DESIGN AND FABRICATION OF POLYMER-BASED MICROFLUIDIC PLATFORMS FOR BIOMEMS APPLICATIONS

DISSERTATION

Presented in Partial Fulfillment of the Requirements for

The Degree Doctor of Philosophy in the Graduate

School of The Ohio State University

By

Siyi Lai, M.S.

* * * * *

The Ohio State University
2003

Dissertation Committee:

Professor L. James Lee, Adviser

Professor S. T. Yang

Professor Kurt W. Koelling

Approved by

_____

Adviser

Chemical Engineering Graduate Program

ABSTRACT

The goal of this study is to design and fabricate polymer microfluidic devices for BioMEMS applications. The emphasis is on the design of microfluidic functions and the development of a new packaging technique.

A microfluidic platform was designed on a compact disk (CD) for medical diagnostics, which includes functions such as pumping, valving, sample/reagent loading, mixing, metering, and separation. The fluid propulsion was based on the centrifugal force. A passive capillary valve, which is based on a pressure barrier that develops when the cross-section of the capillary expands abruptly, was used to control the fluid flow. Micromixing was achieved by impinging mixing and bend-induced vortices. Integration of these microfluidic functions was applied in a two-point calibration system for medical diagnostics and a cascade micromixer for protein reconstitution. A specific application was for enzyme-linked immunosorbent assays (ELISA). It has been demonstrated successfully to realize the necessary microfluidic functions for the ELISA process on a CD. The preliminary analysis of rat IgG from hybridoma culture showed that the microchip-based ELISA has the same detection range as the conventional method on the 96-well microtiter plate, and has advantages such as less reagent consumption and shorter assay time over the conventional one.

A new technique, resin-gas injection, was developed for bonding and surface modification of polymer microfluidic devices. This method can easily bond biochips with complex flow patterns. By adding surface modification agents, the interfacial free energy of the substrate with water can be controlled. Local modification of the channel surface can also be achieved through sequential resin-gas injection in conjunction with the masking technique. For application, this technique was used to form a layer of dry monolithic stationary hydrogel on the walls of a microchannel, serving as a sieving material for electrophoresis separation of DNA fragments. The regent loading, and the electrophoresis separation efficiency of this new technique were compared experimentally with the conventional linear polymer solution method used in the microchannel based DNA sequencing process. It was found that our method has the advantages of more user-friendly operation, easier and faster sample loading, and better separation efficiency.

Dedicated to my parents

ACKNOWLEDGMENTS

First I would like to express my sincere appreciations to my adviser, Professor L. James Lee, for his invaluable guidance, discussions, supports and encouragements throughout my four years stay at The Ohio State University. Many thanks to him for his frequent discussions with me about my general research directions and technical details which not only expanded my horizons but also stimulated my creativity and imagination.

I would also like to acknowledge Professor Marc Madou for bringing me into this wonderful field and provide partial financial support to me. Thanks to Professors Kurt Koelling and S.T. Yang for serving on my dissertation committee and for their invaluable comments and suggestions, to Dr. Paula Stevenson for proofreading all the manuscripts I submitted for publishing.

Thanks also go to my collaborators, Dr. Sylvia Daunert, Dr. Leonidas Bachas, Daniel Johnson, Phillip Douglass and Brett Wenner on the CD project, Dr. S. T. Yang, Jun Luo on the ELISA project, and to Dr. Yifar Chen and Lynn Kim for their help and support during my stay at Burstein Technologies in summer 2000.

To all the fellow graduate students in our lab, especially to those who collaborated with me (Chee Guan Koh, James Shih, Roger Juang, Yumin Lu, Liyong Yu, Yong Yang, Shengnian Wang, Xia Cao and Kai Kang), thank you very much for your friendship and I

cherish the moments we shared together very much! Experimental assistances from Yeny Hudiono are greatly appreciated.

I also want to give my special thanks to Paul Green for his endless help on the CNC-machining work and his assistance on the construction of the clean room (KL 431) together with Carl Scott and Leigh Everad.

Last but not least, I want to thank my parents for their love and dedications for raising me, supporting me and educating me. Great appreciations to my wife, Yunying, for her love, accompany, encouragement, and support through all these years.

VITA

March 26, 1972	Born - Kaihua, Zhejiang, P.R. China
September 1990 - July 1994	B.S. Chemical Engineering, Zhejiang University Hangzhou, Zhejiang, P.R. China
September 1994 - January 1997	M.S. Chemical Engineering, Zhejiang University Hangzhou, Zhejiang, P.R. China
February 1997 - June 1998	Instructor Chemical Engineering Zhejiang University Hangzhou, Zhejiang, P.R. China
September 1998 – August 1999	Department Fellowship Chemical Engineering The Ohio State University Columbus, Ohio, USA
July 2000 – September 2000	Research Intern Burstein Technologies, Inc. Irvine, California, USA
September 1999 – Present	Graduate Research Associate Chemical Engineering The Ohio State University Columbus, Ohio, USA

PUBLICATIONS

1. Siyi Lai, L. Yu, S.-K. Kuo, S. Wang, J. Luo, L.J. Lee, K. Koelling, C.H. Menq, and S.T. Yang “Design and fabrication of BioMEMS devices and simulation of micro-molding,” Proceedings of National Science Foundation Design, Service and Manufacturing Grantees and Research Conference, Birmingham, Alabama (Jan. 2003).

2. P.M. Douglass, B.R. Wenner, Siyi Lai, L. Bachas, and S. Daunert, "Centrifugal Microfluidics in Pharmaceutical Analysis: Phenothiazine Detection Employing Fluorescently-Labeled Calmodulin as the Biorecognition Element," Analytical Chemistry (2002).

3. Siyi Lai, Y. Hudiono, L. J. Lee, S. Daunert, and M. J. Madou, "Gas-resin injection technique for bonding and surface modification of polymer-based microfluidic platforms," Annu. Tech. Conf. - Soc. Plast. Eng. 60th (Vol. 3), pp. 2703-2707 (2002).

4. Siyi Lai, L. J. Lee, L. Yu, K. W. Koelling, and M. Madou, "Micro- and nano-fabrication of polymer based microfluidic platforms for BioMEMS application," Materials Research Society Symposium Proceedings, 729 (BioMEMS and Bionanotechnology), pp.17-27 (2002).

5. Siyi Lai, L.J. Lee, K.W. Koelling, and C.H. Menq, "Polymer based micro/nano-fabrication for BioMEMS applications," Proceedings of NSF Design, Service and Manufacturing Grantees and Research Conference, San Juan, Puerto Rico, (Jan. 2002).

6. L.J. Lee, M.J. Madou, K.W. Koelling, S. Daunert, Siyi Lai, C.G. Koh, Y-J. Juang, Y. Lu and L. Yu, "Design and fabrication of CD-like microfluidic platforms for diagnostics: microfabrication," Biomedical Microdevices 3(4), pp. 339-351 (2001).

7. M.J. Madou, L.J. Lee, S. Daunert, Siyi Lai and C.H. Shih, "Design and fabrication of CD-like microfluidic platforms for diagnostics: microfluidic functions," Biomedical Microdevices 3(3), pp. 245-254 (2001).

8. R.D. Johnson, L.H.A. Badr, G. Barrett, Siyi Lai, Y. Lu, M.J. Madou, L.G. Bachas, "Development of a fully integrated analysis system for ions based on ion-selective optodes and centrifugal microfluidics," Analytical Chemistry 73(16), pp. 3940-3946 (2001).

9. X. Cao, Siyi Lai and L.J. Lee, "Design of a self-regulated drug delivery device," BioMedical Microdevices 3(2), pp.109-117 (2001).

10. M.J. Madou, Y. Lu, Siyi Lai, C.G. Koh, L.J. Lee and B.R. Wenner, "A novel design on a CD disc for 2-point calibration measurement," Sensors and Actuators A 91(3), pp.301-306 (2001).

11. Siyi Lai, Y. Hudiono, L. J. Lee, S. Daunert, and M. J. Madou, "A novel bonding method for polymer-based microfluidic platforms," Proceeding of SPIE, Micromaching and Microfabrication Process Technology VII, v4557, pp. 280-287 (2001).

12. M.J. Madou, L.J. Lee, K.W. Koelling, Siyi Lai, C. G. Koh, Y-J. Juang, L. Yu and Y. Lu, "Design and fabrication of polymer microfluidic platforms for biomedical application," Annu. Tech. Conf. - Soc. Plast. Eng. 59th (Vol. 3), pp. 2534-2538 (2001).

13. P.M. Douglass, B.R. Wenner, S. Shrestra, B. Sharma, Siyi Lai, M.J. Madou, and S. Daunert, "Genetically designed biosensing systems for high-throughput screening of pharmaceuticals, clinical diagnostics, and environmental monitoring, Proceedings of SPIE - The International Society for Optical Engineering v 4252, pp.59-70 (2001).

14. M.J. Madou, Y. Lu, Siyi Lai, Y-J Juang, L.J. Lee and S. Daunert, "A novel design on a CD disc for two-point calibration measurement," Solid-state Sensor & Actuator workshop, Hilton Head, pp.191-194 (2000).

15. M.J. Madou, Y. Lu, Siyi Lai, L.J. Lee and S. Daunert, "A centrifugal microfluidic platform – a comparison," Proceedings of the μTAS 2000 Symposium, pp. 565-570 (2000).

FIELDS OF STUDY

Major Field: Chemical Engineering

Studies in BioMEMS, Microfluidic and Polymer Microfabrication

TABLE OF CONTENTS

Page

LIST OF TABLES

Table **Page**

LIST OF FIGURES

Figure **Page**

CHAPTER 1

INTRODUCTION

1.1 Background

Over the past 20 years, many micro-electro-mechanical systems (MEMS) have been developed for a diverse range of applications from automotive to medical devices. Recent advances of microsystem technology (MST) to medical applications (BioMEMS) promise to revolutionize the field of medical and life sciences through the development of miniature analytical devices with sophisticated functionality. Microsystems (so called lab-on-a-chip, biochips, microchips), which are based on integrating large parallel arrays of miniaturized fluidic components and sensors into the smallest possible space, can greatly reduce reagent volume, sample contamination, and power consumption. It can also provide faster and more efficient compounding and separations in biomedical and analytical applications. The small size and portability of lab-on-a-chip systems are very advantageous. For example, a physician can perform diagnostic testing at a patient's bedside or at an accident spot and know the testing results in a few minutes. The

miniaturization also results in a significant improvement of lab safety. For example, spills, explosions, and other laboratory accidents that can occur during conventional sample preparation procedures are not a problem with the lab-on-a-chip devices due to the extremely small amount of sample used.

The demand for high-precision miniature devices and efficient processing technologies for micro-/nano-fabrication has been growing rapidly in recent years. Emerging markets include chemical and medical devices (e.g. gene-chips, hearing aids, drug delivery systems, bio-sensors, fuel cells) [Freemantle, 1999]; telecommunication components; optical components (e.g. diffraction gratings, miniature lens and mirrors); automotive crash, acceleration and distance sensors; camera and watch components [Snyder, 1999]; and mechanical devices (e.g. printer heads, micro heat exchangers). According to the NEXUS (The Network of Excellence in Multifunctional Microsystems) MST market analysis, total world market for microsystems is expected to grow from $ 30 billion in the year 2000 to $ 68 billion by the year 2005. The main fields of application within this market will be dominated by IT peripherals, biomedical, automotive, household and telecommunications. The application field of biomedical contributes a value of $ 8 billion in year 2000 to $19 billion by the year 2005. Within the biomedical applications, the worldwide market for microarrays, microfluidics devices, and other biochips is expected to grow at an annual rate of 65% and reach $3.3 billion by 2004, as reported by Technical Insights (San Antonio, TX, 2002).

1.1.1 Microfluidics

The major technical challenges in making these microsystems include: design and implementation of necessary microfluidic functions; integration of these functions with complete automation; and development of cost-effective manufacturing technology [Madou 1997]. Microfluidics is the manipulation of fluids in channels having at least two dimensions at the micron scale. It is a core technology in a number of miniaturized systems developed for chemical, biological, and medical applications [Freemantle, 1999]. Microfluidics is one of the fastest growing sectors of the life science research market. According to Frost & Sullivan report in April 2001, the microfluidics market will surge from $17 million in 1999 to $77 million in 2000 and to $395 million in 2004.

Major microfluidic components include sample introduction or loading (and in some cases, sample preparation); propulsion of fluids (such as samples to be analyzed, reagents, and wash and calibration fluids) through micron-sized channels; valving; fluid mixing and isolation as desired; small volume sample metering; sample splitting and washing; and temperature control of the fluids. A wide range of microfluidic components, such as micropumps, microvalves, micromixers, flow sensor, etc., has been demonstrated. The main challenge in making miniaturized systems is the integration of different microfluidic components to perform certain functions at high speed and high throughput. Integrated microfluidic systems have the potential for applications such as microreaction technology, on-chip flow-through-PCR (polymerase chain reaction), bio-separation, clinical diagnostics, drug discovery and delivery, lab-on-a-chip technology, air bag triggers, and ink jet nozzles [McDonald et al., 2000].

1.1.2 Microfabrication

Most of these devices are currently built on single crystal silicon (Si) and polycrystalline silicon (Poly Si) materials. The main reason for choosing silicon-based materials is that micro-fabrication methods for these materials have been extensively developed for the microelectronics industry over the last four decades. However, for many applications (particularly in the biomedical field) these materials and the associated production methods are too expensive, or else the material properties often induce problems like lack of optimal clarity, low impact strength and poor bio-compatibility. Currently, fabrication of miniature devices is taking a new turn towards non-silicon materials, in particular polymers because polymeric materials offer a wide range of physical and chemical properties. They also have the advantages of low cost, good processibility for mass production, and are recyclable. The largest markets are expected to be in medical and chemical devices. However, polymer microfabrication techniques are still not well developed.

A number of polymer-based micro-components have been fabricated for demonstration in academia and industry by combining various bulk or surface machining techniques and conventional manufacturing methods, such as silicone rubber casting, injection molding, hot embossing, and reaction injection molding [Becker and Dietz, 2000]. However, the processes have not been thoroughly analyzed and most technologies are developed by trial-and-error. For these reasons, the cycle time is very long and the yield tends to be very low, closer to prototyping than mass production. As a result, there is considerable potential for developing new molding methods and improving existing

processes through greater technical understanding and innovation. Although a growing number of researchers are at work in this emerging new manufacturing field, most research activities are in Europe and Japan. There is relatively little effort in the U.S., except for polydimethylsiloxane (PDMS) casting [Xia and Whitesides, 1998].

1.1.3 Bonding and surface modification

After fabrication, these devices need to be sealed in order to perform microfluidic functions. The channel surface may need to be modified in order to provide proper physical, chemical, and/or biological functions. Examples are hydrophilicity for easy reagent loading, hydrophobicity for capillary valving, immobilization of protein, enzyme or immunomolecules, and electric charge on the surface (for strong electroosmotic flow, a high static charge is preferred; while a charge-free surface is preferred for pressure flow and electrophoresis). Currently packaging (bonding, surface modification, and reagent loading) is still a challenging issue in the design and fabrication of polymer-based microfluidic devices.

Bonding (i.e. sealing a device with a lid) between silicon and silicon or other materials (e.g., glass, metal, etc.) is well developed and can be achieved by different methods such as anodic bonding, fusion bonding, eutectic bonding, and adhesive bonding [Schmidt, 1998]. These approaches involve high temperature, high pressure, or high voltages. Among them, only adhesive bonding can be applied to polymer-based microfluidic devices. When using the adhesive bonding method, care needs to be taken in order to prevent the adhesive from flowing into the micro channels. Other techniques

such as adhesive tape bonding (lamination), thermal (IR, hot-plate, laser) bonding, ultrasonic welding, and solvent bonding (i.e., partially dissolve the bonding surfaces, and evaporate the solvent) have also been tried in academia and industry [Becker and Gartner, 2000]. In general, these approaches alter the surface of the microdevices by using external sources (e.g. solvent, adhesive, heat) and applying pressure to bring two halves together. They have problems with either blocking the microchannels or changing their dimensions and are mainly applicable for relatively large microchannels (several hundreds of microns to millimeters).

In most BioMEMS applications, biocompatibility is one of the main requirements for a substrate due to protein adsorption and cell adhesion on the substrate surface. Factors that affect protein adsorption include protein concentration, surface energy/tension, surface roughness, crystallinity, surface charge, etc. Therefore, surface modification is necessary to produce surfaces that are able to resist cell adhesion and protein adsorption.

1.2 Objective of study

The overall goal of this study is to design and fabricate of polymer-based microfluidic platforms for BioMEMS applications. This study focuses on the design of microfluidic functions and development of a new packaging technique. Low-cost microfabrication techniques are used as tools to produce the polymer-based microfluidic devices for research studies.

The more specific objectives of this study are:

1. To design microfluidic functions, such as pumping, valving, sample/reagent loading, dilution, mixing, metering, and separation on a plastic compact disc. The fluid propulsion is based on centrifugal force, which is achieved through rotationally induced hydrostatic pressure. It is simple, uses a single low-cost motor, and is capable of fine flow control through proper design of the location, dimensions and geometry of channels and reservoirs based on fluid properties. A passive capillary-valve, which is based on pressure barrier that develops when the cross-section of the capillary expands abruptly, is used to control the fluids flow. No moving parts and external actuation is required. Micromixing is achieved by impinging mixing and bend-induced vortices by flowing fluids through an S-shaped channel. Integrating these microfluidic functions can be applied in a two-point calibration system for medical diagnostic, a cascade micromixer for protein reconstitution, and an enzyme-linked immunosorbent assay (ELISA) for hybridoma cell culture.
2. To develop a packaging technique for polymer-based microfluidic platforms. As mentioned in the above section, packaging of polymer microfluidic platforms is still a challenging issue. This newly developed method, called resin-gas injection technique, is able to bond the polymer-based microfluidic platforms, to modify the surface properties (such as changing the hydrophilicity, protein adsorption and rejection properties etc.) of the microchannel, and to provide more functionality onto the microchannel.

1.3 Outline

A general introduction about the project is given in Chapter 1 together with its significance and our objective. Chapter 2 reviews the background information about BioMEMS applications (genomics and proteomics), microfluidic functions, polymer-based microfabrication, bonding methods for polymer-based microfluidic platforms, and polymer surface modification method to improve the biocompatibility, especially in inhibiting protein-adsorption and modifying the surface wettability (hydrophobic vs. hydrophilic).

In Chapter 3, the design and fabrication of a CD-like microfluidic platform for medical diagnostics are discussed. Results from design and performance of different microfluidic functions such as centrifugal pumping, capillary valving, flow sequencing, washing, and micromixing are described. By combining these microfluidic functions, two potential applications, a two-point calibration system for medical diagnostics and a cascade micromixer for protein reconstitution, are studied and the results of these two applications are presented.

Chapter 4 describes the newly developed method, resin-gas injection assisted technique, for bonding and surface modification of polymer-based microfluidic platforms. The application of this new approach on coating polyacrylamide gels serving as the sieving materials in microchip-based capillary electrophoresis for DNA separation is also discussed.

Chapter 5 presents the design of a CD microfluidic platform for enzyme-linked immunosorbent assay (ELISA). The results and performance on analysis of rat IgG from hybridoma cell culture are discussed.

In Chapter 6, all the research work conducted is summarized and recommendations for future work are also listed.

CHAPTER 2

LITERATURE REVIEW

2.1 Microfluidic systems in bio-analytical applications

Most molecular and biological assays and tests are very tedious and time consuming. As shown in Figure 2.1, following sample preparation procedures are usually included: obtaining a cellular sample (e.g. blood, tissue, etc.); separating out the cellular material of interest; lysing the cells to release the crude DNA and RNA by external forces; purifying the crude lysate; performing necessary enzymatic reactions such as denaturing, cleaving, and amplifying the lysate by polymerase chain reaction (PCR); sequencing DNA/gene in gel electrophoresis; and finally detecting and reducing data. This process requires skilled technical people working in well-equipped biomedical laboratories for several days to analyze a single sample. Much of today's diagnostic equipment is costly and bulky. They have limited uses in medical diagnostics and are unsuitable for emergency response at the site of a chemical/biological-weapon attack. To improve public health, there is a great need to develop efficient and affordable methods and devices that can simplify the diagnostic process and be used as portable units.

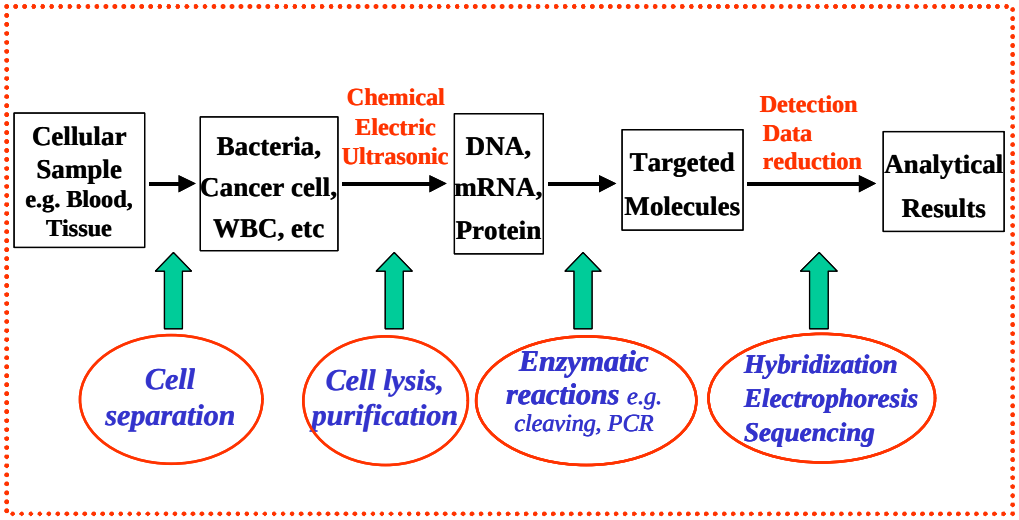

Figure 2.1. Protocol for molecular diagnostics.

On the other hand, micro-instrumentation, based on integrating large parallel arrays of miniaturized fluidic systems and sensors, can greatly reduce reagent volume and sample contamination. It can also provide faster and more efficient compounding and separation in biomedical and analytical applications. Tasks that are now performed in a series of conventional bench-top instruments can be combined into a single portable unit. For example, sample transport, sample pretreatment, separation, and detection are automatically carried out in a single device. Due to the miniaturized size, fabrication of devices with massively parallel analysis and detection is possible to improve the accuracy. The portability of the systems also enables the point-of-care testing. In the future, households might be equipped with small and user-friendly deices to monitor the daily health status based on measurements of small samples. Furthermore, polymer-based microfabrication technologies make cheap and disposable systems feasible.

Integrated microfluidic systems have the potential for applications such as microreaction technology, bio-separation, medical diagnostics, drug discovery and delivery, lab-on-a-chip technology, micro total analysis systems (μTAS), air bag triggers, and ink jet nozzles [McDonald, 2000]. The review in this section aims at the applications of microfluidic systems in genomic and proteomic applications.

2.1.1 Genomics

2.1.1.1 Capillary electrophoresis chips (CE chips)

Electrophoresis has been extensively used in separating, sizing, and sequencing

genetic materials. The advantages of microfabricated capillary electrophoresis devices are that only very small amounts of sample are required and the electrophoresis separation is 10 to 100 times faster than conventional techniques (e.g., slab gel electrophoresis, capillary electrophoresis), in which separation times are usually larger than 10 minutes. The throughput of genetic analysis can be improved by an order of magnitude by the application of CE chips. The first capillary electrophoresis experiments using a chip-like microstructure were introduced in 1992 by Manz and his coworkers [Manz et al., 1992] for the separation of fluorescent dyes with different charges. Since then, separations of fluorescence-labeled amino acids, metal ion complexes, DNA fragment, PCR products, short oligonucleotides, and blood serum cortisol have been demonstrated [Woolley et al., 1997] in capillary electrophoresis chips.

The fast separation of CE chips is due to its ability to apply a high electric field (the Joule heating problem can be solved by the high energy dissipation due to the large surface-to-volume ratio in microchannel) and to inject a very small sample plug. Figure 2.2 shows a commonly used design for capillary electrophoresis separation. The sample is injected by applying a voltage between reservoirs 3 and 4. A very small plug (of pl volumes) can be introduced, with dimensions approximately the same as the channel width. Larger plugs of sizes can be injected by using an offset double T-injection system as shown in Figure 2.2b. The separation is performed by applying a voltage between reservoirs 1 and 2 and detection is usually carried out at the point near reservoir 2. The separation channel may be filled with sieving materials, such as polyacrylamide gel, to prevent broadening the separated band.

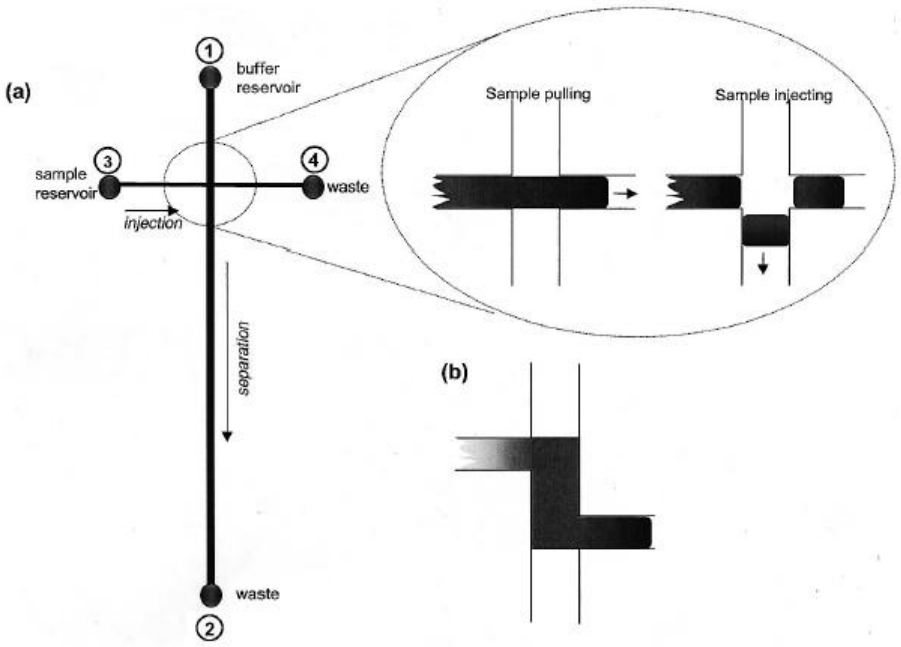

Figure 2.2. (a) A common design for capillary electrophoresis chips with cross injection and (b) double T injection design (from Sanders and Manz [2000] with permission from the author).

Injection-molded acrylic CE chips have been used in electrophoresis to separate two major components of mRNA (18s and 28s rRNA) [Ogura et al., 1998]. The microchannel for separation is about 100 micron wide, 40 microns deep, and 1 cm long. Microchannels were filled with hydroxypropyl methylcellulose as sieving polymer and ethidium bromide for RNA staining. The assay can be finished in less than 3 minutes and the results are reproducible. Very small amount of sample (about 1-2 μl) is sufficient. The detection limit was found to be 100-fold lower than that for conventional agarose gel electrophoresis.

The potential of using capillary electrophoresis chip for high-throughput sequencing has been recently developed by Mathies' group [Woolley et al., 1997; Simpson et al., 1998; Medintz et al., 2001]. Capillary array electrophoresis (CAE) chips have been demonstrated by analyzing 96 different DNA samples in less than 8 minutes [Igor et al., 2001]. A 384-channel CAE microplate on a 200mm diameter wafer have also been proposed for further increases in the throughput by allowing parallel analyses.

A number of companies are now commercializing the technology of microfabricated capillary electrophoresis devices. Caliper Technologies Corporation [http://www.calipertech.com] and Agilent Technology have released an instrument that used disposable glass chips (LabChip®) for integrated analysis of DNA, RNA, and protein, providing fragment size and concentration information within 30 minutes. Aclara Biosciences Inc. [http://www.calara.com] intends to provide a disposable microfluidic system (LabCard™) where ready to use plastic chips are pre-filled with gel that can be used for rapid DNA fragment sizing.

2.1.1.2 Polymerase chain reaction (PCR) chips

Polymerase chain reaction (PCR) has rapidly become one of the most widely used techniques in molecular biology since it was first reported in 1986. It provides inexpensive and simple means of producing relatively large numbers of copies of DNA molecules from minute quantities of specific region of a DNA chain. For example, a 40 cycle PCR would amplify a specific region of DNA chain 1 billion times (2^{40}) theoretically. A PCR cycle involves three major steps: melting or denaturization, annealing, and extension or elongation. The first step (melting or denaturization) usually takes place at 95°C, at which the double strand of a DNA opens to single-stranded DNA, and all enzymatic reactions from a previous cycle stops. It is then annealed at a lower temperature, usually at 50~60°C, at which primers stick to the single-stranded DNA. A primer is a short segment of nucleotides that is complementary to a section of the to-be-amplified DNA. Primers are annealed to the single-stranded DNA template to provide an initiation site for the extension of the new DNA molecule. The final step is the extension at 72°C, at which the polymerase reaction is most active. These steps are repeated for 30 or 40 cycles until a sufficient number of DNA is generated for subsequent analysis. Using a conventional thermocycler device (e.g., Perkins Elmer 9700 Thermal Cycler), a single amplification cycle can be performed within about 4 minutes because each cycle involves heating and cooling processes. The whole PCR process would take about 2~4 hours. The efficiency of the PCR depends highly on rates of heating and cooling and the accuracy and uniformity of the temperature control.

Microfabricated devices have high surface area vs. volume ratio. Energy

dissipation in these systems is rapid, and therefore, fast heating and cooling can be realized to minimize the PCR cycling time. In addition, PCR on microfabricated devices can reduce the consumption of expensive reagents, the power consumption, and the space. A number of groups have investigated PCR systems in microfabricated devices (PCR chips). The PCR thermocyclers are realized by several methods in the laboratory. Single reservoir thermocyclers [Fujii, 2001], array thermocyclers [Lagally et al., 2001; Waters et al., 1998], and flow-through devices [Kopp et al., 1998; Schneegab et al., 2001] have been demonstrated

In the early stage of PCR chip development, the PCR material has been incorporated into one or more of the reservoirs on the microdevices; and the whole device is then thermally cycled, just like the conventional PCR system except the size [Waters et al., 1998]. Systems, on which only the reservoirs with PCR materials is thermally cycled, have also been demonstrated. The heating and cooling rate for the PCR reaction can be improved to 20 ^{0}C/s by using microfabricated heating and temperature sensing elements [Lagally et al., 2001]. Capillary electrophoresis (CE) has also been coupled with PCR chip to create a completely integrated DNA analysis system [Lagally et al., 2001]. The DNA micro-analyzer is capable of performing amplification and electrophoretic DNA analysis much faster than conventional techniques without any manual sample manipulations. This system demonstrated high-speed PCR amplification and CE detection in less than 15 minutes.

Continuous-flow PCR systems have also been reported [Kopp et al., 1998; Schneegab et al., 2001]. As shown in Figure 2.3, PCR materials are pumped to flow

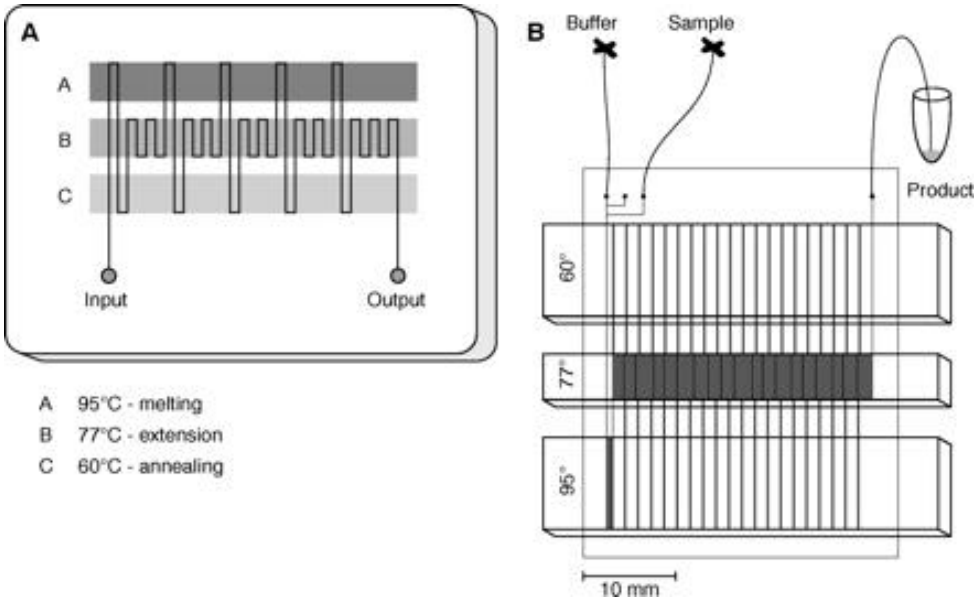

Figure 2.3. (a) Schematic of a continuous-flow PCR on a chip system and (b) layout of device of a 20-cycle PCR microdevices. (Kopp et al.[1998] with permission from the author).

between regions of different temperatures. Three well-defined zones are kept at 95^0C, 60^0C, and 77^0C by means of the thermostated copper blocks. The melting, annealing, and extension steps are defined by the materials passing through these three different temperature zones. A 20-cycle PCR amplification of a 176-base pair DNA fragment can be performed within 20 minutes [Kopp et al., 1998]. In flow-through PCR chips, only the temperature of the flowing PCR materials is changed. The temperature of the walls remains constant, while fast temperature changes of the devices are usually necessary in stationary PCR chips. However, relatively large volumes of sample are necessary in flow-through PCR chips.

2.1.1.3 Integrated DNA analysis systems

The integrated DNA analysis devices are still in the early stage of development and initial efforts at integration are limited to two to three functions. PCR-based sample preparation and electrophoresis separation have been integrated to develop a miniaturized DNA analysis system [Lagally et al., 2001]. The fully integrated system includes microfabricated heaters, temperature sensors, and PCR chambers directly connected to capillary electrophoresis separation channels. Valves and hydrophobic vents provide controlled and sensorless sample positioning and immobilization. PCR amplification and detection of nanoliter volumes of DNA can be performed within 15 minutes. Integrated glass system of cell lysis, PCR, and electrphoretic sizing has also developed [Waters et al., 1998]. The entire microchip is thermally cycles to lyse cells and to amplify DNA, and

the products are then analyzed using a sieving medium (e.g., polydimethylacrylamide gel) for size separation.

Burns and coworkers [Burns et al., 1998; Brahmasandra et al., 2001] have demonstrated a more sophisticated integrated DNA analysis device as shown in Figure 2.4. This device consists of different microfluidic components such as sample loading, metering, mixing, thermal reaction, electrophoresis separation, and fluorescence based detection. It is capable of metering nano-liter aqueous regent and DNA containing solution, mixing the solutions together, amplifying or digesting the DNA to form discrete products, and separating and detecting those products.

2.1.2 Proteomic applications

2.1.2.1 Enzyme assays

Hadd and coworkers [Hadd et al., 1997] published the first work on developing an automated, microchip assay for ß-galactosidase using a fluorogenic substrate. Electrokinetic flow was used to actively and precisely control the transportation, dilution and mixing of the reagents in an enzyme assay. On-chip fluorescence detection allows automated studies of enzyme kinetic and inhibition determinations. An enzyme assay can be preformed on the microchip in 20 minutes and the reagent consumptions can be reduced to 4 orders of magnitude compared to a conventional assay.

Cohen et al. [Cohen et al., 1999] applied the microchip for enzyme assay of phosphatase and protease where fluorogenic assays are not readily available. This microchip design is more sophisticated and capable of incorporating several sets of paired

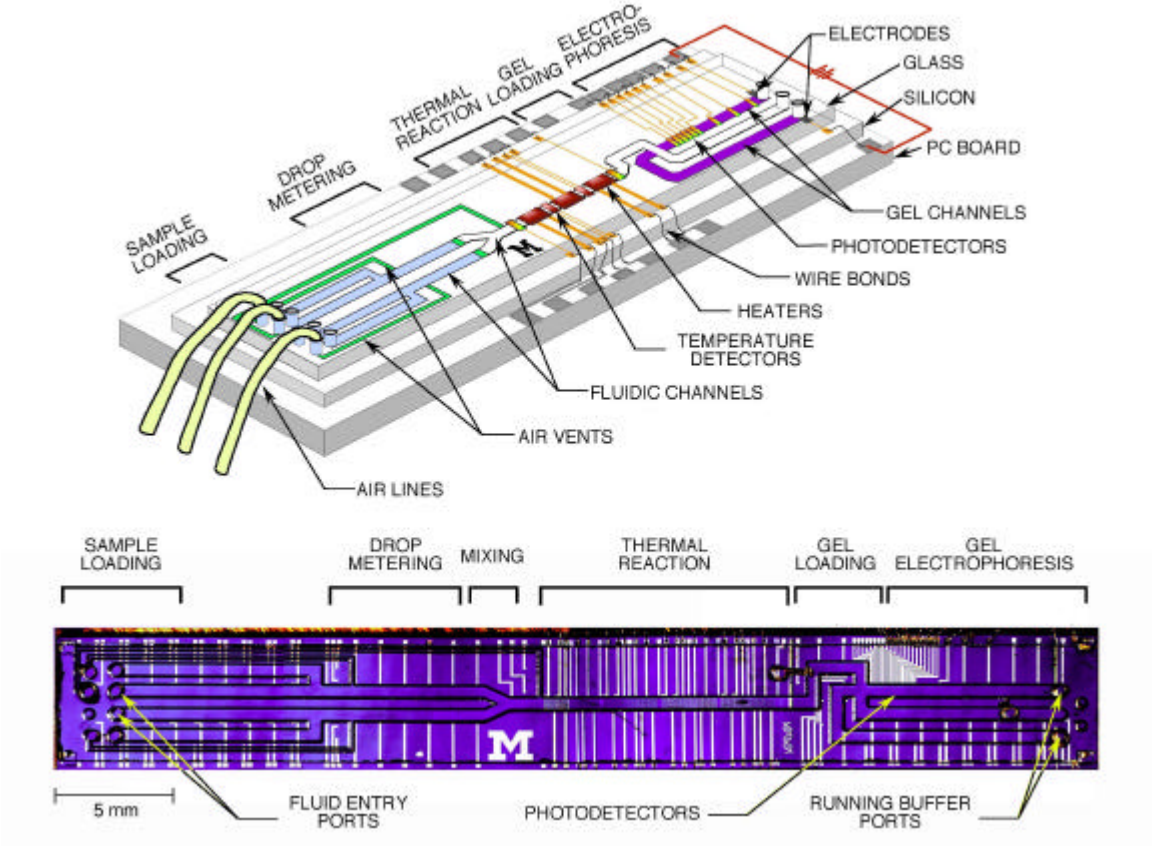

Figure 2.4. Schematic of an integrated device (from Burns et al. [1998] with permission from the author).

reagent wells so that the concentration of each component of the inhibition reaction could be independently controlled. It allows an enzyme and its inhibitors to be characterized in an automated fashion. Two designs of the microchip were demonstrated to offer different possibilities for performing enzyme assays. One design is actually a reactor attached to a separation capillary while the other allows complex titration of various assay components to be carried out on the chip without any manual pipetting steps. Both phosphatase and protease reactions were demonstrated and good agreements between on-chip determined Michaelis-Menten constants and off-chip ones were achieved.

2.1.2.2 Immunoassays

Immunoassay (IA) is an indirect method, which measures the effect of varying concentrations of a compound/analyte in the test fluid on the reaction of the specific antibody (Ab) and the antigen (Ag). According to the design of the experiment, they can be used to detect either antibody or antigen. A wide variety of compounds can be quantified by immunoassays. These range from large polymeric proteins, nucleic acids, receptors, and structural proteins, to small molecular weight haptens of drugs or their metabolites. Immunoassays can be classified as competitive and noncompetitive IAs [Wild, 1994; Lee and Colbrun, 2002].

2.1.2.2.1 Non-competitive IA

Non-competitive IA is based on the separation of Ag-Ab complexes from free Ab and/or Ag. For the analysis of antigens (or fragment of Ag) in a sample, an excess

amount of labeled Ab (Ab*) could be added to the sample to form complexes with the antigens in the sample (Ag-Ab*).

$$Ag + Ab^* \text{ (excess)} = Ag\text{-}Ab^* + Ab^* \text{ (excess)} \qquad (2.1)$$

The formation of complex should be quantitative and directly dependent on the amount of Ag present in the sample. After separation of the Ab* and the Ag-Ab* complex, it is possible to quantify the amount of Ag in the mixture based on the amount of complexes formed and/or the decrease in the amount of free labeled Ab*. The non-competitive IA has high sensitivity, but is limited by the nonspecific binding (the binding of the antigen/ antibody to the supporting surface).

2.1.2.2.2 Competitive IA

The antibody (limited amount) binds the antigen (Ag) and also labeled antigen (Ag*) in the sample. Therefore there is competition between labeled and unlabeled antigen for the antigen binding sites.

$$Ag + Ab = Ag\text{-}Ab \qquad (2.2)$$

$$Ag^* + Ab = Ag^*\text{-}Ab \qquad (2.3)$$

As the amount of unlabelled antigen in the sample increases, the amount of labeled antigen bound to antibody will decrease. Therefore the amount of bound labeled antigen is proportional to the amount of unlabeled antigen in the sample. A fixed amount of labeled antigen is added to the system so at the end of the reaction either the amount of bound or the amount of unbound labeled antigen can be measured. From this, the amount of antigen present in the sample can be determined from a standard curve. Standard

curves are constructed with increasing amounts of known antigen and so from this curve the amount of antigen in the unknown sample can be determined.

2.1.2.2.3 Capillary electrophoresis-based immunoassays

The use and development of immunoassay technology in clinical, food safety, and environmental applications is wide spread in all three of these areas because of its extremely high selectivity and sensitivity. However, most conventional immunoassays are carried out manually. They require a relatively long assay time and involve troublesome liquid-handling procedures and many expensive antibody reagents. Microchip-based immunoassay seems to be effective to overcome these drawbacks. It can enhance the reaction efficiency, simplify procedures, reduce assay time and sample or reagent consumption, and provide highly portable systems. In conjunction with the exponential growth in microfabricated devices research, several developmental advances have been realized in miniaturization of capillary electrophoresis-based immunoassays [Bao, 1997; Schmalzing et al., 2000; Colyer et al, 1997; Sanders and Manz, 2000].

Koutny et al. recently developed a microchip for competitive immunoassay of cortisol [Koutny et al., 1996]. As shown in Figure 2.5a, the microchip was used only for the separation part of the immunoassays. The reagent mixing and incubation, which dominates the total assay time, were carried out off-chip. A similar competitive immunoassay for theophylline was described by Chiem and Harrison [1997] as shown in Figure 2.5b. An integrated electrophoretic microdevice, where reagent mixing, incubation, and subsequent electrophoretic analysis were performed on-chip, has been

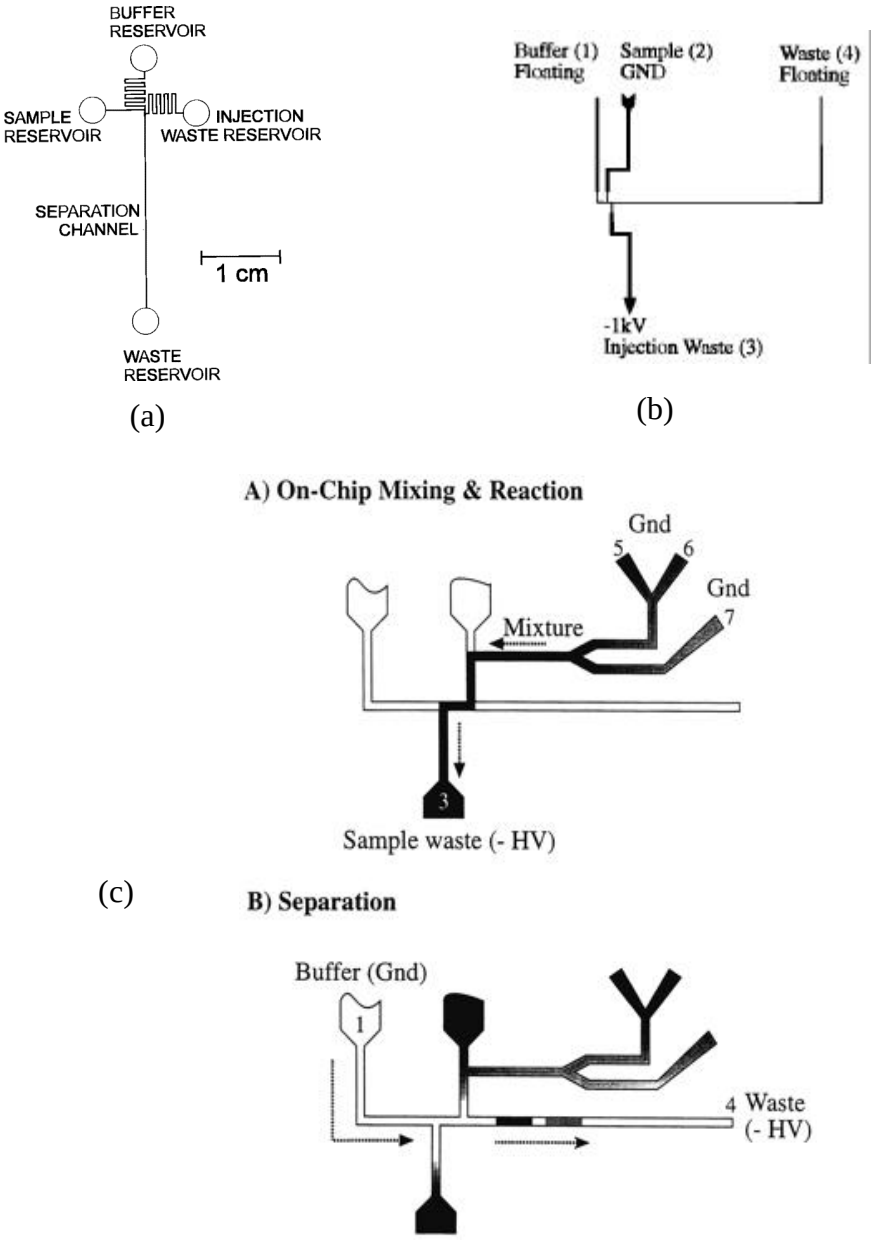

Figure 2.5. Difference microchip designs for capillary electrophoresis-based immunoassays: (a) from Koutny et al [1996]; (b) from Chiem and Harrison [1997] (with permission from the author); and (c) Chiem and Harrison [1998] (with permission from the author).

reported to perform a competitive immunoassay for theophylline [Chiem and Harrison, 1998]. In this design (Figure 2.5c), solution of theophylline, labeled theophylline, and antibody in reservoirs 5, 6, and 7 respectively, were electroosmotically pumped along the shaded area by applying electrical ground (Gnd) to these reservoirs and negative high voltage (-HV) at the sample waste (reservoir 3). This forms a plug of the on-line incubated mixture at the double-T intersection. The reagents and products were separated by switching Gnd to reservoir 1 to –HV to the separation waste (reservoir 4). The theoretical minimum detection limits of competitive capillary electrophoresis-based immunoassay has also been investigated [Taylor et al., 2001].

2.1.2.2.4 Enzyme-linked immunosorbent assay

Enzyme-linked immunosorbent assay (ELISA), in which antigen and antibodies are immobilized on a solid surface, has also been incorporated into microchips. Several microchip-based ELISA have also been developed, based on the immunoreaction on surfaces of a single microchannel [Rossier et al., 2001] or on micro-beads, which was trapped in the microchannel [Sato et al., 2000 and 2001]. A sandwich immunoassay of D-Dimer in plasma was carried out in a disposable plastic microchip [see Figure 2.6a]. The time required for assay is only 5 to 15 minutes, whereas a few hours are usually required for a quantitative ELISA. Sato and coworkers [see Figure 2.6b] have integrated an immunosorbent assay system into a glass microchip for immunoassays of human secetory immunoglobulin A (s-IgA) and determination of carcinoembryonic antigen for cancer diagnosis. The integration reduced the time necessary for the antigen-antibody reaction

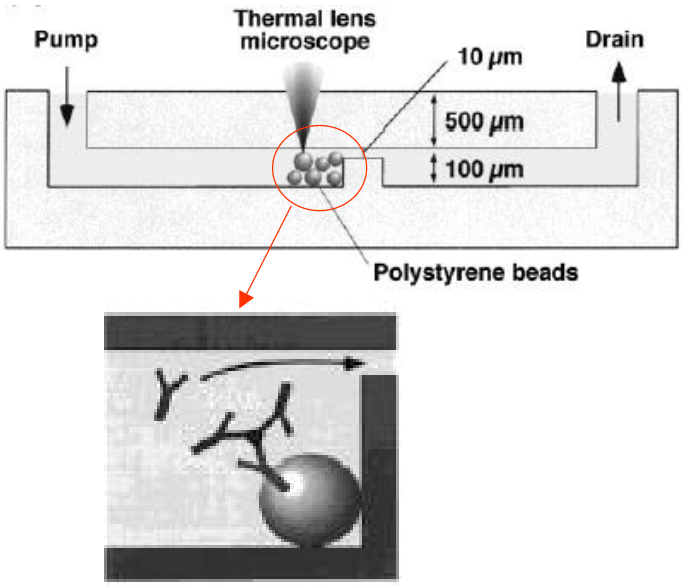

(a)

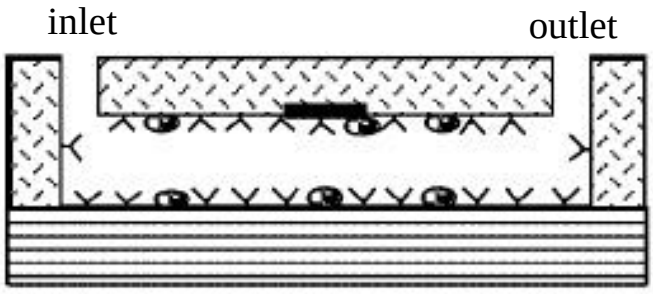

(b)

Figure 2.6. Microchip-based ELISA designs: (a) from Sato et al [2001] (with permission from the author) and (b) Rossier and Girault [2001] (with permission from the author).

and shortened the overall analysis time from 45 hours to 35 minutes. These microchip-based immunoassays took the advantages of the high surface to volume ratio of the microchannel for fast immunoreaction and carried out the whole process of immunoassays on the microchip. However, each step of the ELISA was still carried out manually.

2.1.2.3 Integrated Protein chips

Integrated protein microchips have also been developed for immunoassay and enzymatic reactions [Arenkov et al., 2000]. Different proteins such as antibodies, antigens, and enzymes were immobilized within the 100 μm × 100 μm × 20 μm gel pads of protein microchips. A modified polyacrylamide gel has been developed to accommodate proteins of a size up to 400,000 Daltons. Electrophoresis in the microchip reaction chamber speeded up antigen-antibody interaction within the gel. This chip has been used in immunoassays for detection of antigens or antibodies, as well as to carry out enzymatic reactions and to measure their kinetics in the absence or presence of an inhibitor.

2.1.3 Biochip companies

There are a number of companies participating in the market of biochips or lab-on-a-chip for genomic and proteomic applications. Most of their products are microarray-based systems with biomolecules such as DNA probes, enzymes, and antibodies being immobilized on the chip surface, or simple microfluidic systems capable of either DNA

sequencing by electrophoresis. The biochip companies (partial list) and their main products/ technologies are summarized on Table 2.1.

2.2 Ideal Scales

2.2.1 Volume

Figure 2.7 shows a logarithmic graph of concentration vs. sample volume [Petersen, 2001]. This figure illustrates several basic principles regarding microfluidic and its applications. Different bio-substrates (e.g., DNA, antibodies, virtues, bacteria) have different concentration in the solutions. To ensure that there is at least one 'target' molecule per sample volume, a test system must operate above the diagonal line. For concentrations of chemicals above 10^{15} molecule/ml (~1μM), sample volumes less than one pico-liter are adequate (suitable for clinical chemistry). For concentrations between 10^{9} ~ 10^{17} molecule/ml (1pM~100μM), sample volumes less than one micro-liter are adequate (suitable for immunoassays). However, genomic DNA/RNA exists in blood at a concentration of about 10^{6} or 10^{7} molecule/ml and pathogenic DNA (viruses and bacteria) exists in blood and food at concentrations as low as 10 to 10^{6} molecule/ml. As a result, DNA test systems must be designed to work with samples as large as several milliliters and amplifications of the target molecules (PCR) are necessary. Smaller volumes will not contain even one target molecule.

Companies	Products	Descriptions	Homepage
Lap-on-a-chip systems			
ACLARA BioSciences	LabCard™ microfluidic platforms	RNA and DNA analysis--and high-throughput pharmaceutical drug screening.	http://www.aclara.com
Burstein Technologies	BCD™ technology platform	Use CD or DVD discs to deliver a wide range of tests using a compact disc reader attached to a personal computer.	http://bursteinlabs.com
Caliper/Agilent	LabChip®	Integrated analysis of DNA, RNA, and protein, provide fragment size and concentration information.	http://www.calipertech.com
Cepheid	I-Core® module and Fluidic systems	Sample preparation (extraction, concentration, purification), rapid amplification (PCR) and DNA detection	http://www.cepheid.com/pages/home.html
Gyros AB (SE)	Gyrolab MALDI SP1	In the form of a compact disk, sample preparation for protein analysis and identification. Can perform concentrate, desalt, mix with matrix and crystallize.	http://www.gyros.se/
Motorola Life Sciences	CodeLink™ Bioarray	Gene expression, SNP genotyping and pharmacogenetic profiling.	http://www.motorola.com/lifesciences
	eSensor™ DNA Detection	DNA testing, not inhibited by common components of blood, serum, plasma and urine.	
Nanogen	Nanochip® Electronic Microarray	Molecular diagnostics: SNPs, STRs, insertions, deletions and other mutation analyses.	http://www.nanogen.com

Table 2.1. Companies participating in the market of biochips/lab-on-a-chip for genomic and proteomic applications (Continued)

(Table 2.1 continued)

Companies	Products	Descriptions	Homepage
Protein microarray systems			
Aclara Bioscience	eTag™ reporter	Solution-based antibody assay, profile 18 proteins I solution with eTag reporters, highly sensitive	http://www.aclara.com
Affymetrix	GeneChip® expression arrays	Qualitatively and quantitatively measure gene expression levels in a number of biologically relevant organisms.	http://www.affymetrix.com/index.affx
Ciphergen Biosystems	ProteinChip® Systems	Detect and accurately calculate the mass of compounds ranging from small molecules and peptides of less than 1000 Da up to proteins of 500 kDa or more based on measured time-of-flight.	http://www.ciphergen.com/
Zyomyx	Biochip™ System	Conduct simultaneous measurement of many proteins from very small samples of complex biological mixtures, such as serum or cell lysates.	http://www.zyomyx.com
Others			
Illumina	Oligator™ platform	DNA synthesis	http://www.illumina.com
	BeadArray™ technology platform	SNP Genotyping	
Molecular Staging	RCAT™ technology	Antibody based microarray, profile 136 cytokines, highly sensitive	http://www.molecularstaging.com/

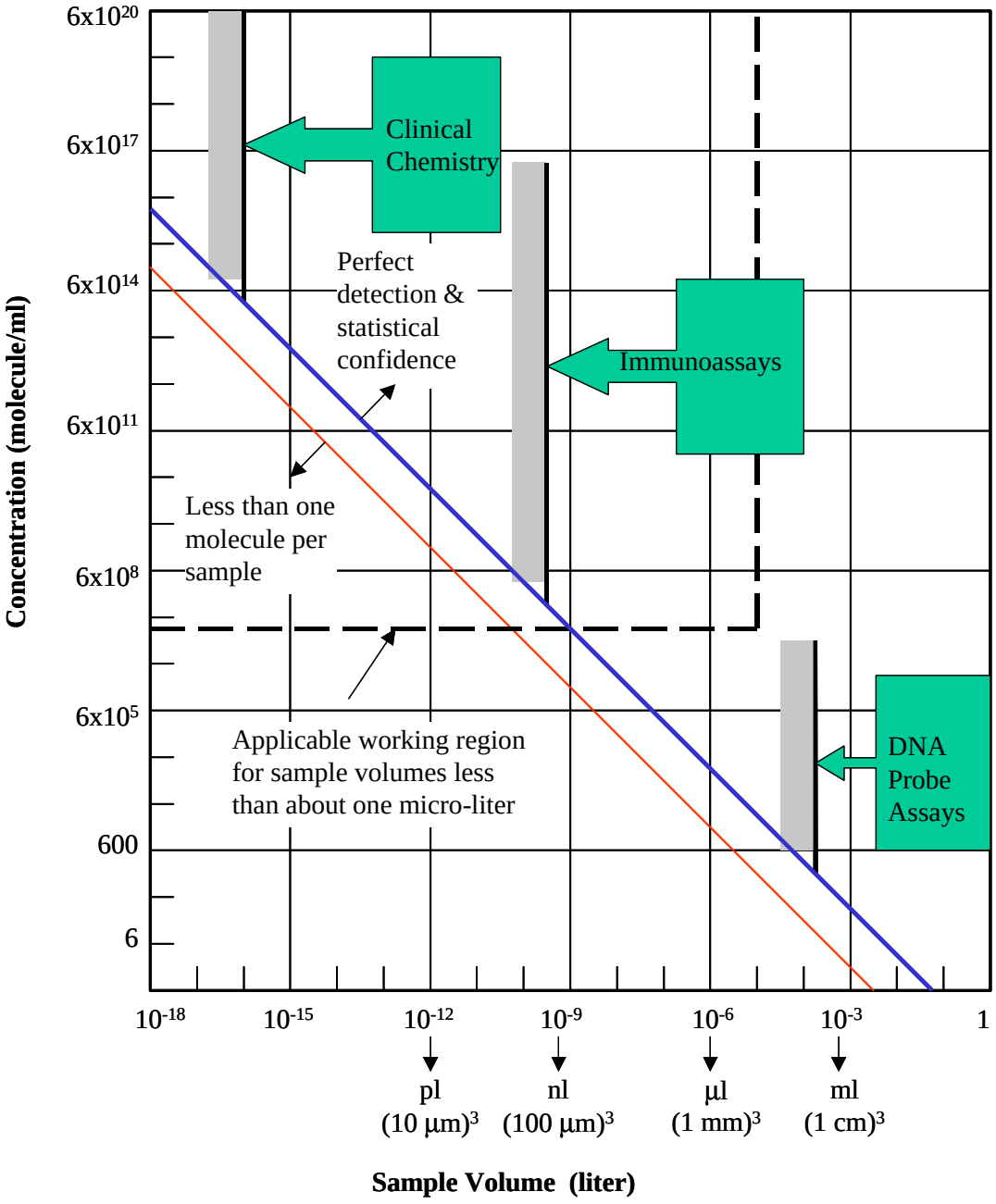

Figure 2.7 Concentration vs. sample volume graph (Petersen [2001] with permission from the author).

2.2.2 Length

Mixing is a process normally necessary during sample preparation in microfluidic devices for biological analysis and separations. Because of the dimension of micron-sized flow channels, the Reynolds number of fluid flow in the microfluidic systems is extremely small (usually less than 1). The lack of turbulent flow makes the mixing in microdevices a very challenging issue. Molecular diffusion is the main driving force in micro-mixing due to the nature of laminar flow. The characteristic time required for a molecule to diffuse through a distance L is give by the relation

$$t = \frac{L^2}{2D} \tag{2.4}$$

where D is the diffusivity of the molecule. For example, a moderately sized DNA molecule ($D \sim 10^{-6}$ cm^2/s) would require a few hours to diffuse in a 1 mm wide channel. If the width of the channel is reduced to 50 μm, the required diffusion time is about several seconds. Therefore, it is generally considered that the optimal dimension of microfluidic-channels in BioMEMS application is between 10 μm to 100 μm [Bousse et al., 2000]. Above that, mixing is too slow or additional mixing devices are required. Below that range, the detection will be difficult. For example, a microchannel with a dimension of 50 μm × 50 μm × 1mm contains only 2.5 nl sample, which may not have sufficient molecules for detection or for amplification.

In addition, the shear rate (dU/dr) in the microchannel is extremely high (usually large than 1000 s^{-1}). In very small channel, the shear rate could reach 10^6 s^{-1}. Such high shear rate may damage the biomolecules flowing inside the channel.

2.3 Microfluidic functions

The major technical challenges in making a miniature biomedical instrument include: design and implementation of necessary microfluidic functions; integration of these functions with complete automation; and development of cost-effective manufacturing technology [Madou 1997]. Microfluidics is the manipulation of fluids in channels, with at least two dimensions in the micron scale. Microfluidics is a core technology in a number of miniaturized systems developed for chemical, biological, and medical applications [Freemantle, 1999].

Major microfluidic components include sample introduction or loading (and in some cases, sample preparation); propulsion of fluids (such as samples to be analyzed, reagents, and wash and calibration fluids) through micron-sized channels; valving; fluid mixing and isolation as desired; small volume sample metering; sample splitting and washing; and temperature control of the fluids. A wide range of microfluidic components such as pumps, valves, mixers, and flow sensors has been demonstrated [Gravesen et al., 1993]. The main challenge in making miniaturized systems is the integration of different microfluidic components to perform certain functions at high speed and high throughput.

2.3.1 Pumping

Various microfluidic propulsion technologies have been reviewed and compared by Madou et al. [1998, 2000] with regard to the choice of materials, the maturity of the technology, and the achievable volumetric flow rates. In general, the fluid propulsion can be generated mechanically, electrically, or thermally. In the pressure-based approach, a mechanical pump is often used to provide the driving pressure. The pump can be as

simple as a roller in the blister pouch design [Madou and Kellogg, 1998; Findlay et al. 1993] or as complicated as a miniaturized syringe or acoustic pump [Madou and Kellogg, 1998; Moroney et al., 1990]. The former is simple, low cost, and readily available, however, there is little opportunity of it for further miniaturization or for high throughput tests. The latter is costly and the choice of materials is limited to piezoelectrics for acoustic pumping. Pressure-based propulsion does have the attractive feature of being generic for the kinds of fluids that can be pumped. Syringe pumps and silcon or plastic diaphragm pumps with piezoelectric activators can offer suitable low flow rates.

On the other hand, electrokinetic techniques such as electro-osmosis or electrophoresis [Effenhauser et al., 1997; Deshpande et al., 2000], electrodynamics [Jacobson et al., 1994], and electrowetting [Colgate and Matsumoto, 1990] have the advantages that they scale favorably for miniaturization. Eelectrokinetic pumping has been established as the method of choice for transporting and separating liquid samples in microchannels. In electro-osmosis or electrophoresis, the driving forces for flow are generated by the interaction of applied electric fields with ionic species in the fluids. In electrodynamics, the flow is generated by the interaction of electric fields with induced electric charges in the fluids. Electrowetting is based on the principle that the contact angle between a liquid and a solid surface can be changed through the application of an electrical potential. This change may result in capillary forces that provide a driving pressure in a small flow channel. An advantage of electrokinetic techniques over mechanical pumping is that electroosmotic flow is plug flow, and it will cause less dispersion than the parabolic flow in the traditional pressure-driven system [Paul et al., 1998]. Electroosmotic flow can be quite significant, reaching velocities of around 5

cm/min. However, they need high electric fields and depend strongly on the properties of fluids to be pumped (such as pH or charges). Many organic compounds and solvents may not be able to meet the charge and pH requirements [Zheng and Dasgupta, 1994]. Moreover, the on-chip electrophoresis systems must be made in an insulating substrate in order to avoid electrical breakdown [Bousse et al., 2000].

Thermal methods can also be used for fluid propulsion. Sammarco and Burns [1999] manipulated the contact angle between a liquid and a solid surface by changing the local fluid temperature. The resulting capillary force is used to drive the fluid as in electrowetting. In the case of phase-change pumping [Jun and Kim, 1998], the driving pressure arises from the volume change due to the phase change from liquid to gas, as the liquid is heated. Considering the high heat exchange rate in small channels, this mechanism scales well down to the micro-domain. Thermal methods are still in the early research stage and they require careful control of the local temperature. By contrast, in centrifugal pumping, fluid propulsion is achieved through rotationally induced hydrostatic pressure. It is simple, uses a single low-cost motor, and is capable of fine flow control through proper design of the location, dimensions and geometry of channels and reservoirs based on fluid properties. It can also be easily integrated with the information-carrying capacity of the CD.

2.3.2 Valving

Another essential component in the microfluidic system is the ability to stop and start the fluid flow. Different designs use different methods of actuation, such as magnetic, pneumatic, hydraulic or thermal-electric. The majority of micro-valves consists

of a diaphragm [Sammarco and Burns, 1999; Kaetsu et al., 1999; Liu et al., 2000; Cao et al., 2001] that is actuated externally to open or close a flow port. Conventional diaphragm valves can fulfill the valving task, but they usually require moving parts and an external actuation mechanism such as a change in temperature, pH or charge. Controlling the liquid flow electro-kinetically has been recently demonstrated [Jacobson et al., 1999]. This method, however, requires a high electric field, is sensitive to the properties of the fluids, and may lead to the occurrence of Joule heating. In order to improve the performance of a single valve, an array of micro-valves has been developed for a linear and more flexible control of the flow [Bousse L., et al, 1996; Wroblewski et al., 1998]. An alternative approach is to use a passive capillary-valve that relies on the capillary force to stop the flow in micro-channels. The principle of operation is based on a pressure barrier that develops when the cross-section of the capillary expands abruptly. Capillary valving has the advantage of not requiring any moving parts and external actuation. Recently, this type of valve has attracted a great deal of attention and has a strong appeal for applications in various microfluidic systems [Zeng et al., 2000; Duffy et al., 1999; Madou et al., 1998, 2000].

2.3.3 Micromixing

Mixing of liquids inside microchannels has received increasing attention in recent years. It is a process normally necessary during sample preparation in microfluidic devices for biological analysis and separations. Because of the dimension of micron-sized flow channels, the Reynolds number of fluid flow in the microfluidic systems is extremely small (usually less than 1). The lack of turbulent flow makes the mixing in microdevices

a very challenging issue. Molecular diffusion is the main driving force in micro-mixing due to the nature of laminar flow. For example, a moderately sized DNA molecule (D ~ 10^{-6} cm^2/s) would require a few hours to diffuse in a 1 mm wide channel. If the width of the channel reduced to 50 μm, the required diffusion time is about several seconds.

Design of micromixers is generally based on increasing the contacting time, enlarging the contact area, and creating more chaotic flows. Several miniaturized mixers have been developed. The most common method is based on increasing the contact surface between two fluids. The enlargement of the contact surfaces can be achieved in many different ways. Static-type micromixers (i.e., no moving parts) based on the concept of lamination or separation-reunification have been developed and studied [Bertsch et al., 2001; Branebjerg et al., 1996; Koch et al., 1998; Hinsmann et al., 2001; Schwesinger et al., 1996, He et al., 2001]. A similar approach is to divide each flow into several partial flows in order to increase the contact surface. Injecting one liquid into another liquid with microplumes can also achieve the same goal [Koch et al., 1998, Elwenspoek et al., 1994]. The basic principle of these micromixers is to divide and rearrange the fluid streams to decrease the diffusion distance required for mixing. Some of the static micromixer designs can be complicated, e.g. the lamination type where very precise alignment is required [Woias et al., 2000]. Numerical simulations of these micromixers by using the computational fluid dynamics program have also been applied to evaluate the mixing efficiency of micromixers [Bertsch et al., 2001; Hinsmann et al., 2001; Ehlers et al., 2000].

A chaotic flow field can be generated with two pumps connected via source and sink to a mixing chamber [Evans et al., 1997]. This design employs chaotic advection for

mixing. It is more efficient than static mixers, but requires expensive instrumentation. In electro-kinetic based microfluidic systems, convective mixing can be achieved by inducing surface charges at the interface of liquid samples that have different conductivities [Choi and Ahn, 2000]. The surface charges react with the applied electric fields to generate electric shear forces. The separate flow streams mix when passing the electrodes. Successful mixing results have been demonstrated. Lee et al. [2001] have applied unsteady pressure perturbations superposed to a mean stream to achieve chaotic-like mixing in microchannels and use time-dependent dielectrophoretic forces to induce folding and stretching for micromixing. One can also place a solid post in the middle of the micro-flow channel. By applying one electric field to the surface of the channel wall and an opposite electric field to the surface of the post, convective mixing can be achieved when the fluids pass the post [Brahmasandra, 2001]. In addition, the composite drop may be moved to create recirculating streamline to facilitate convective transport of species through the drop [Anderson et al., 1998]. However, this kind of mixer depends on the physiochemical properties of fluids and therefore limits its general applications.

2.3.4 Sampling/Metering

Delivery of precisely metered fluids from one reservoir to another in a well-controlled sequence is important in many microfluidic applications. Several methods have been developed for this purpose. An on-chip technique to meter discrete nanoliter-sized liquid drops inside microchannels was developed, using a combination of a hydrophobic surface treatment and air pressure [Handique et al., 2000]. This technique involves spontaneously filling the microchannel up to a hydrophobic stop and splitting a

liquid drop by injecting air through a hydrophobic side channel as shown in Figure 2.8. Accurate liquid volumes, ranging from 0.5 to 125 nl, were metered using this technique. Another method is to draw a liquid sample from a larger reservoir to a number of smaller capillaries and let the excess liquid flow into an overflow chamber. The capillaries containing metered liquid samples can then be released in sequential order by capillary valving [Madou and Kellogg, 1998]. Two-phase flow in microchannels with a constriction has also been applied to sample metering in microfluidic system [Madou et al., 2001] because a fixed amount of liquid is trapped between two bubbles that are snapped-off.

2.4 Polymer-based microfabrication

2.4.1 Materials commonly used in BioMEMS applications

Silicon, glass, and polymer materials are the most common materials used in different BioMEMS applications. The comparison of these three kinds of materials in their properties important to BioMEMS applications is summarized in Table 2.2.

2.4.1.1 Silicon

The *advantages* of using silicon are: (a) there are available microfabrication methods (lithography, etching) that have been extensively developed fro the microelectronics industry over the last four decades. (b) They have the high thermal conductivity, which suitable for application involving with heat transfer (e.g., PCR). (c)

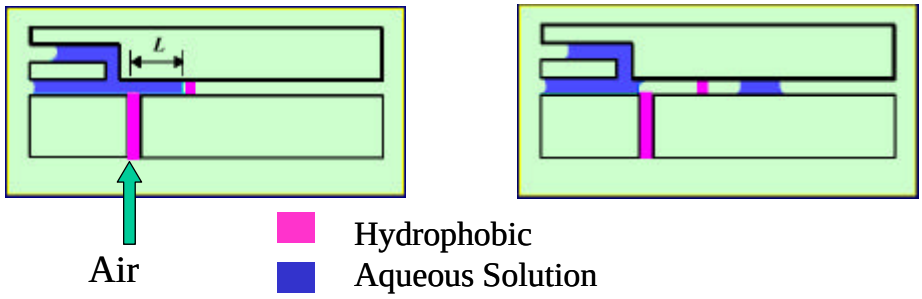

Figure 2.8. Schematic of capillary metering by using hydrophobic stop [Handique et al., 2000].

Materials	Silicon	Glass	Polymers
Cost of row materials	Expensive (~ 1 dollar/cm^2)	Less expensive (20~40 cents/cm^2)	Cheap (~1 cent/cm^2)
Ease in fabrication	Available in IC industry, involved series of processes and chemicals	Geometry limitation due to the isotropicity (shallow, semicircular cross-section)	High processibililty
Mass production	Yes, slow process, high cost	Yes, slow process, high cost	Yes (not well-developed), fast process, low cost
Optical	Opaque	Transparent	Transparent, may absorb the ultraviolet light
Thermal conductivity	1.4 W/mK	~ 1 W/mK	~ 0.1 W/mK
Biocompatibility	Usually need surface modification	OK	Depends on polymers and applications
High temperature sterilization	OK	OK	Tend to deform
Electric conductive	Semiconductor	Electric insulator	Electric insulator

Table 2.2. Summary of the commonly used materials in BioMEMS.

They can endure high temperature, which is suitable for application with high temperature sterilization.

The *disadvantages* of using silicon are: (a) the cost of row materials is expensive, about ~1 dollar/cm^2 for single crystal silicon. (b) Fabrication process has to go through a series of steps (cleaning, resist coating, photolithography, development, and wet etching), which has long fabrication time, the risk of low yield, and therefore raises costs. In addition, lots of harmful chemicals (solvents, KOH, or HF) are usually involved during the process. Any residual chemicals on the devices may be dangerous for later application. The process costs are also largely due to the chemical reagents involved as well as their waste disposal. (d) Geometries of the cross section of microchannels and the aspect ratio (height vs. width) are limited due to the isotropicity. It could be enhanced by the advanced silicon dry etch processes (DRIE). (e) Silicon is opaque, which posts problems for any optical-based detection. (f) The semi-conductivity of silicon (semiconductors) may cause problem in the commonly used electroosmosis pumping (electrical breakdown). (g) Silicon is hydrophobic and biomolecules (oligonucleotides, DNA, or proteins) tend to stick to silicon surfaces.

2.4.1.2 Glass

The *advantages* of using glass are: (a) fabrication techniques are available in IC industry. (b) Glass has good heat conduction ability for application involved with heat transfer (e.g., PCR). (c) Glass (electric insulator) has proved to be a better substrate than silicon for applications involved in high electric field (electroosmosis). (d) Glass is transparent and does not absorb any light, which is perfect material for optical-based

detection and flow visualization. (e) Glass can endure high temperature sterilization. (f). Glass is good biocompatible material.

The *disadvantages* of using glass are: (a) same as silicon, the fabrication process of glass involves a series of steps and various chemicals, which lengthen the fabrication time and increase the cost. (b) Compared to polymer materials, the row material cost of glass is still expensive. (c). Geometries of the fabricated channel (usually shallow, semicircular cross-section) and the aspect ratio (usually < 1) are limited. (e) Glass is brittle and has low impact strength. (f) The negative charged surface of glass posts problems for the electrophoresis applications.

2.4.1.3 Polymers

The *advantages* of using polymers are: (a) the row material cost of polymers is much cheaper than silicon and glass. (b) Polymers have high processibility and are possible mass production in a very fast manner (e.g., several seconds a piece in injection molding). (c) The high cost mold insert only needs to be fabrication once. The mold insert can replicate thousands of pieces. This will lower the fabrication cost. (d) Some polymers are transparent and suitable for optical-based detection and flow visualization. (e) Polymers can provide variety of materials choice with various phyiso-chemical properties to meet different applications. (f) Polymers are good materials for electrophoresis applications.

The *disadvantages* of using polymers are: (a) various mass replication methods (casting, injection molding, embossing) are available but not well developed. (b) Polymers has low thermal conductivity, therefore, may not be suitable for applications

involved with heat transfer (e.g., PCR). (c) Most of the polymers are not thermal stable. At high temperature, polymers tend to deform due to the residual molding stress. (d) Most polymers have strong adsorption of lights at certain wavelengths. Careful screens are necessary for absorbance detections.

The basic principle of polymer-based microfabrication protocol is the replication of a microfabrication mold insert or master, which has the negative structure of the desired microfluidic structure. Therefore, the expensive microfabrication process is necessary only once for producing the mold insert. A good recent review paper on polymer-based microfabrication, including a section on polymer bonding, is by Becker and Gartner [2000].

2.4.2 Prototyping

For testing the design concept of microfludic devices, low-cost prototyping techniques are highly desirable. If the feature size is larger than 50 μm or different feature depths are required, computer numerically controlled (CNC) milling can easily be used to mechanically manufacture the device. CNC machining does not provide a smooth surface finish (surface roughness around several μm), a high aspect ratio (height vs. width ratio is limited to less than 2), or good dimension control (often 10% large than design). It does, however, have no material limitations, and various metals, glass, and plastics can all be used. For feature sizes smaller than 50 μm (but larger than several micrometers), micromilling or laser ablation can either be used alone or in conjunction with CNC machining for prototyping fabrication.

Laser ablation is also widely used in fabrication of microfluidic devices on polymeric materials [Pethig et al., 1998; Schwarz et al., 1998]. In this process, the laser energy is used to remove the polymer material from the ablation region. Depending on the energy available per laser pulse and substrate materials, typical ablation rates per laser pulse range between hundreds of nanometers to 5 μm [Schwarz et al., 1998]. The accuracy of laser ablation in the x-y direction is typically on the order of a few microns and the depth control is on the order of 0.1 micron. Laser ablation offers a high degree of geometrical freedom and it has large materials choices. A wide range of materials, such as PMMA, PS, PC, PET, cellulose acetate, polyimide, and photoresists, has been structured [Becker and Gartner, 2000]. However, laser ablation is a time consuming process and its high energy tends to melt the plastic channel wall, and therefore, causes rough surfaces.

2.4.3 Mass production

All of these prototyping fabrication processes are labor intensive and slow, and it typically takes hours or even more to produce a single device. Therefore, they are expensive manufacturing processes and may be only suitable during the trial and error of microfluidic pattern design stage. Polymer replication, on the other hand, enables high-volume production of low-cost disposable microfluidic devices. Mass production of polymer-based microdevices typically involves three steps: pattern defining, mold insert or master fabrication, and polymer replication. Figure 2.9 shows the typical protocol for polymer-based microfabrication.

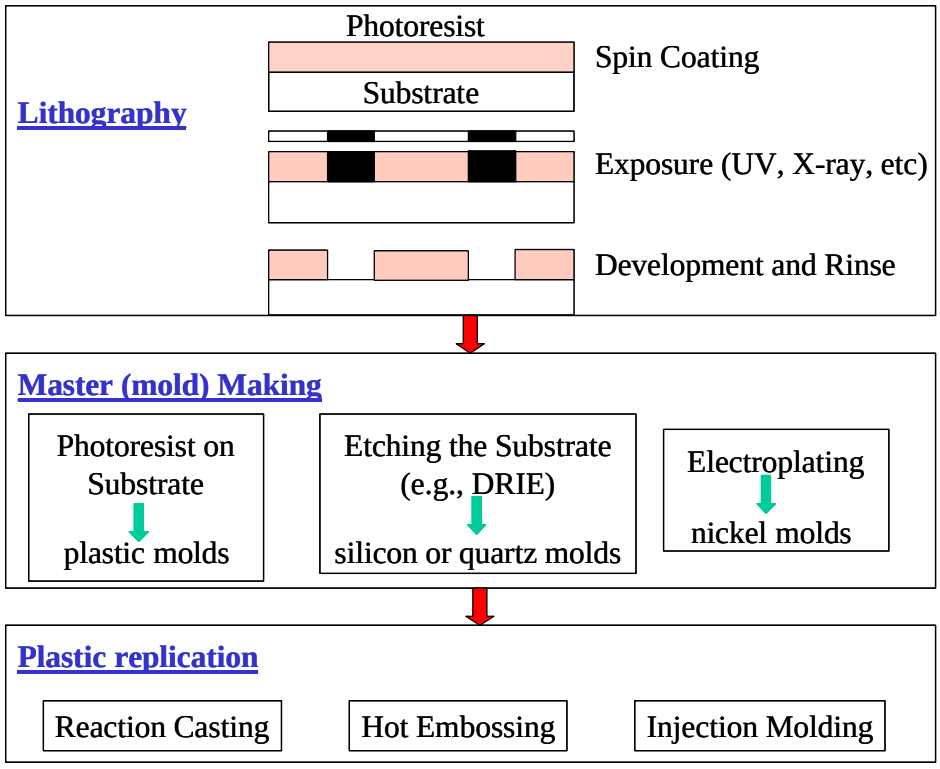

Figure 2.9. Protocal for polymer-based microfabrication.

2.4.3.1 Scale limitation of lithography

Microfabrication techniques for BioMEMS include the "top-down" strategy (lithography) and "button-up" strategy (self-assembly). The self-assembly approach is still in reaching stage and not ready for mass production. The lithography approach for BioMEMS, which is adopted from the traditional semiconductor industry for producing the integrated circuit, is a mature technique for mass production of microdevices on silicon/glass materials. The downscaling limitations have already been identified both in terms of fundamental limits in physics and in manufacturing. According to the International Technology Roadmap for Semiconductors (ITRS), the conventional (refractive) optical lithography currently (year 2002) sustains the 0.13 μm technologies. Technologies of 0.11 μm will be available for mass production in 2003. Significant issues arise in terms of availability of the light sources and the need for new photoresist materials. A number of candidates for next generation lithographies have been proposed which include extreme UV lithography (EUV), Electro-projection lithography (EPL), electro-beam direct-write (EBDW), and proximity X-ray lithograpy (PXL). The scale projections of the minimum feature size (MFS) are shown in Figure 2.10.

2.4.3.2 Pattern defining

Typically photolithography is applied to define the designed microfluidic pattern on a flat material (substrate) such as silicon wafer, glass, or plastic sheet for further

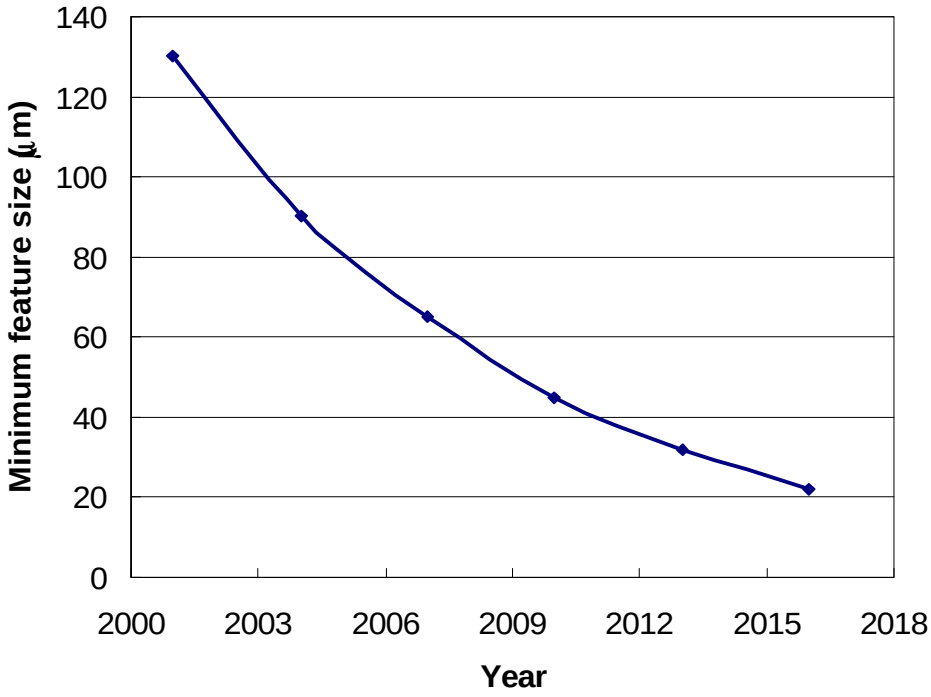

Figure 2.10. Scaling projection of the minimum feature size (MFS) of lithography technology [Source: ITRS Roadmap, 2001].

process. Photolithography is the photochemical process of transferring designed pattern on a mask to the substrate surface. A mask with designed microfluidic pattern is firstly produced. This will typically be a chromium pattern on a glass plate. Recently a low-cost transparency mask has been applied by printing out the designed microfluidic pattern on transparent polymer film through high-resolution (usually larger than 3000 dpi) image setting system [Xia and Whitesides, 1998]. The latter is much cheaper than the former, several dollars vs. several hundreds dollars. However, the pattern on transparent mask has to be larger than 20 microns, limited by the resolution of the image setting system. In addition, the pattern produced through the transparency mask has much rougher edges than the chromium mask [Lee et al, 2001]. The process of photolithography usually involves several steps: substrate cleaning, photoresist application, soft baking, mask alignment, exposure and development, and hard baking.

2.4.3.3 Master making

The mold inserts (or masters) can be fabricated by a variety of techniques [Madou 1997]. For large features (>50 μm) with tolerances and repeatability in the range of about 10 μm, traditional CNC-machining of materials like tool steel and stainless steel are often accurate enough. The advantage of this technique is that materials used are the same as those in conventional polymer molding, so their design, strength, and service life are well established. Complicated 3D structures can also be easily machined. The main drawbacks are that it is difficult to make sharp corners or right angles, and the surface quality is usually poor. Diamond-based micromilling or microdrilling [Warrington, 1998], and excimer or femtosecond laser-based [Momma et al., 1997] direct removal processes can

reduce the surface roughness to 1 μm or less [Robert et al., 1997]. While diamond-based methods can also make features smaller than 10 μm, they are only applicable to 'soft' metals such as nickel, aluminum, and copper. For smaller feature sizes (down to sub-micron), LIGA (German acronym for X-ray lithographie-lithography, galvanoformung-electroplating, abformung-molding) [Becker et al., 1986] and LIGA-like methods (e.g., UV-LIGA, Laser-LIGA) have to be employed [Madou, 1997].

Patterned thick photoresists (e.g., SU-8) by photolithography can be used as mold inserts for small quantity production and low-pressure processes (e.g., reaction casting) since the photoresist usually cannot survive long through the polymer replication processing conditions.

Silicon wafers or quartzes fabricated through bulk machining (wet etching and dry etching.) can also be utilized directly as a mold insert for small quantity production. A wet etched <100> silicon wafer has a wall angle of 54.7^0 due to the orientation of the silicon crystal. Therefore, a trapezoidal channel is formed which will facilitate the mold release. If high aspect ratio and vertical sidewall are necessary in an application, dry etching methods (e.g., Bosch-processed deep reactive ion etching) are available. The roughness of the bulk machined silicon mold largely depends on the etching rate. The faster the etching process, the rougher the surface produced. However, silicon mold inserts are often too brittle to endure very high molding pressure; therefore, one improvement is to anodically bond the silicon wafer to a thick glass support.

Metal is the ideal mold insert material for plastic replication due to its high mechanical and thermal strength. LIGA technique can produce features with small sizes and high aspect ratio. The LIGA process uses synchrotron radiation to create a pattern in

an x-ray resist, usually polymethyl methacrylate (PMMA). It is ideally suited for making parts with depths significantly greater than nominal lateral dimensions and parts that require a particularly smooth or straight sidewall. Electrodepostion is then used to produce mold inserts made of ‘soft’ metals like nickel. Before lithography, if the substrate is not conductive, a seed layer (e.g., gold or titanium) is necessary to put on the substrate through vapor deposition or sputtering. After the deposition of the metal in the electroplating bath, the substrate and the photoresist are dissolved to release the metal mold. Nickel mold inserts with good surface and high aspect ratio vertical structures have been fabricated by this method. Given the cost of the LIGA equipment, various LIGA-like processes (such as UV-LIGA, Laser-LIGA etc.) took center stage. These methods involve transferring designed patterns by alternate lithography means such as laser ablation (Laser-LIGA) or UV lithography (UV-LIGA) of thick photoresist (such as SU-8 100).

2.4.3.4 Polymer replication

Various approaches have been tried to replicate the micro-machined features on polymers. Reaction casting, hot embossing, and injections molding are the successful methods to produce polymeric microdevices.

2.4.3.4.1 Reaction casting

Micromolding based on low viscosity liquid resins (instead of high viscosity polymer melts) is a very attractive approach, since mold inserts made by photolithography techniques are limited to soft metals (e.g., nickel), silicon, quartz, and

plastics. During liquid resin molding, the low viscosity reactive polymer components are mixed shortly before injection into the mold cavity, and polymerization takes place during the molding process. Both reaction injection molding (RIM) and transfer molding, two techniques widely used in conventional processing of thermoset resins, are options for mass production [Lee et al., 2001]. For new design of microfluidic devices, casting is an attractive method for rapid prototyping. Whitesides and his group at Harvard University [Qin et al., 1998; Xia and Whitesides, 1998] combined a photolithography technique with PDMS molding for microfabrication. The PDMS resin was cast onto a photoresist mold produced by photolithography on a silicon wafer and cured at elevated temperatures. The polymer replica of the master containing a negative relief of features could be easily peeled away from the silicon wafer and either used as the microdevice directly [Xia et al., 1996, 1997], or as a master for micro-contact printing [Xia et al., 1996], micromolding in capillaries [Xia et al., 1998], or micro-transfer molding [Kim et al., 1995]. This method, called soft lithography, has also been used by other researchers [Effenhauser et al., 1997] because of its simplicity. The long cycle time (several hours) and limitation to only PDMS rubber, however, make it difficult to use for mass production in most large scale BioMEMS applications.

2.4.3.4.2 Injection molding

Injection molding is based on heating a thermoplastic material until it melts, thermostatting the parts of the mold, injecting the melt with a controlled injection pressure into the mold cavity, and cooling the molded polymer. Injection molding is probably the most widely used technique in macroscopic production of polymer parts.

Injection molding of parts with small features and low-aspect ratios (like CDs) has been widely applied. Currently, the main challenge is to extend this technique to the fabrication of components with a smaller feature size but larger aspect ratio, needed in many medical and bio-chemical applications. In recent years, some research work has been initiated in Europe. Ehrfeld and his co-workers at the IMM (Institut fur Mikrotechnik) in Mainz, Germany [Dunke et al.,1995; Ehrfeld et al., 1995], used precision injection molding machines, similar to those commonly used for the fabrication of CDs, to mold MEMS-components based on mold inserts made by LIGA. Another group at the Institut fur Materailforschung in Karlsruhe, Germany [Fahrenberg et al, 1995; Ruprecht et al., 1995; Goll et al., 1997; Piotter et al., 1997 & 1999], used CNC-machined and laser ablated metal molds in microinjection molding. Wimberger-Friedl in the Netherlands [1999] fabricated sub- m grating optical elements by injection molding. The mold inserts were made by E-beam lithography together with nickel electroplating, and by RIE in SiO_2 (fused quartz). In the United States, Edwards et al. [2000] used SU-8 molds and Kelly [1999] used LIGA-produced nickel molds for injection molding to make devices such as micro heat exchangers. In general, these studies showed that the molds need to fill rapidly in order to prevent early freezing. A mold temperature above the 'no-flow' temperature can guarantee a complete filling. Shape deviation and damage of the fragile mold walls occur quite easily, possibly due to shrinkage of the polymer or defective filling and release. Since the mold cavity is filled at a mold temperature that exceeds the melting point or the glass transition temperature T_g of the polymer, the mold needs to be cooled down to obtain a sufficient strength before part ejection. In addition, conventional venting of the cavity is not feasible due to the presence of microfeatures in

the mold inserts. Therefore, prior evacuation of the mold cavity is needed. As a result, the cycle time is five minutes or longer, including the time needed for evacuation, heating and cooling of the mold. Molding of microfeatures with large aspect ratios or the use of materials with a higher viscosity leads to even longer cycle times.

2.4.3.4.3 Hot embossing

Hot embossing (or relief imprinting) [Ramos et al., 1996; Becker et al., 1999] provides several advantages compared to injection molding, such as relatively low costs for embossing tools, a simple process, and a high replication accuracy for small features. The basic principle of embossing is that the polymer substrate is first heated above its glass transition temperature, T_g (or softening temperature). A mold (or master) is then pressed against the substrate, fully transferring the pattern onto it (embossing). After a certain time of contact between the mold and the substrate, the system is cooled down below T_g (or softening temperature), followed by separating the mold and the substrate (de-embossing). Replication of micro- and nano-size structures has been successfully achieved [Becker et al., 1999; Kopp et al., 1997; Chou et al., Schift et al., 1999; Jaszewski et al., 1998; Casey et al., 1997 &1999; Gottschalch et al., 1999]. Adding an anti-adhesive film to reduce the interaction between the mold and the replica during embossing has also been studied [Jaszewski et al., 1997 & 1999]. Instead of the conventional nickel molds, the possibility of using silicon molds has been demonstrated due to their excellent surface quality and easy mold release [Becker and Heim, 1999; Lin et al., 1996]. Also, the use of a plastic mold in the embossing process was recently illustrated [Casey et al., 1999]. This can be achieved in either a cyclic or continuous

process [Lee et al., 2001]. In a cyclic process, a metal master is placed in a hydraulic press. A heated polymer sheet is stamped by applying the appropriate force, thus replicating the structure from the master to the polymer. This constitutes a low-cost method for making prototypes. For mass production, a continuous process is preferred. A polymer sheet stretches through a temperature chamber and several masters, mounted on a conveyor belt to continuously produce parts. The process also may incorporate a lamination station to enclose certain features.

Processing parameters include thermal cycle, compression force and compression speed. The temperature difference between embossing and de-embossing determines the thermal cycle time, typically from 25°C to 40°C. In principle one could, after hot embossing, cool down the whole device to room temperature before de-embossing or, at the other extreme, one could de-emboss just below or at the glass-transition temperature. A compromise is needed: the quality of the replication may not be good if one tries to remove the master when the polymer is still soft, while cooling all the way down to room-temperature takes too long. A narrower small temperature cycle leads to smaller induced thermal stresses. Such a narrower temperature cycle also reduces replication errors due to different thermal expansion coefficients of the tool and substrate. By actively heating and cooling the upper and lower bosses, a cycle time of about 5 minutes can be achieved.

Lee and coworkers [Lee et al., 2001] have summarized the advantages and disadvantages of these three molding methods from various aspects as shown in Table 2.3.

	Liquid Resin Molding	Injection Molding	Hot Embossing
Mold Inserts	Any molds	Metal molds (Silicon molds suitable for prototyping)	Metal and silicon molds (Plastic molds suitable for prototyping)
Feature Size	No limit	Good for small features with low aspect ratio, or large features with high aspect ratio Good for 3D features	Good for small features Difficult for high aspect ratios Difficult for multiple depth Planar features only
Materials	Liquid resins (thermosets provide high chemical resistance)	Mainly low molecular weight thermoplastics	Low and high molecular weight thermoplastics
Processing	Simple (except for RIM) Easy mold filling Closed mold process Long cycle time (hr) Mold release problem for some resins	Short cycle time (sec ~min) Closed mold process High automation	Simple Medium cycle time (min) Potential for continuous production Open mold process
Replication Accuracy	Less dimensional control (polymerization shrinkage)	Excellent dimensional control	Less dimensional control
Part Quality	Low molded-in stresses Contamination (resin residue)	High stress on mold insert High molded-in stresses	High molded-in stresses
Cost	Low tooling cost (except for RIM) For prototyping and low volume production	High tooling cost For large volume production	Low tooling cost For low and medium volume production

Table 2.3. Comparison of Micro-molding Methods [from Lee et al., 2001].

2.5 Bonding and surface modification

After fabrication, these microfluidic devices need to be sealed in order to perform microfluidic functions. Currently packaging (i.e., bonding, surface modification, and reagent loading) is still a challenging issue in the design and fabrication of polymer-based microfluidic devices.

2.5.1 Bonding

Bonding (i.e., sealing a platform with a lid) between silicon and silicon or other materials (e.g., glass, metal, etc.) is well developed and can be achieved by different methods such as adhesive bonding, eutectic bonding, anodic bonding, and fusion bonding [Schmidt 1998]. Adhesive bonding has been in widespread use for over 30 years. Adhesives can be made electrically/thermally conducting (e.g. silver loaded epoxy) or electrically isolating. Typical adhesive materials include epoxy thermoset resins, acrylic thermoplastic resins, and silicone resins. High pressure (>1 MPa) is usually necessary for adhesive bonding. An eutectic bond is formed by heating two (or more) materials (e.g. Au and Si) in a joint such that they diffuse together to form an alloy composition that melts at a lower temperature than the base materials (e.g. a Au-Si eutectic melts at 363°C). For fusion bonding, temperatures above 1000 ^{o}C need to apply for silicon fusion bonding, while temperatures around 600 ^{o}C are necessary for glass fusion bonding. The bonding of silicon to glass (anodic bonding) is performed at a temperature ranging from 300 to 500 ^{o}C, with an applied voltage ranging from 500 to 1000 volts. These methods

usually involve high temperature, high voltage, or high pressure. Several low temperature-bonding technologies (100 ~ 200 ^{o}C) have been developed [Sayah et al., 2000]. However, they usually need assistance from hydrofluoric acid (HF), plasma, or high pressure (up to 50 MPa). Therefore, among these bonding techniques for silicon/glass materials, only adhesive bonding may be applied to polymer-based microfluidic devices.

Several techniques such as lamination (adhesive tape, thermal adhesive film), thermal (IR, hot-plate, laser) bonding, ultrasonic welding, and solvent bonding (i.e., partially dissolve the bonding surfaces, and evaporate the solvent) have been tried [Becker and Dietz, 1998; Becker and Gartner, 2000; Gandhi et al., 2000; Lee et al., 2001; Robert et al., 1997; Lum and Greenstein, 1999; Rossier et al., 1999; Dreuth and Heiden, 1998; Madou et al., 2001; Glasgow et al., 1999] on polymer-based microdevices. McCormick et al. [1999] successfully applied a thermal activated adhesive (Top flight MonoKote, Great Plane Model Distributors, Champaign, IL) to bond a Mylar sheet with an injection molded acrylic microchip for DNA separations. Rossier et al. [1999] used a 5 μm thick polyethylene adhesive layer to seal a UV laser photo-ablated polyethylene terephthalate (PET) microchannels with a PET film for electrophoretic separations. Dreuth and Heiden [1998] applied a thin adhesive film on a substrate and the adhesive was then transferred to the elevated microstructures by stamp printing. Lamination by adhesive tapes or thermal adhesive films probably is the simplest and fastest one, but at the risk of creating channels with different top and bottom surfaces. Moreover, when using the adhesive bonding method, care needs to be taken in order to prevent the adhesive from flowing into the micro channels.

2.5.1.1 Solvent bonding

A solvent can be applied to partially dissolve the bonding surfaces, and evaporating the solvent will bring two halves together. This can solve the problem with dissimilar materials as sidewalls. Lum and Greenstein [1999] prepared microdepressions on one substrate and microprojections on the other so that the substrates can be mated together to secure the relative position. A layer of monomer or pre-polymer was deposited on the microprojections before being mated and further polymerized to provide a bonding effect. Photoresist itself can also be used (e.g., SU-8 and Polyimide [Metz et al., 2001]) as a bonding agent to fabricate photoresist-based microfluidic devices. Glasgow et al. [1999] introduced a solvent bonding technique in which a layer of polyimide precursor and solvent with dissolved precursor was placed in contact with patterned structures made of uncured polyimide precursor. The two halves were then cured with weights on top of the upper plate. They found that the bond quality was affected by the vent spacing for solvent evaporation, soft-bake duration, spin-coat speed during solvent application, and the concentration of the dissolved polyimide precursor in the solvent. However, as the solvent dissolves the bonding surface, it also partially dissolves the microchannel itself. Dimension control becomes quite difficult for very tiny channels. In addition, thermoset plastics or dissimilar materials cannot be effectively jointed by solvent bonding. Stress cracking of components occurs more likely in this method than other bonding methods. Furthermore, the use of solvents in a production line becomes more problematic, as environmental regulation and operator safety become prime issues for manufacturers throughout the world.

2.5.1.2 Ultrasonic welding

Ultrasonic welding is also a widely used welding method for joining plastic materials together due to its simplicity of use and rapid joining potential. In ultrasonic welding, high frequent ultrasonic energy is applied to produce mechanical vibration. Usually horns and traps need to be fabricated around the designed joint area. The material at the joint surface (horn) melts resulting from the heat generated due to the mechanical vibration. Traps are used to prevent molten plastic material flowing the designed joint area. This can pose problem for boding of microfluidic device with very tiny channels (e.g., less than a hundred microns) because it would be difficult to fabricate even smaller horns and traps around the microchannels. This process can be done in a very fast manner (e.g., several seconds) depending on substrate materials, joint design, and the ultrasonic energy applied. However, the ultrasonic welding limits to thermoplastic materials with similar melting point. In addition, significant investment of capital equipment is necessary.

In general, these bonding techniques alter the surface of the microdevices by using external forces (e.g. solvent, adhesive, ultrasonic, laser) and applying pressure to bring two halves together. However, the same driving force that allows the bonding also tends to deform the channel shape. Therefore, these methods have problems with either blocking the microchannels or changing their dimensions and are mainly applicable for relatively large microchannels (several hundreds of microns to millimeters).

2.5.2 Surface modification

Many microfluidic devices have been fabricated for the biomedical applications, such as biosensors [Zhang et al., 1998], clinic diagnostics, DNA/RNA analysis systems, bioseparation nanofilters, drug delivery, and tissue engineering. In most of these applications, the microfabricated devices are introduced into contact with biological fluids, or tissues. When any foreign material is brought into contacting biological environment, one common phenomenon is the accumulation and adhesion of biological materials on the contacting interface. This uncontrolled accumulation of biological material on the surface of devices may cause adverse biological reaction in the living host system such as fibrous encapsulation [Kingshott et al., 1999]. For instance, the cell adhesion to an implant surface can lead to collagen deposition and subsequent walling of the capsule implant by disposition of a fibrous layer [Zhang et al., 2001]. This problem is generally referred as bioincompatibility [Alcantar 2001]. Biocompatibility is a fundamental characteristic that makes a substance very well tolerated in biological environment so as not to interfere with normal bodily functions. The term 'biocompatible surfaces' is used to define surfaces that are introduced in the human body without causing any allergic or rejective reactions. A truly generally biocompatible material will show absolutely no reactivity and no cell toxicity. For example, blood-compatible materials are required to eliminate, or largely reduce, the adsorption of blood proteins, to avoid surface-induced thrombosis.

In the molecular level, the bio-adhesion all begins with the rapid adsorption of proteins to the device surface therefore makes the surface for the subsequent adhesion of other molecules and cells. For example, blood thrombosis starts with deposition and

aggregation of platelets on the surface of the prosthesis [Chen and Ruckenstein, 1991]. A decrease in protein adsorption usually leads to a decrease in cellular attachment. Therefore, it is generally considered that reduction or prevention of protein adsorption is the primary objective in the design and fabrication of surfaces with resistance to bioadhesion [Kingshott et al., 1999]. To improve the biocompatibility of microdevices and to develop the substrate surfaces with reduced protein adsorption and cell adherence is one of the major considerations for microfluidic devices for BioMEMS applications.

Factors that affect protein adsorption include protein concentration, surface energy/tension, surface roughness, crystallinity, surface charge, etc. The surface free energy has been considered to be the dominant factor in protein adsorption [Lyman et al., 1965]. The thermodynamic driving force for protein deposition is low if the interfacial free energy between the substrate and the bio-fluids is low enough [Chen and Ruckenstein, 1991]. It is believed that an interfacial free energy with water on the order of 1~3 mJ/m^2 could be a criterion for a material being biocompatible [Chen and Ruckenstein, 1991]. Generally, the interfacial free energy between polymeric materials and bio-fluids is too large to meet the biocompatibility criterion. Therefore, surface modification is necessary to lower the interfacial free energy to produce surfaces that are able to resist cell adhesion and protein adsorption. Surface modification is generally considered as an applicable method to improve the biocompatibility of a substrate surface through proper manner while still keeping the bulk properties intact.

In the literature, a great deal of effort has been devoted to the surface modification of biomaterials to improve their biocompatibility. Various approaches have been reported to modify the surface of biomaterials, such as physical adsorption, surface

grafting, plasma modification, etc. Hydrophobic and electrostatic interaction play important roles in protein adsorption and cell adhesion. Therefore, increased hydrophobicity and positive charge of support surface is favored by protein adsorption and cell adhesion. Prevention of cell adhesion to supports has been focused on modifying surface hydrophilicity. Hydrophilic materials such as glass are known to discourage bacterial adhesion [Bower et al., 1996]. Therefore, the materials used to coat the substrate surface usually involve a hydrophilic polymer, such as polyethylene oxide (PEO) [Prime and Whitesides, 1993; Kiss et al., 1996], polyethylene glycol (PEG) [Desai et al., 1999], poly(N,N-dimethyacrylamide), poly(vinyl alcohol), ethylene-vinyl alcohol copolymer, phospholipid, polyacrylamine, polysaccharide, poly(methyl propenoxy fluoroalkyl siloxane) and poly(perfluoroacrylate) [Tsibouklis et al., 1999 & 2000], surfactants such as sodium dodecyl sulfate (SDS) [Chen and Ruckenstein, 1991], PEO-PPO-PEO triblock copolymer (Pluronics surfactant), and other coatings. Among the wide variety of materials, PEG/PEO and PEG containing materials are wide recognized as effective coating materials due to its non-interaction nature with protein and cell. Coating surfaces with PEG-containing substances is currently one of the most promising approaches to improve the biocompatibility of foreign biomaterials. [Harris, 1992; Alcantar et al., 2001] For example, it was demonstrated both in vitro and in vivo that grafting PEG on solid surfaces limit platelet adhesion, therefore leading to reduced risk of thrombus formation, tissue damage, and other cytotoxic effects [Kaelble, 1971]. It was found that PEG-functionalization of leptosomes increases their blood circulation times by nearly an order of magnitude [Sheth, 1997]. Furthermore, no antigenic activity on PEG-modified substances was also reported [Chen and Ruckenstein, 1991; Brady, 1997; Lyman et al.,

1965]. These properties are thought to be directly related to PEG's ability to repel protein [Ruckenstein and Lee, 1987].

2.5.2.1 PEG/PEO properties.

Polyethylene glycol (PEG) is a linear or branched polymer, available in a variety of molecular weight. Its molecular structure is shown in below:

$$HO—(CH_2\text{-}CH\text{-}O)_n—CH_2\text{-}CH_2\text{-}OH \quad \text{(polyethylene glycol)}$$

PEG is also referred as polyethylene oxide (PEO). In general, PEG refers to polyols of molecular weights below about 20,000, and PEO refers to higher molecular weight polymers [Harris 1992]. The PEG commonly used in biomedical and biotechnical application has molecular weighs ranging from a few hundred to tens of thousand.

PEG is generally considered as a hydrophilic polymer due to its high solubility in aqueous solutions. This is a very unusual property of PEG because both polypropylene oxide (PPO, one more methylene group than PEG) and polymethylene oxide (one less methylene group than PEG) are hydrophobic and insoluble in water [Sheth 2000]. PEG also demonstrates some aspects of hydrophobic characters by being soluble in most of the organic solvents, forming thin monolayers at the air-water interface, and adsorbing to hydrophobic surfaces. In certain aspect, PEG can be considered as an amphiphilic molecule, such as surfactant and lipid, which have distinct hydrophilic and hydrophobic moieties.

2.5.2.2 Mechanism of protein rejection of PEG

It is well known that PEG coating has extraordinary ability to reduce or eliminate protein adsorption, and is extensively used in both fundamental research and biomedical applications [Malmsten et al., 1998]. There have been extensively theoretical and experimental studies [Griffith, 2000] over the last couple of decades regarding the molecular mechanism behind this phenomenon and different hypotheses have been suggested. It is considered that the protein rejecting properties are due to a combination of different effects such as steric repulsion, van der Waals attraction, and hydrophobic interaction between protein in solution and the PEG surface [Sheth, 2000]. The steric repulsion (where the PEG prevents the protein from reaching the substrate surface to adsorb) and lack of strong interaction between protein and PEG-coated surface are generally considered to be most important.

The major driving forces for protein adsorption are hydrophobic interactions, electrostatic interaction, and van der Waals force. Hydrophobic interactions are due to the dehydration of nonpolar components in an aqueous environment, which results in an increase of the entropy of the water molecules released from those components, and therefore, in lowering the Gibbs energy of the system. The hydrophobic interactions are considered as the primary driving force for protein adsorption and cell attachment.

In the case of PEG-covered surface, the driving force for protein adsorption is weak due to the absence of strong adsorption mechanisms. For example, the PEG-coating is uncharged and typically also masks any electrostatic effects from the underlying substrate surface, which provides little incentive for protein adsorption driven by electrostatic. Furthermore, the PEG-coated layer is hydrophilic. Therefore, the

electrostatic interaction is expected to be of minor importance for PEG-covered surface. Due to the quite dilute coverage of the PEG-coating layer, the van der Waals contribution to the attractive force was found to be smaller than the hydrophobic interaction between the protein and the hydrophobic surface, so the van der Waals interaction is expected to be weak. Consequently, it was found that the degree of protein adsorption onto hydrophobic surfaces is roughly a decimal order of magnitude greater than their adsorption onto hydrophilic surface. And protein adsorption on hydrophilic surfaces are reversible (can complete desorption with the original aqueous solvent) while protein adsorption onto hydrophobic surface is much more irreversible [van Oss, 1995]. Therefore, for a protein to be able to adsorb directly at a PEG-coated surface, it has to diffuse through the hydrophilic PEG layer to reach the hydrophobic substrate surface.

Furthermore, when a protein tries to penetrate the PEG-coating layer, a steric repulsion force is generated due to an excluded volume and the compression and desolvation. The excluded volume is an elastic response from the loss of conformation. When a protein approaches to a PEG-coated surface, the available volume for each PEG segment is reduced. Therefore, a repulsive force is developed due to the loss of conformational freedom of the PEG chains [Israelachvili et al., 1997]. The compress and desolvation of PEG are also unfavorable. The desolvation of PEG forces more water molecules near the hydrophobic surface and the compression and constrained of the stretched and mobile chains causes a decrease in entropy.

2.5.2.3 Coating methods

Various techniques have been applied to immobilize PEG/PEO to substrate surfaces, including direct adsorption of PEG in the forms of a surfactant or a block copolymer (e.g., PEO-PPO-PEO triblock copolymer), covalent grafting of PEG which has reactive chain-ends, graft copolymerization of PEG macromonomer, chemical coupling, and self-assembled monolayers (SAMs) of PEOs etc [Otsuka, 2001].

Physical adsorption of PEG directly onto a substrate surface is the simplest way to achieve a PEG coated surface. It has been demonstrated that successfully reducing protein adsorption and cell attachment can be realized on a PEG coated glass through physical adsorption. However, physical adsorption may not be the most reliable method because the physically adsorbed PEO tends to desorb when they come in contact with blood by proteins or cells with a higher affinity for the interface. Many proteins and cells in biological fluids can readily displace the adsorbed PEO from the surface. An important consideration for the protein rejecting ability of PEG-containing layers is their anchoring to the underlying surface. Particularly in the presence of large proteins, there is a possibility for interfacial exchanges, i.e., replacement of the adsorbed polymer layers by the protein. In order to avoid this detrimental effect, it is essential that the polymer layer be firmly attached. Adhesion strength for physical adsorption of PEG can be enhanced by using PEO-containing amphiphilic block copolymers, such as Pluronics surfactants (BASF Co.) [Green et al., 1998], which are commercially available amphiphilic ABA block copolymer made up of a central PPO chain with a PEO chain attached at each end. The use of PEO-containing copolymers has advantages such that they are able to form a more stable adsorbed layer, with central hydrophobic PPO block stabilizing the molecule

to a hydrophobic surface, allowing the hydrophilic PEO chains to extend out into the bulk aqueous medium. The PEO-PPO-PEO triblock copolymers have been used widely to reduce protein adsorption in a host of biomedical applications such as coatings for implants and in controlled drug release systems [Malmsten et al, 1998]. The stability of block copolymer on a substrate surface can be enhanced by crosslinking of polymer chains via UV or Gamma irradiation, plasma treatment or by using a hydrophobic priming layer to which both material surface and PPO can covalently bind. A simple technique for the plasma-induced immobilization of PEG onto poly (vinylidene fluoride) microporous membrane has been reported [Wang et al., 2000]. Several other studies were reported to introduce PEG chains into the bulk mass or onto the surface of PLGA and PLA mostly based on the used of tri or di-block copolymers of PLA (PLGA) and PEG [Jeong et al., 2000].

Covalent bonding of PEO onto a substrate is an effective approach to prepare the permanent, PEO-modified surface. However, direct coupling method requires functional groups (e.g., methacrylate) or coupling agent on the substrate surface with which derivatized PEO can react. An alternative method for obtaining PEG-modified surface is through graft-polymerization with PEG-containing macromonomer. Graft polymerizations by plasma and photo-induced coupling have been successfully introduced PEG onto glass. It has been demonstrated that the PEG coating deposited by these methods have excellent ability in eliminating protein adsorption and cell adherence. End-grafting PEO from solution, through widely practiced and suitable for some applications, yields surfaces with moderate coverage and thus several approaches have been developed to increase the polymer segment density in the vicinity of the surface.

Alternative approaches include radiation grafting, formation of interpenetration networks, and modification of one of the polymer ends with an oligomeric or polymeric segment, which has a thermodynamic driving force to assemble at the interface [Griffith, 2000].

Self-assembly monolayers (SAMs) technique has also been applied to form PEG/PEO layer on silicone, gold and silver in Whitesides' group [Prime and Whitesides, 1993; Harder et al, 1998]. An approach was developed based on monolayer self-assembly of end-modified alkane trhiols on gold-coated substrates. Initial experiments using monolayers containing systematically varied rations of unmodified (hydrophobic) alkanethiol chains to alkanethio chains modified with hydrophilic oligoethylene glycol segments (which create a dense PEO brush) demonstrated protein adsorption—and thus cell adhesion—could be tuned by the degree of hydrophilicity (i.e., the fraction of hydrophilic terminated alkanethiol chains). SAMs on gold and silver provide interesting insights intro relationships between the structure of PEG surfaces and their ability to resist protein adsorption, confirming and extending previous work with those SAMS on Au.

2.5.2.4 Detection of protein adsorption

Protein adsorption to PEG-coatings has been investigated by using techniques such as radiolabeling, X-ray photoelectro spectroscopy (XPS), fluorescence microscope, reflectometry. The radiolabeling method appears to be the most commonly used one. In this method, proteins are labeled with radioactive agents (e.g., Iodobead reagent) just prior to the usage and the amount of adsorbed protein was determined by using a gamma counter [Jeong et al, 2000]. However, the radioactivity decays during measurements. The

protein-adsorbed surfaces can also be analyzed by X-ray photoelectro spectroscopy (XPS) [Zhang et al, 2001; Wang et al, 2002]. The XPS N1s core-level signal was used as a marker. The relative intensity of the nitrogen signal from the peptide bonds of the protein is employed as an indicator and the relative amount of the protein adsorbed onto the surface can be represented by the [N]/[C] ration. Alcantar and coworker [Alcantar et al, 2001] have applied fluorescence microscope to measure the ability of PEG-coating to resist protein adsorption. The bovine serum albumin (BSA) was labeled with a Texas red probe. Low fluorescence-intensity indicates low or absent protein adsorption. Quantitative analysis of protein adsorption was done by comparing the normalized adsorption intensity (NAI) of scans for the substrates.

CHAPTER 3

DEVELOPMENT OF CD-LIKE MICROFLUIDIC PLATFORMS

3.1 Introduction

In this chapter, a compact disk (CD)-like microfluidic platform for biomedical diagnostic applications was designed and fabricated. The CD platform integrates a number of microfluidic functions such as pumping, capillary valving, washing, and mixing. By spinning the disc, the centrifugal force overcomes the capillary force and the fluid is pumped from the center towards the edge of the disc. Control of fluid transfer from one reservoir to another is achieved by manipulating the spin velocity of the disc. By coupling the CD drive with a detection system, samples on the CD can be analyzed (e.g. based on adsorption or fluorescence). This microfluidic CD platform has the advantages of low-cost, easy operation, parallel detection, fast response (suitable for point-of-care), and minimum sample usage (usually in sub-microliter range). A user only needs to place a drop of sample (e.g. blood or urine) on the CD, and a computer with a CD reader does the rest of the work. The user can also transmit the results via the

Internet to the hospital or doctor's office for medical consultation or for storing the data in a central data bank.

The focus of this chapter is on the design of polymer-based CD-like microfluidic platforms by manipulating both centrifugal and capillary forces. Flow sequencing is achieved by centrifuge-based fluid propulsion and capillary valving. A two-point calibration design is used as an example to show how the release and flow of fluids can be precisely controlled by the rotation speed of the CD. By combining the capillary valving and micromixing, a cascade micro-mixing design allows sequential mixing on the CD. A typical application of cascade micromixing is reconstituting lyophilized protein.

3.2 Experimental

3.2.1 Materials

The testing fluids include DI water (from the university reagent lab) and bovine serum albumin (BSA) buffer solution. For demonstration purposes, diluted food dyes (purchased from a local grocery story) were used. The materials used for reaction casting is polydimethylsiloxane (PDMS) (Sylgard® Elastomer 184, Dow Corning). The polymethyl methacrylate (PMMA) and polycarbonate (PC) sheets with different thickness for computer numerically controlled (CNC) machining were purchased from American Plastics. Photoresist SU-8 series (SU-8 5, 25, 50, and 100) and their developer PGMEA (propylene glycol methyl ether acetate) were purchased from MicroChem Corp. (Newtonm, MA).

3.2.2 Characterization

The cross section and surface of fabricated microdevices were examined by a scanning electron microscope (Philips XL 30, Philips Electron Optics). The dimension and surface roughness of the fabricated microchannels were characterized by an optical profilometer (WYKO NT3300 Profiling System, Veeco Metrology Group, Tucson, AZ). The surface tension of different fluids and the contact angles between the surface of the microfluidic device and fluids were measured by a Dynamic Contact Angle Analyzer (DCA-322, CAHN Instruments Inc., CA).

3.2.3 Fabrication

For prototyping, we have applied computer numerically controlled (CNC) machining (for PMMA CD) and soft lithography (for PDMS CD) to fabricate the CD microfluidic platforms.

3.2.3.1 CNC machining

The designed microfluidic patterns were drawn using commercial AutoCAD software (AutoCAD 2000, AutoDesk, Inc). Channels and reservoirs (with depths ranging from 60μm to 800μm and widths ranging from 127μm to 762μm) were generated on a polymethyl methacrylate (PMMA) plate (12cm in diameter) by a CNC machine (Dynapath Delta CNC, Chevalier®). The end mills (single-end two-flute sub-miniature end mill) were purchased from McMaster-CARR (Chicago, IL) and the diameter of the mills ranged from 0.005” to 0.03”. Figure 3.1 shows CNC-fabricated plastic CD platforms with a two-point calibration structure and a cascade micromixer.

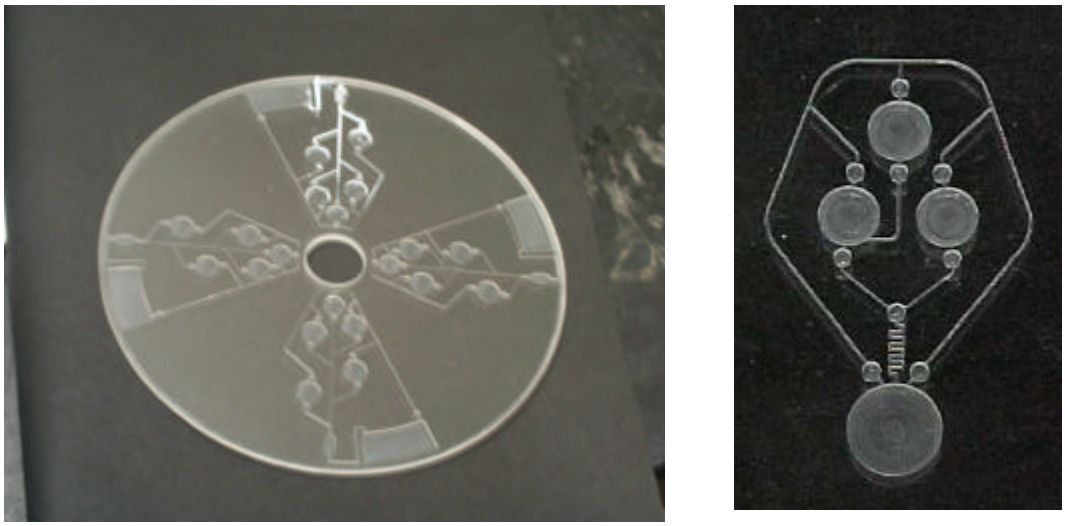

(a) (b)

Figure 3.1. CNC-machined CD microfluidic platforms: (a) a two-point calibration design and (b) a cascade micromixer.

3.2.3.2 PDMS CD

Soft lithography [Xia et al., 1998] was also applied to fabricate the PDMS CD for the case that all feature sizes have same depth. The designed pattern was drawn using AutoCAD software and was then printed on a transparent film using a high-resolution (3386 dpi) image setting system (Yeager Graphics, Columbus OH). The resulted transparent film was then place onto a 4"×4" glass plate and was used as the mask in the photolithography process. For the photolithography process of a feature depth of 300 μm, the negative photoresist SU-8 100 (MicroChem Inc.) was used. The process conditions of the SU-8 100 photolithography process were listed in Table 3.1. The pictures of the resulted SU-8 structure are shown in Figure 3.2a and b.

For PDMS casting, a mixture of the elastomer precursor (part A) and its curing agent (part B) was prepared at the ratio of 10:1 (A: B) and degassed in vacuum oven (20~25 inch Hg) at room temperature until the air bubble disappeared. The mixture was then poured onto the resulted SU-8 mold from above photolithography process and cured at elevated temperature (e.g., 65 ~70 ^{0}C for 1 hour) or room temperature (for 24 hours). The cured PDMS feature was then peeled off from the SU-8 mold. Figure 3.2c shows an SEM photo of the replicated PDMS structure.

3.2.4 Sealing and Sample loading

For PMMA CD, the channels and reservoirs were sealed with a piece of Scotch adhesive tape. To fill the reservoirs, a syringe tip was used to create a hole in the sealing layer above the center of each reservoir. Solutions were then introduced into the reservoir

Step	Equipment/ Material	Condition	Purpose
Coating	Spin coater	500 rpm for 10s (@ramp 100 rpm/s) 1000 rpm for 30s (@ramp 300 rpm/s)	Define the feature/film thickness
Soft bake	Hot plate	65 ^{0}C for 30 minutes 95 ^{0}C for 1.5 hours	Remove the solvent in SU-8; densify the film
Exposure	Cobilt Masker Aligner (365nm)	55s @ 12mW/cm^2	Define the feature
Post exposure bake	Hot plate	65 ^{0}C for 15 minutes 95 ^{0}C for 30 minutes	Cross-link the exposed portion of SU-8
Development	SU-8 developer PGMEA	15~20 minutes	Remove the unexposed portion of SU-8
Hard baking (Optional)	Convection oven	150-200 ^{0}C for 1 hour	Increase the mechanical strength and resistance to further processes

Table 3.1 Process conditions for the photolithography process of SU-8 100 (feature depth 300 μm on silicon wafer)

.

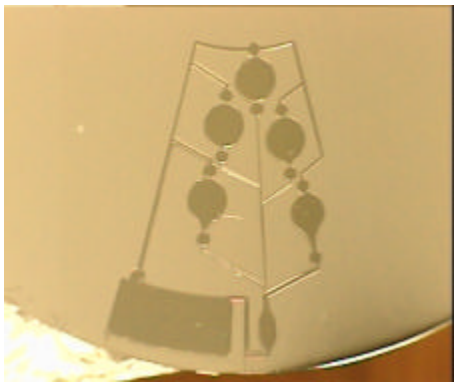

(a)

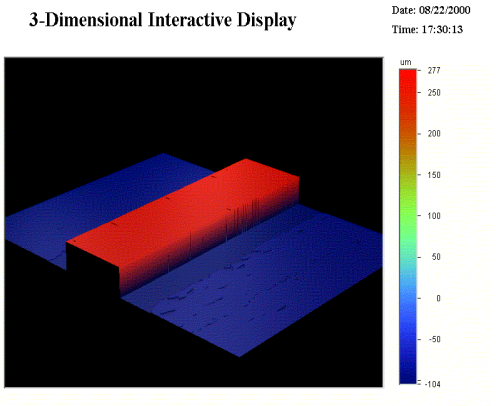

(b)

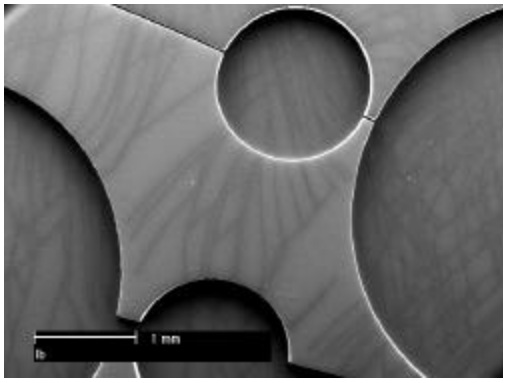

(c)

Figure 3.2. (a) A picture of photoresist (SU-8) mold, (b) the 3-D display of a microchannel in (a), and (c) an SEM photo of replicated PDMS structure.

through the hole with a micropipette. Finally, a second layer of adhesive tape was placed over the entire fluidics system to ensure an airtight seal to avoid fluid leakage. Before reuse, the disk was washed with ethanol and de-ionized water.

For PDMS, small holes were punched through the PDMS layer for loading. The PDMS was then directly placed onto a regular disk (the base, 1.2mm thick and 12 cm in diameter). For better results, another thin CD cover (0.6mm thick) with loading holes was placed on the top of the PDMS as shown in Figure 3.3. This type of sealing is reversible and the PDMS is easily peeled off for reuse.

3.2.5 CD microfluidic testing setup

The experimental setup for microfluidic testing is shown in Figure 3.4. The disc was mounted on a motor plate (up to 5000 rpm) designed by Gamera Bioscience. The motor control was constructed of a five-stage stepper motor, a 12-V power supply, and a controller (PIC-Servo, HdB Electronics, Redwood City, CA). The setup allows accurate monitoring of both position and acceleration/deceleration profiles as the motor was running. In addition, the motor could be recalled to a preset home position allowing accurate positioning of the disk for analysis. The motor was controlled directly via an RS232 serial port connection to a desktop PC, allowing integrated software control. The rotation speed of the disk was gradually increased until the release of fluid from the reservoir occurred. The motor was connected to an encoder to trigger a strobe (Monarch, DA 115/Nova Strobe) for synchronized imaging. When the same position of the CD passed under a CCD camera (Panasonic GP-KR222), the strobe was triggered. Therefore, only a fixed portion of the CD was highlighted during each turn. The flow in

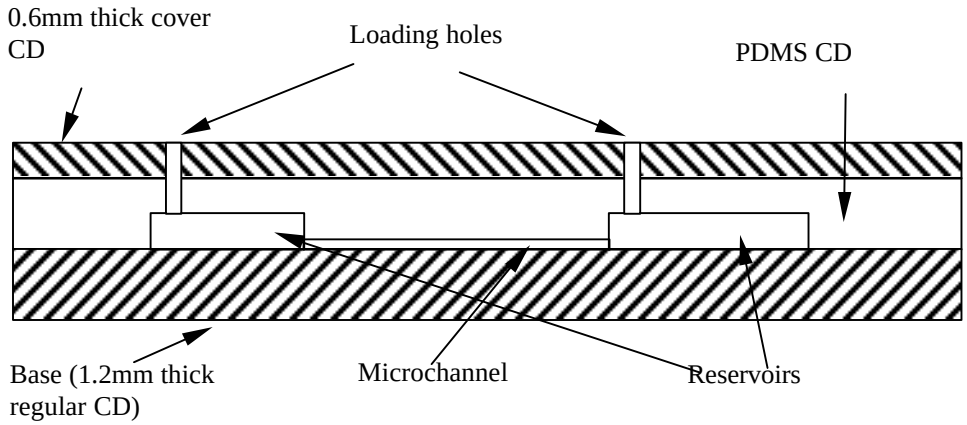

Figure 3.3. The schematic of the sealing of PDMS microfluidic platforms.

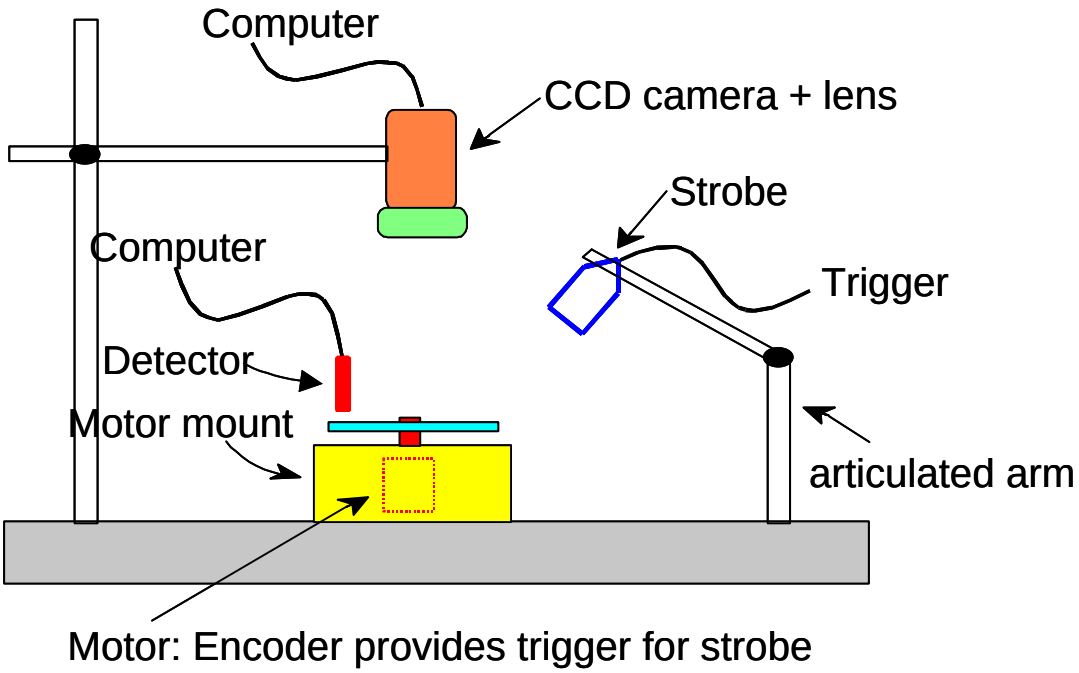

Figure 3.4. Schematic and picture of experimental setup for CD microfluidic testing. (continued)

(Figure 3.4 continued)

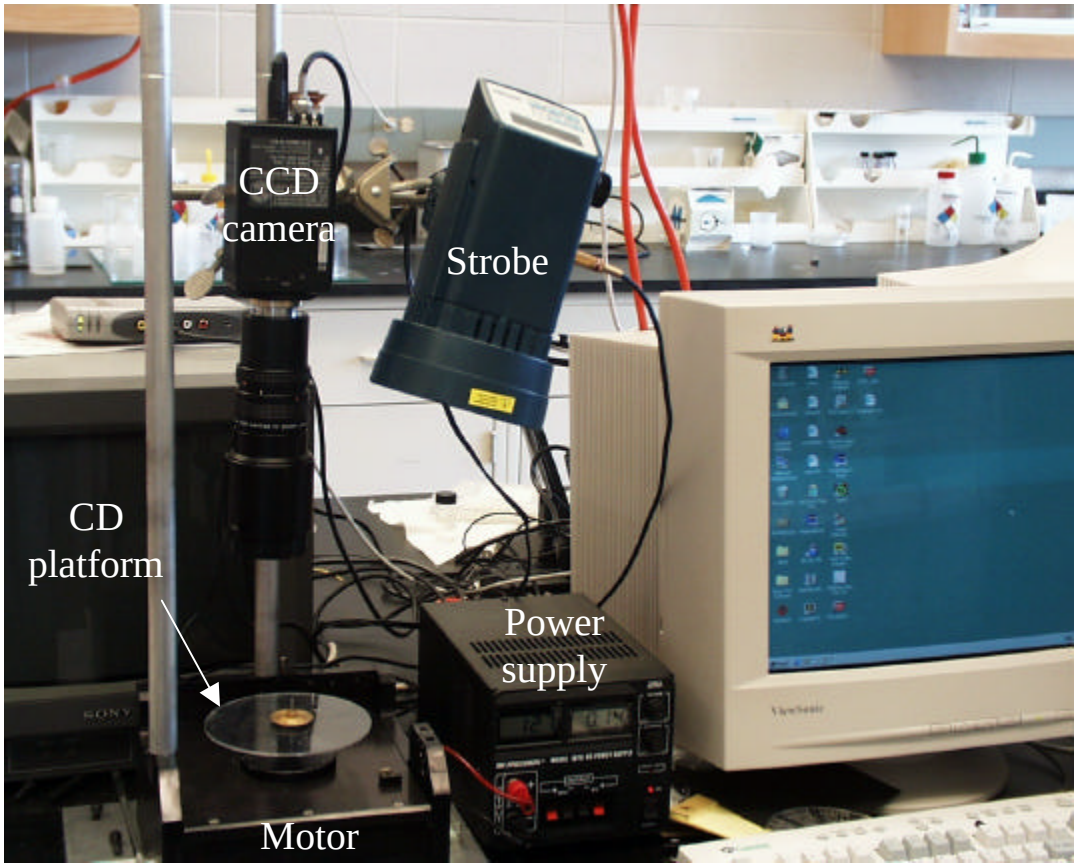

this portion of the CD was videotaped through the CCD camera and a VCR (Panasonic AG-1960). After the experiment, frames were grabbed from the motion video by the commercial video software Adobe Premiere® 5.0.

3.3 Results and discussion

3.3.1 Centrifugal Propulsion and Capillary Valving

In the CD microfluidic platform, the centrifugal force provides the pumping pressure. The pumping force per unit area (P_c) due to the centrifugal force is given by:

$$\frac{dP_C}{dr} = \rho w^2 r \qquad (3.1)$$

where ρ is the density of the liquid, w is the angular velocity of the CD platform, and r is the distance of a liquid element from the center of the CD.

Integration of Eq. 3.1 from $r = R_1$ to $r = R_2$ gives:

$$\Delta P_C = \rho w^2 (R_2 - R_1)(\frac{R_1 + R_2}{2}) = \rho w^2 \cdot \Delta R \cdot \overline{R} \qquad (3.2)$$

where $\overline{R}$ is equal to $\frac{R_1 + R_2}{2}$, and R_1 and R_2 are the two distances of the liquid elements from the center of the CD as shown in Figure 3.5a.

It is very important for a CD microfluidic platform to be able to deliver the solution from each reservoir in a pre-specified manner. The delivery of solution from a single reservoir allows the measuring reservoir to be filled without releasing solutions in other reservoirs. Capillary burst valves were incorporated into the microfluidics platform design for this purpose. When the fluid comes to the junction through the microchannel,

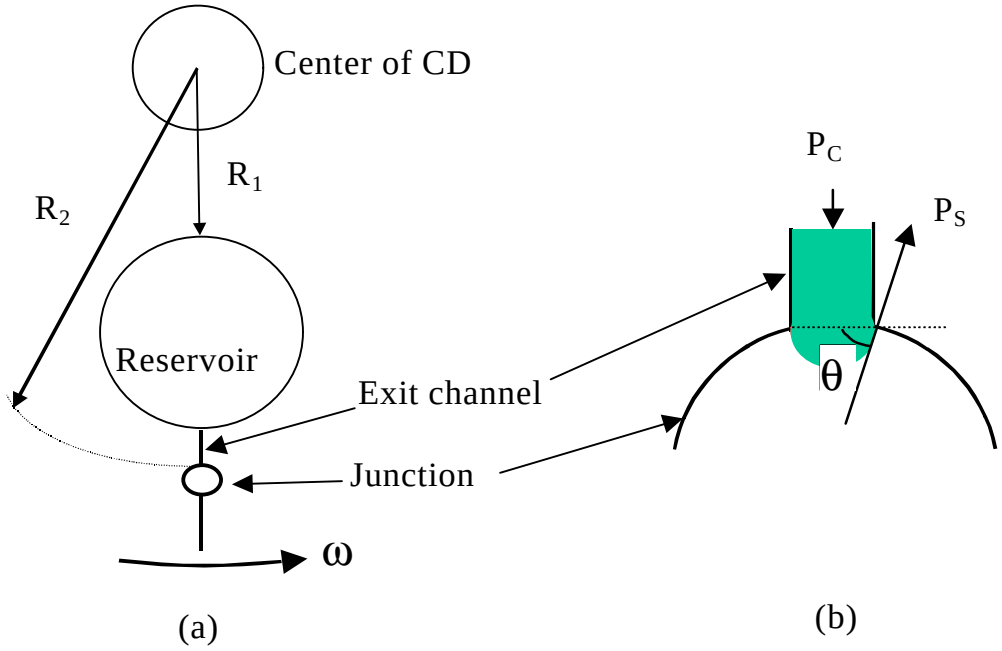

Figure 3.5. (a) Schematic illustration of fluid propulsion and (b) close view of the liquid front at the junction where the liquid is held by capillary force

the capillary force at the end of the microchannel due to a change of the geometry tends to hold the fluid as illustrated in Figure 3.5b. The capillary force per unit area (P_s) due to surface tension is given by:

$$\Delta P_s = \frac{Cg \sin q}{A} \tag{3.3}$$

Where g is the surface tension of the fluid, q is the contact angle, A is the cross-section area of the microchannel, and C is the associated contact line length.

The burst frequency is defined as the angular frequency at which DP_c is greater than or equal to DP_s. At this rotation speed, the liquid overcomes the pressure generated by capillary force (DP_s) and flows through the capillary valve, releasing liquid from the reservoir. The burst frequency, f_b, calculated from Eqs. 3.2 and 3.3 is given by:

$$f_b = \left(\frac{g \sin q}{p^2 r \cdot \Delta R \cdot \overline{R} \cdot d_H}\right)^{\frac{1}{2}} \tag{3.4}$$

where d_H, equal to $4A/C$, is the hydrodynamic diameter of the channel connected to the junction. The capillary burst valve is a passive valve that requires no moving parts. It is controlled by the angular speed of rotation, fluid density, surface tension, and geometry and location of the channels and reservoirs.

A simple experiment was carried out to demonstrate the valving function by the capillary force as shown in Figure 3.6. In this experiment, a reservoir (2.62 mm in diameter and 610 μm in depth) is connected to a larger microchannel A (508 μm wide and 508 μm deep) and a smaller microchannel B (127 μm wide and 63.5 μm deep) and sealed with adhesive tape. The reservoir was filled with food dyes, and fluids were held at the end of channels A and B by the capillary force as shown in Figure 3.6a. Applying

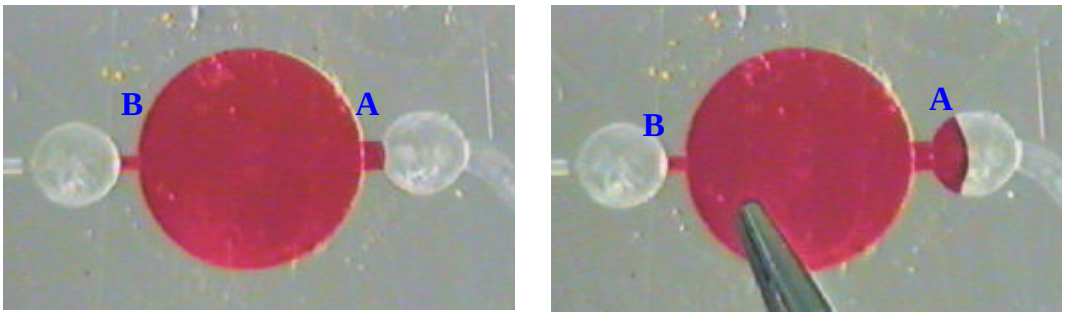

(a) (b)

Figure 3.6. Capillary valving experiment. (a) Reservoir is filled with food dye and liquid is held by capillary valving at the end of channels A and B, (b) food dyes is releasing through channel A but not through channel B. (Channel A is 508 μm wide and 508 μm deep; and channel B is 127 μm wide and 63.5 μm deep.)

a gentle pressure by pressing the adhesive tape on the top, the food dyes burst off the capillary valve at the end of channel A but not channel B (see Figure 3.6b). According to Eq. (3.2), the capillary force per area by channel B is about 6 times of that by channel A. Therefore, liquids burst through channel A but not channel B.

3.3.2 A two-point calibration system

With nearly constant fluid properties and uniform substrate materials, precise flow sequencing can be realized by appropriately choosing the channel dimensions and the junction size and location. To demonstrate this flow sequencing function, a two-point calibration design for medical diagnostics is described [Madou et al., 2000]. In this design (see Figure 3.7), the pre-loaded liquids should flow to the optode reservoir in the order of calibrant 1, wash 1, calibrant 2, wash 2, and the sample by increasing the rotation speed of the CD platform. The same optode reservoir is used for measuring both calibrant and sample fluids, in order to eliminate systematic errors common with devices using separate reservoirs for measuring sample and calibrates. An integrated analysis system for ions, which incorporates this two-point calibration microfluidic system and a potassium-selective optode, has been constructed [Johnson et al., 2001]. The simplest case of a calibration system based on two potassium standards has been demonstrated. It has been found that the error for determination of the test sample by using a two-point calibration system improved from 21% to 2.6% by using a single point calibration. This major improvement reflects the shortcoming of the one-point calibration system (i.e., only a single point is applied to fit a calibration curve, therefore, any error existing in the

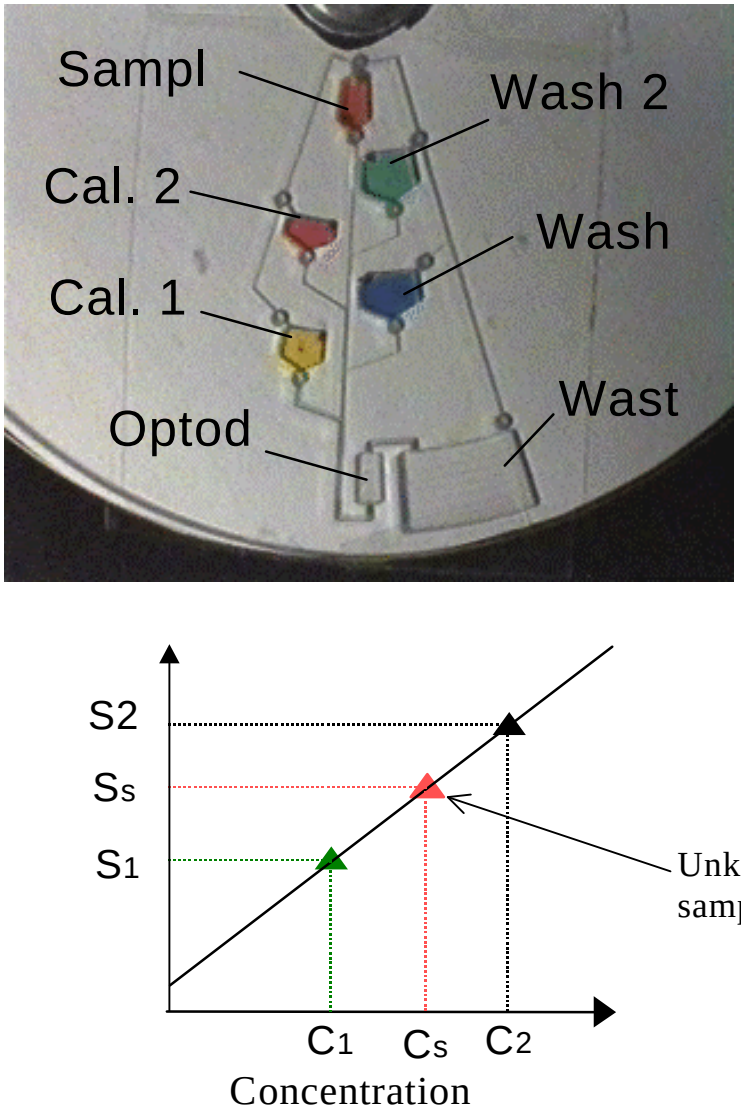

Figure 3.7. A two-point calibration microfluidic platform. Flow order: Cal. 1 → Wash 1 → Cal.2 → Wash 2 → Sample

measurement is translated into the calibration curve). Without the washing steps, it is also possible that a calibration based on three or four standards can be performed if desired.

3.3.2.1 Flow sequencing on PMMA CD

In order to test the burst frequency of each reservoir, CNC-machined PMMA discs, 12 cm in diameter, were made with a two-point calibration design. De-ionized water containing different colors of food dye was used as the test fluid. Table 3.1 summarizes the channel dimensions and burst frequencies for the experiments. Burst frequencies of the reservoirs were designed to release at rotation speeds ~200 rpm greater than the preceding reservoir. In the experiment, different food dye solutions were filled into different reservoirs. Their releases from different reservoirs were visualized and recorded by a CCD camera. The burst frequency was determined when each burst valve release its solution.

Figure 3.8 shows a series of snapshots taking during a test run. At a low rotation speed (524 rpm), only the calibrant 1 fluid went to the optode reservoir, while the other fluids stayed in their reservoirs. When the rotation speed increased in steps, the fluids of wash 1, calibrant 2, wash 2, and the sample moved to the optode reservoir in the right order. Figure 3.9 shows the burst frequency test results on two CNC-machined CDs.

The experimental results indicate that the separations of burst frequencies are large enough to provide the desired fluid control. For example, the worst case of burst frequency separation in the experiment occurred between reservoir cal. 1 and reservoir wash 1 (98 rpm). It should also be noted that the burst frequencies occur as governed by theory. For example, reservoir cal. 1 had the lowest burst frequency due to its greatest

Reservoir	Channel dimensions (μm)		Burst frequencies (rpm)	
	width	depth	calculated	experimental
Sample	127	63.5	1222	1126
Wash 2	127	63.5	1032	1026
Cal. 2	254	127	832	822
Wash 1	254	127	623	622
Cal. 1	508	254	427	524

Table 3.2. Channel dimensions and burst frequencies for two-point calibration system on PMMA.

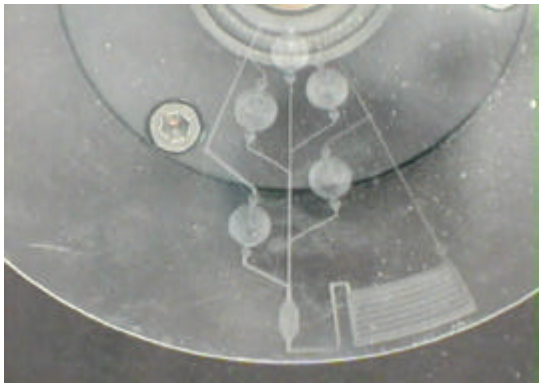

Beginning

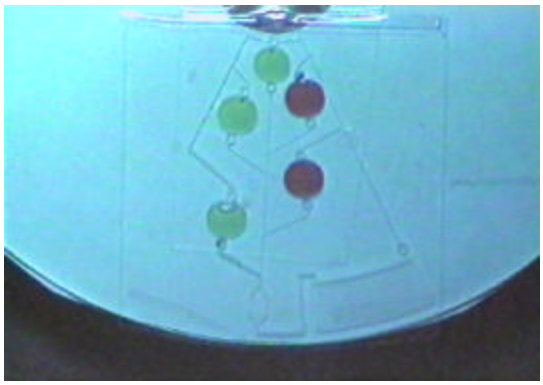

Calibration 1 @ Ω_1= 524rpm

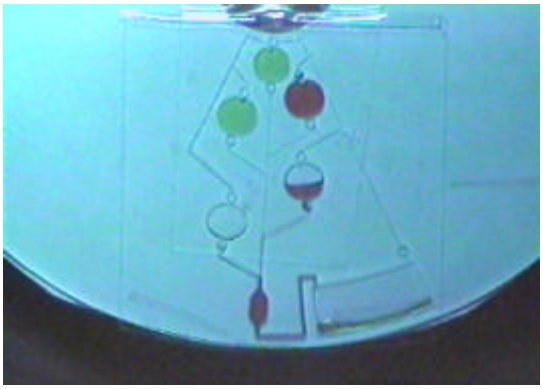

Wash 1 @ Ω_2 =622 rpm

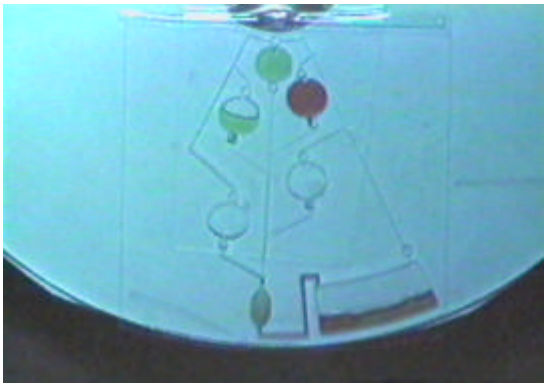

Calibration 2 @ Ω_3 =822 rpm

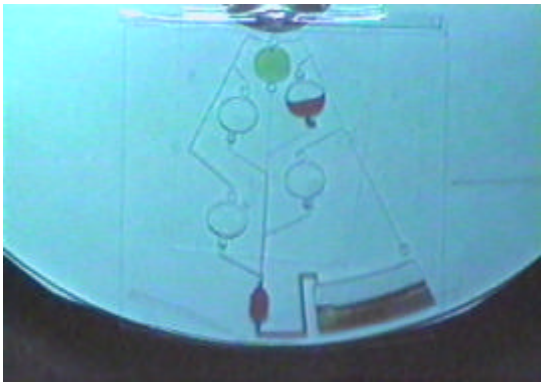

Wash 2 @ Ω_4 =1026 rpm

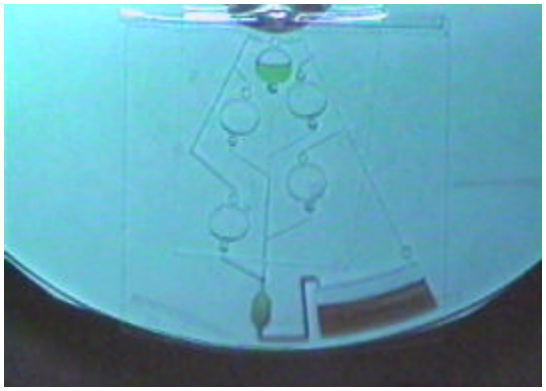

Sample @ Ω_5 =1126 rpm

Figure 3.8. Flow sequence of a two-point calibration system on PMMA.

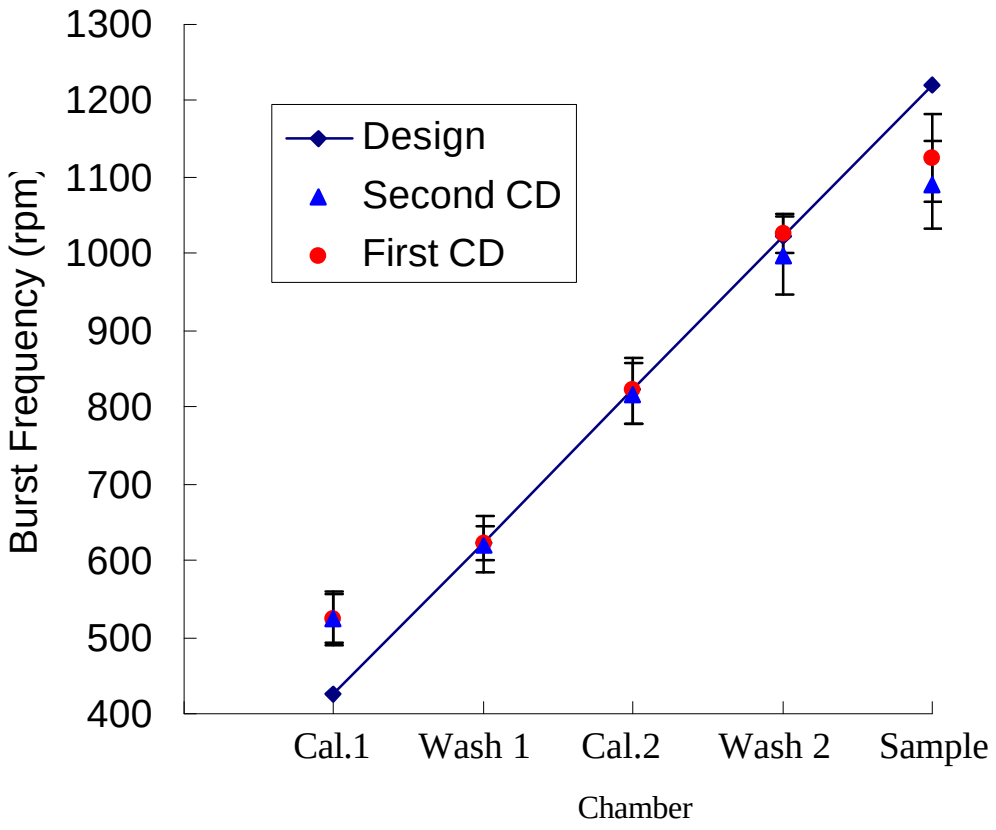

Figure 3.9. Burst frequencies of the CNC-machined CD platform based on DI-water.

distance from the center and largest exit channel (with a 508 μm wide and 254 μm deep). Similarly, reservoir wash 1, having the same exit channel dimension (254 μm wide and 127 μm deep) as reservoir cal. 2, released fluids at a lower rotation speed than reservoir cal. 2 due to its further distance from the center of rotation. The same observation was true for reservoir wash 2 and sample reservoir (exit channel 127 μm wide and 63.5 μm deep) with reservoir wash 2 releasing at a lower rotation speed.

Considering the tolerance of CNC machining, the experimental results agreed reasonably well with the calculated burst frequencies. For testing the design concept of microfluidic devices, low-cost prototyping techniques are highly desirable. If the feature size is larger than 50 μm or different feature depths are required, CNC milling can easily be used to mechanically manufacture the device. CNC machining does not provide a smooth surface finish (surface roughness around several μm), a high aspect ratio (height vs. width ratio is limited to less than 2), or a good dimension control (often 10% large than the design). It does, however, have no material limitations, and various metals and plastics can all be used. Yet this fabrication process is labor intensive and slow, and it typically takes several hours to make a single CD platform.

The observed deviations in burst frequencies for a given reservoir were most likely caused by the manner in which the reservoirs are filled. For instance, trapped air in the channel between the reservoir and burst valve can provide a force counteracting the centrifugal force, thus causing a slight increase in burst frequency. This factor, however, only creates slight changes in the value of the burst frequency, and it was found that the

200 rpm separation designed into the architecture is great enough to ensure the desired separation of burst frequencies.

3.3.2.2 Flow sequencing on PDMS CD

A two-point calibration system was also design with same feature depth (300 μm) by the soft-lithography approach on PDMS. De-ionized water containing different colors of food dye was used as the test fluid. Table 3.3 summarizes the channel dimensions and burst frequencies for the experiments. Figure 3.10 shows a series of snapshots taking during a test run on PDMS CD. The observed burst frequencies were consistently higher than the calculated values.

3.3.2.3 Sealing

During the experiment of the PMMA CD, it was observed that upon the rotation, the sealing of two-layer adhesive tapes (refer to "soft cover") tended to bulge because of the flexibility of the adhesive tapes. This caused the burst frequencies of each reservoir is much higher than designs. Another method (refer to "harder cover") was tried using a small piece of polycarbonate (PC) plate with small holes drilled at proper locations as inlets for loading solutions. The detail procedure of this approach is:

(a) First cover the CD with a layer of adhesive tape;

(b) Use another layer of adhesive tape to secure the PC plate on the CD at proper position. Load solutions into corresponding reservoirs;

(c) Cover inlets with a third layer of adhesive tape.

Reservoir	Channel dimensions (μm)		Burst frequencies (rpm)	
	width	depth	calculated	experimental
Sample	60	300	302	400
Wash 2	60	300	515	650
Cal. 2	100	300	590	770
Wash 1	100	300	774	850
Cal. 1	500	300	864	1000

Table 3.3. Channel dimensions and burst frequencies for two-point calibration system on PDMS.

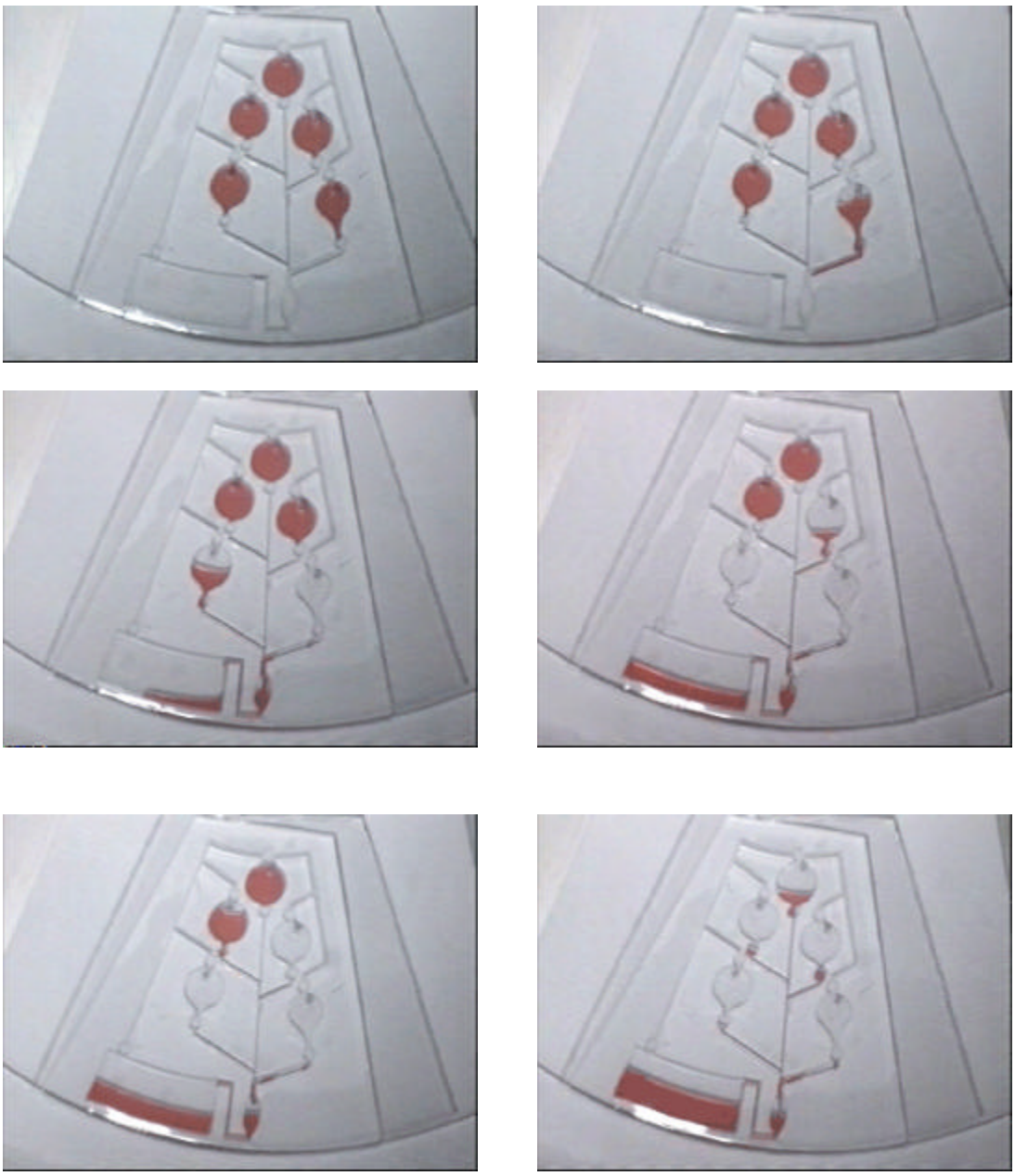

Figure 3.10. Flow sequence of a two-point calibration system on PDMS.

Table 3. 4 summarizes the burst frequencies by using these two sealing methods. It can be seen that the method of sealing cover did affect the burst frequencies and the hard cover method worked better than the soft cover one. However, the hard cover method is pretty complex and needs three layers of adhesive tape and one layer of PC plate. Further development of a new sealing method to cover the CD with one layer of PC plate is necessary.

For the PDMS CD, the sealing method of directly placing PDMS CD onto a regular disk (base) can sustain the rotation speed up to 1000 rpm. Above that rotation speed, leakages were observed. To improve the sealing, a layer of the curing agent (Sylgard® Elastomer 184 kit, Part B) was spin coated (at rotation speed of 5000 rpm for 15 seconds) on the base before the PDMS CD was placed onto. The sandwich structure was then placed in the oven at 70 ^{o}C for one hour. This improvement allows PDMS CD to sustain the rotation speed up to 2000 rpm. Both sealing methods mentioned above were reversible and the PDMS was easily peeled off from the base for reuse.

For applications in which a higher rotation speed (above 2000 rpm) was desirable, a tight and irreversible sealing method can be adopted [Duffy et al, 1998]. In this approach, both the PDMS and the base were treated with oxygen plasma and immediately placed together to form a tight and irreversible seal. It can be applied to seal PDMS to a range of materials such as PDMS, glass, silicon, polyethylene (PE), and polystyrene (PS). The mechanism is that the oxygen plasma treatment converts $-OSi(CH_3)_2O-$ group at the surface of PDMS to $-O_nSi(OH)_{4-n}$ and introduces polar function groups (e.g., COOH, OH, ketone) at the surface of polymers, condensation can be occurred between the SiOH

Burst frequency (rpm)					
Reservoir	**Calibration 1**	**Wash 1**	**Calibration 2**	**Wash 2**	**Sample**
Design	**427**	**623**	**832**	**1032**	**1222**
Soft cover sealing	597	672	978	1117	1288
Std. Deviation (rpm)	26	39	24	66	46
Hard cover sealing	524	622	822	1026	1126
Std. Deviation (rpm)	31	22	43	25	57

Table 3.4. Burst frequencies of each reservoir for different sealing methods.

group and the polar function group to form irreversible bonding However, this method is not applicable to polycarbonate (PC) and PMMA [Duffy et al, 1998].

3.3.2.4 Washing

Fluid flow in the employed microfluidics platform is laminar due to fluid velocities and channel dimension. This is a well-known fact associated with flow in microchannels where Reynolds number is much less than the value of 2300 required for turbulent flow. This fact has an influence upon the manner in which each solution fills the measuring area. The microfluidic platform is designed in such a way that liquid from the first reservoir fills the measuring reservoir and is held there until a fluid from the second reservoir begins to flow. When the second liquid reaches the measuring reservoir, fluid 2 physically displaces fluid 1. Since the flow is laminar, there is little mixing of the displaced and displacing fluids, except at the interface of the two liquids some diffusion mixing occurs. Since the fluid reservoirs are designed with a volume (20 μL) that is three-fold larger than the volume of the measuring area (6.5 μL), the diffusional mixing front is quickly pushed out of the measuring area by the initial fluid volume. This front is completely displaced into the waste by the time the measuring area is finally filled. This effect has been observed by placing differently colored liquids in each reservoir and monitoring flow through the measuring area with a strobe lamp synchronized to disk rotation and a CCD camera as shown in Figure 3.11.

For some applications, a washing solution may not be needed. Experimental results have indicated that the inclusion of washing steps does not improve the overall

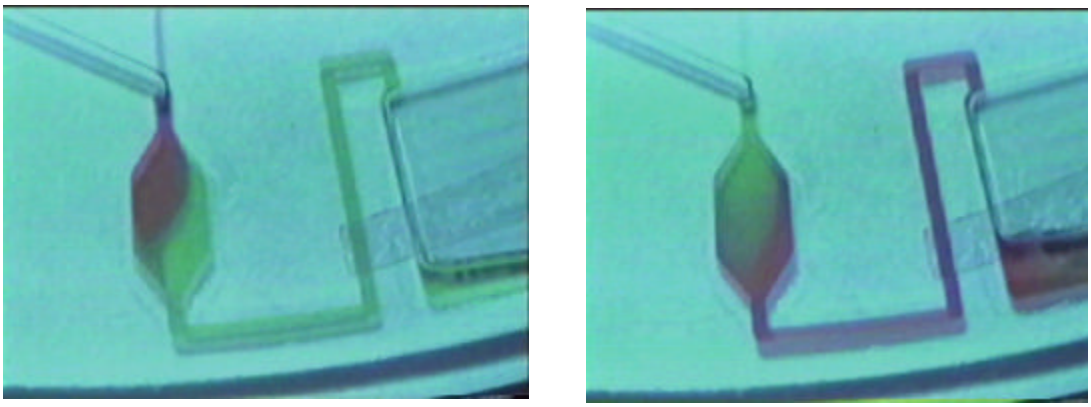

Figure 3.11. Displacement at the optode reservoir.

performance of the integrated system with respect to analysis of the test sample [Johnson et al., 2001]. For instance, when a washing step is included between the two standards and before the test sample, there is little difference in the accuracy and precision of the determination compared to the case where no such washes are included. When individual washing steps were incorporated, the relative error is 1.8% with a standard deviation of 0.2 mM as compared to the protocol with no washing steps, where the relative error was 2.1% with a standard deviation of 0.1 mM. However, for most bio-fluids such as an enzyme solution, washing is essential because of the protein adsorption onto the polymer substrate.

3.3.2.5 Pattern architecture

In designing the microfluidic systems, the shape of reservoirs and channels may play an important role. Figure 3.12 shows three designs of the two-point calibration system. When the shape of the reservoirs was changed from rectangular, to circular, to raindrop-like, sample loading in the reservoirs became easier (i.e. less likely to trap air bubbles) and there was less liquid retained after release. Sharp corners or turns should be avoided in the design of micro-channels and reservoirs, because they tend to cause high residual stresses during disc fabrication. Among the three designs, the raindrop-shaped reservoirs provided the best performance in both microfluidic experiments and disc fabrication.

In order to ensure that the optode reservoir is completely filled and washed after each displacement, the shape of the optode reservoir and the relative location of the optode reservoir and the waste reservoir are important. In Design I of Figure 3.12, the

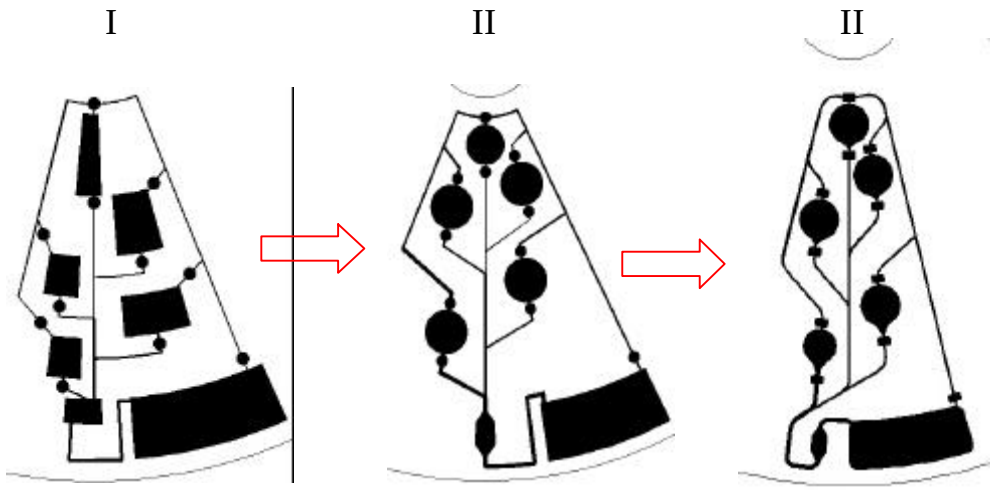

Figure 3.12. Three two-point calibration designs.

incoming fluid passed through the center portion of the optode reservoir, leaving dead space near the corners. In Design II, the optode width is narrower with a rounded inlet and outlet. Although good washing was achieved, the optode reservoir did not totally fill in some cases. In Design III, the incoming fluid moved into the optode reservoir from the bottom to the top, ensuring complete filling and washing.

3.3.3 Cascade micromixing

Mixing is important in many facets of the chemical processes, ranging from simple blending to complex chemical reaction for which the reaction yield and selectivity are highly dependent on the mixing performance. Improper mixing can result in non-reproducible processing and lower product quality, with the associated need for more elaborate downstream purification processes and increased waste disposal costs.

Because of the micron-sized flow channels, the Reynolds number of fluid flow in the microfluidic systems is extremely small (usually less than 1). The lack of turbulent flow makes the mixing in microdevices a very challenging issue. Diffusion is the main driving force in micromixing due to the nature of laminar flow. Design of micromixers is generally based on increasing the diffusion time, enlarging the contact area, and creating more chaotic flows.

Figure 3.13a shows one design for mixing in microchannels on a compact disc. In this design, two fluids are designed to be released from their reservoirs simultaneously and mix at point A by impingement. It is believed that if the impingement velocity is high enough, a chaotic motion occurs in the mixing chamber. Then they go through an S-shaped channel. This channel increases the contact time and also creates bend-induced

vortices to stir the fluid and therefore enhance the mixing process [Yi and Bau, 2000]. Two snapshots taken before and during mixing process were shown in Figures 3.13 b and c. This micromixing CD platform has been applied in genetically-modified binding protein calmodulin (CaM) and phosphate binding protein (PBP) based phenothiazines and phosphate sensing by mixing fluorescence labeled CaM or PBP and analyte solution (chlorpromazine or phosphate) [Wenner et al., 2001].

In the BioMEMS applications, fluids used commonly contain all kinds of proteins. In some instances, preloading bio-fluids into the microfluidic platforms is necessary. It has high risk of protein denaturing if used after a period of storage time. One way to solve this problem is to use the lyophilized protein. Protein is dissolved in the buffer solution only prior to the usage. For reconstituting lyophilized protein, a cascade micromixer structure by combining the capillary valving and micromixing was designed for our CD platform as schematically shown in Figure 3.13d. In this design, a buffer solution in reservoirs 1 is released at a low rotation speed, then flows into reservoir 2 where a solid protein is located (see Figure 3.13e). Such a design reduces the contact time between proteins and buffer solutions, minimizing protein denaturing. As described in flow sequencing, the centrifugal force provides the driving pressure while the capillary valve controls the flow release. After the protein is dissolved, the protein solution and a sample solution are released simultaneously at a higher rotation speed. The mixture is also mixed by impingement mixing and bend-induced vortices when flowing into the optode reservoir for detection. Figure 3.13f shows a snapshot of an impingement mixing experiment during mixing of two water samples containing food dyes.

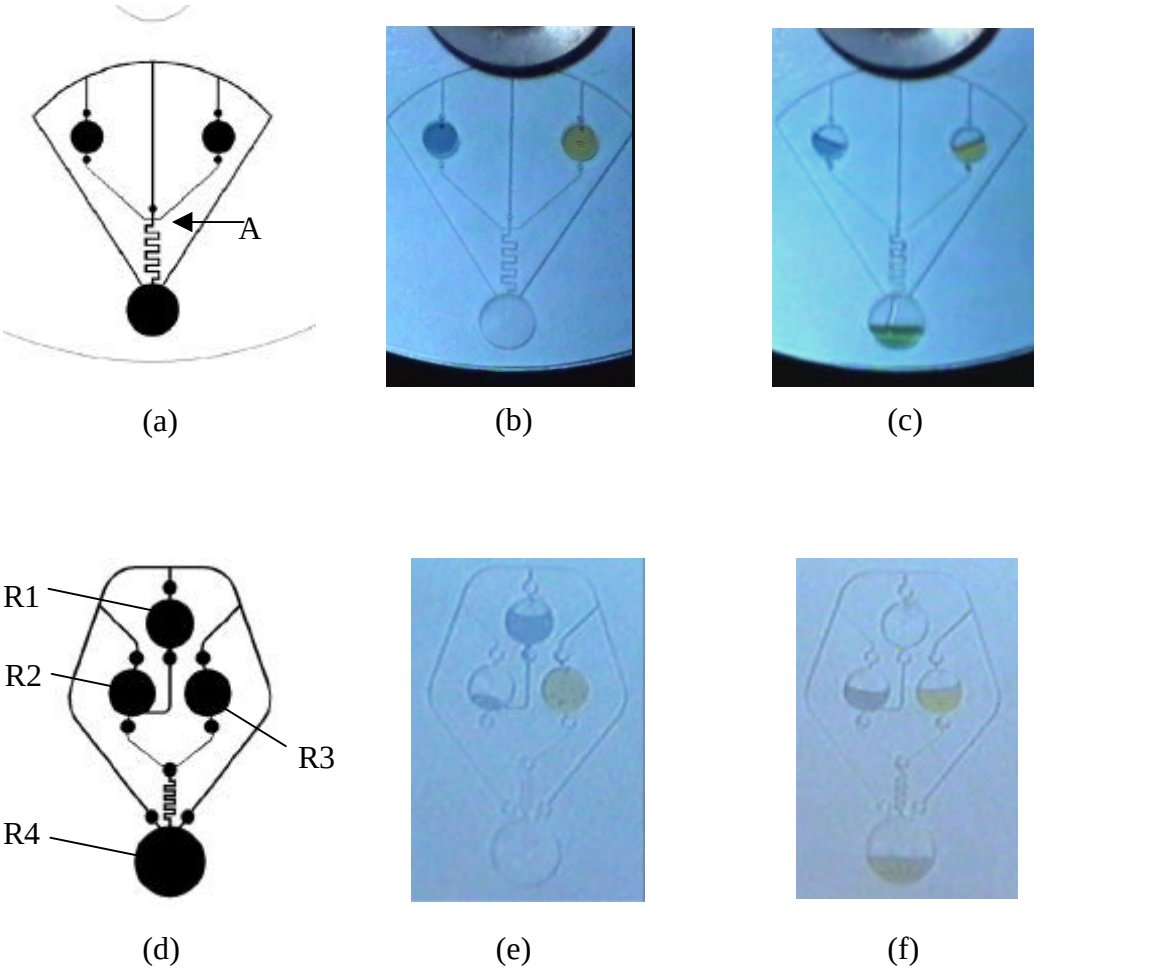

Figure 3.13 Micromixer designs: (a) a micromixer, (b) before mixing, (c) during mixing, (d) a cascade micromixer design, R1-buffer solution, R2- lyophilized protein, R3- sample with analyte, R4- optode; (e) buffer solution release; and (f) sample mixing.

Eight identical sets of the cascade micromixers, which enable complete calibration curves to be performed in a single run, were fabricated by CNC-machining on a 12cm diameter PMMA CD. The burst frequencies of reservoirs R1 and R2/R3 on these structures (results obtained from our collaborator at University of Kentucky [Douglass et al, 2002]) are shown in Figure 3.14. It can be seen that the releases of solutions from R1 and R2/R3 follow very well the designed flow sequence. The average of the burst frequency of R2/R3 is about 170 rpm higher than that of reservoir R1 to ensure reliable release of reconstitution buffer (in reservoir R1) into reservoir R2. This platform has been successfully employed for the detection of chlorpromazine (CPZ), phenothiazine and related tricyclic antidepressants (TCA) by using the fluorescently labeled calmodulin (CaM) [Douglass et al, 2002]. Dry CaM can be stored on the CD for up to ten days and still be able to detect CPZ when reconstituted. The detection limit is about 100 μM for CPZ and mM range for phenothiazine and TCA.

3.4 Summary

A polymer microfluidic platform integrated with different fluidic features has been designed and fabricated. It has been demonstrated to successfully realize some of the basic needs for a microfluidic platform based on centrifuge, such as pumping, capillary valving, washing, mixing, etc. In cases where the fluid properties are nearly constant, substrate material is uniform, and the reservoirs are similarly constructed with respect to geometry, burst valves with well-defined and well-separated critical frequencies can be constructed on the disk by varying channel dimensions and distance of the burst valve

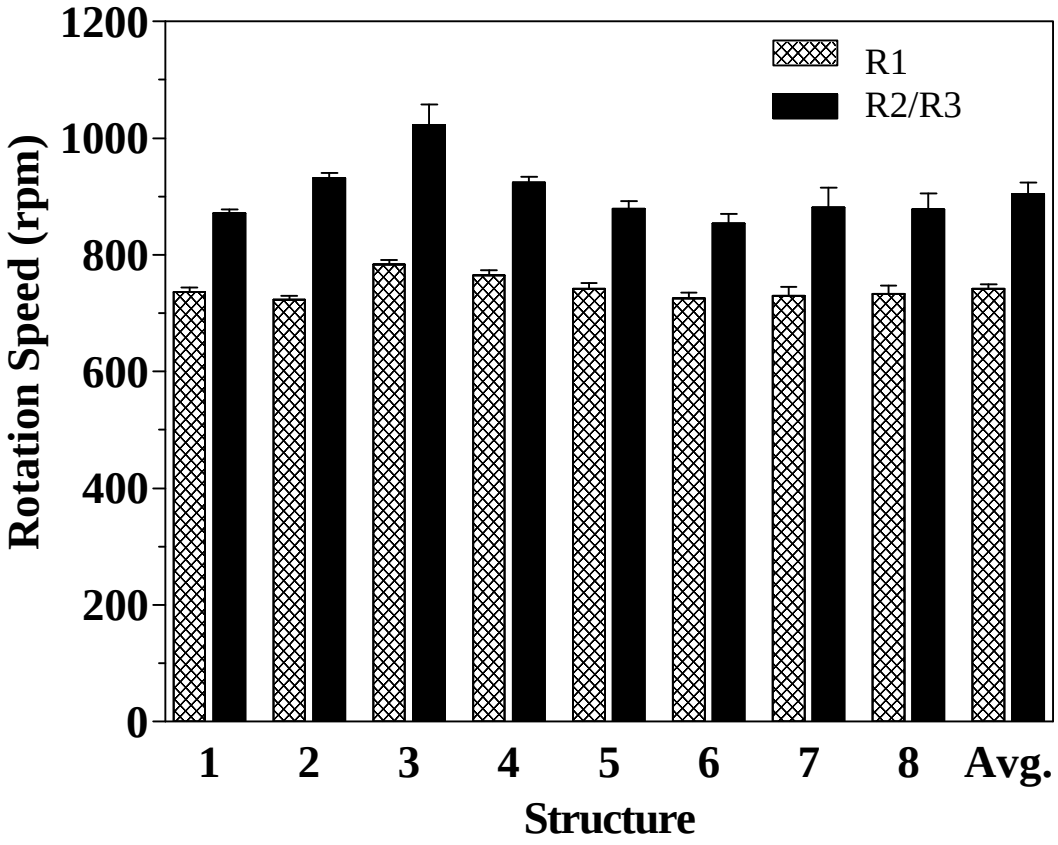

Figure 3.14. Burst frequencies of eight sets of cascade micromixers on a single CD [results from our collaborator at University of Kentucky].

from the center of rotation. By combining different microfluidic functions, two microfluidic systems (a two-point calibration system and a cascade micromixing) have been demonstrated experimentally.

There are several advantages to be gained from using this CD microfluidic platform. The system requires a small power supply and can be interfaced to a laptop or handheld computer and easily further miniaturized. The varieties of architectures that can be constructed on centrifugal microfluidics platforms provide a great deal of versatility in developing dedicated devices for specific applications. The size and architecture of reservoirs govern the number of reservoirs per microfluidic network and the number of networks that can be placed on a single disk. Further miniaturization and changes in the pattern design could easily allow for a greater number of reservoirs or analyses per platform. Furthermore, microfluidic patterns can be constructed such that multiple analyses can be performed on a single disk, demonstrating promise for a single platform devoted for parallel analysis that may be encountered in an application.

CHAPTER 4

PACKAGING OF POLYMER-BASED MICROFLUIDIC PLATFORMS

4.1 Introduction

Polymers have a great potential to be used for BioMEMS applications because many polymers are low cost, can be processed easily, and possess a broad rang of physical and chemical properties. Currently, packaging (i.e., seal the platform with a lid) and surface modification (e.g., hydrophilicity, protein adsorption, electric conductivity), however, are still challenging issues in the design and fabrication of these plastic microfluidic platforms. As reviewed in Chapter 2, several techniques such as lamination, thermal bonding, ultrasonic welding, and solvent bonding have been tried on polymer-based microdevices. In general, these bonding techniques alter the surface of the microdevices by using external forces (e.g. solvent, adhesive, ultrasonic, laser) or applying pressure to bring two halves together. However, the same driving force that allows the bonding also tends to deform the microfeatures. They are mainly applicable for relatively large microchannels.

In this chapter, a new resin-gas injection technique for bonding and surface modification of polymer-based microfluidic platforms was present. A microfluidic device and a lid are encapsulated in a holder. A photo curable resin (glue) was then injected into the platform to fill the micron-sized channels and reservoirs as well as the gap between the platform and the lid. Gas was then injected to replace most of the resin inside the channels and reservoirs. The remaining resin was cured by ultraviolet light. This new approach can easily seal microfluidic devices with micron and sub-micron sized channels without blocking the flow path. It can also be used to modify the channel shape, size and surface characteristics. By applying the masking technique, local modification of the channel surface can be achieved through sequential resin-gas injection.

During the electrophoresis separation, the separation channel is usually filled with sieving materials (such as polyacrylamide or agarose gel) together with the buffer solution. The sieving material is one of the most important components in DNA sequencing analysis because it determines the migration behavior and the resolution of DNA separation. Difficulties are often experienced during loading the buffer solution with gel because the presence of gel greatly increases the viscosity of the buffer solution. Furthermore, air bubbles tend to be trapped in the microchannel, which is problematic in the electrophoresis process. External pumping (vortex or vacuum) is often necessary to eliminate the air bubbles in separation channels.

The resin-gas injection approach was also used to coat a layer of crosslinked polyacrylamide gel on the walls of microchannel, serving as the sieving material for electrophoresis. It eliminates the problems encountered during gel solution loading because only the low viscosity buffer solution needs to be loaded into the empty

separation channel. The hydrophilic wall (hydrogel is usually hydrophilic) also facilitates the loading of buffer solution. After swelling in the buffer solution, the hydrogel serves as the sieving matrix for the electrophoresis separation. The swelling behavior and the electrophoresis efficiency of this new technique were investigated and compared experimentally with the conventional gel solution method on a DNA sequencing chip.

4.2 Experimental

4.2.1 Materials

Hydroxyethyl methacrylate (HEMA, monomer), 2-2-dimethoxy-2-phenylacetophenone (Irg 651, photoinitiator), sodium dodecyl sulfate (SDS, surfactant) were purchased from Aldrich. The probe fluids for contact angle measurements include the distilled water purchased from the university reagent lab and ethylene glycol purchased from Fisher Scientific. The PEO-PPO-PEO tri-block copolymer (Pluronic® F127 Prill, surfactant) was donated by BASF (Mount Olive, New Jersey). Polyethylene glycol with molecular weight of 4000 (PEG-4000) was donated by Union Carbide, now Dow Chemical (Danbury, CT). Photoinitiators (Irgcure® 184, 651, and 819) were donated by Ciba Specialty Chemicals (High Point NC). Polymethyl methacrylate (PMMA) pellets used in injection molding to fabricate microfluidic platforms were obtained from Plaskolite, Inc. PMMA plates with 3.2 mm and 1.6 mm thickness (purchased from American Plastic Inc.) were used as the lid to seal the platforms.

4.2.2 Substrate fabrication

Platforms with micron-sized channel were fabricated using a LIGA-like technique [Lee et al., 2001; Madou et al., 2001]. For a single channel substrate (dimensions are described in Figure 4.1a), the mold insert was made using CNC machining on a steel block. For fabricating the more complex structure, a cascade micromixer as shown in Figure 4.1b (widths of channels range from 127 μm to 508 μm and depths of channels range from 63.5 μm to 610 μm), a female mold was made on a PMMA sheet by CNC machining first, then duplicated twice: first through casting into a male PDMS mold, and then through casting into a female epoxy (PR 500) mold. The epoxy mold was then electroplated to form a nickel mold insert (see Appendix B for details about nickel electroplating). Polymer replication was preformed through injection molding using a Sumitomo 200 ton high-pressure and high-speed machine [Lee et al., 2001].

4.2.3 Gas-resin injection

A schematic and a photo of the experimental setup are shown in Figure 4.2. The microfluidic platform and a lid were encapsulated in a holder. The top plate of the channel holder was made of a 7.5 x 4.8 x 1.2 cm^3 aluminum block with a 3.3 x 1.0 cm^2 view window at the center for the single microchannel and a 7.5 x 6.3 x 2.0 cm^3 aluminum block with a 3.5 x 2.8 cm^2 view window for the micromixer. A 0.5 cm wide x 0.6 cm deep groove was cut around the view window, so that a channel insert could be placed inside the groove. The bottom holder was made of a 7.5 x 4.8 x 2.1 cm^3 PMMA block for the single microchannel and a 7.5 x 6.3 x 2.3 cm^3 PMMA block for the

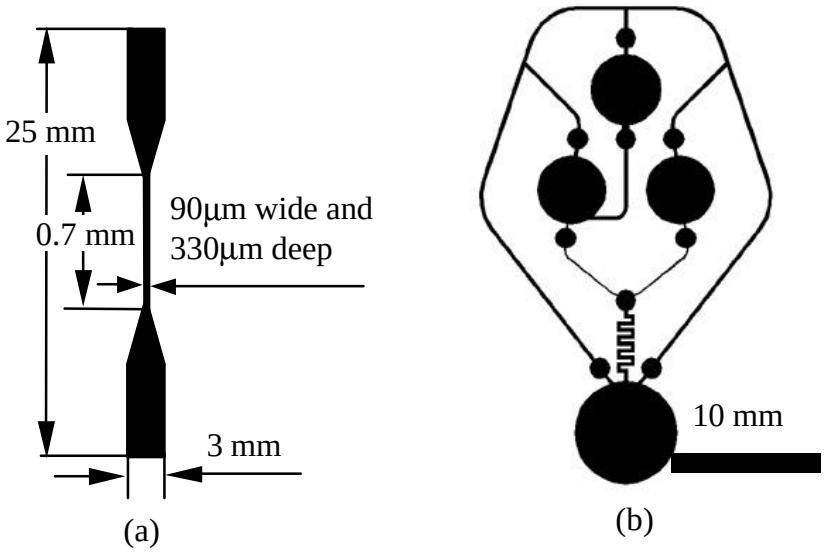

Figure 4.1. Microfluidic devices used for bonding, (a) a single channel, and (b) a cascade micromixer.

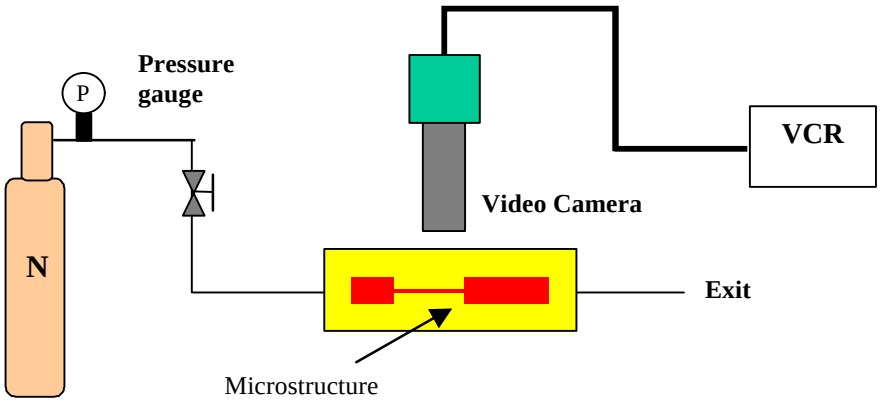

(a)

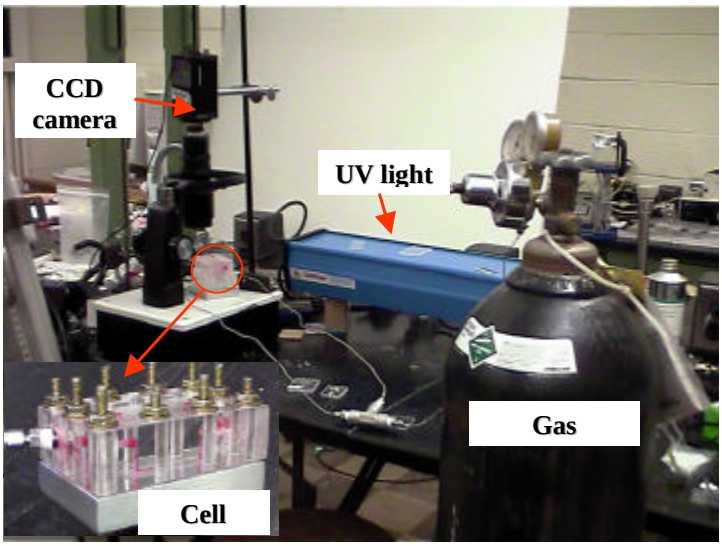

(b)

Figure 4.2. (a) Schematic and (b) photo of experimental setup for bonding and surface modification of microfluidic platforms.

micromixer. After the microchannel insert was placed inside the aluminum groove, the top and bottom holders were tightened with bolts. A nitrogen gas cylinder was used as the pumping unit and a gauge was connected to monitor the pressure. The fluid flow inside the microchannel was monitored by a video system consisting of a Cohu video camera (1.27 cm view detector area), a TV monitor, and a 6.5X zoom lens (D. O. Industries) with a 5X adapter and a 2X eyepiece. With this setup, magnifications greater than 400X can be achieved at a working distance of more than 2.54 cm. After the experiment, frames were grabbed from the motion video by commercial video software Adobe Premiere® 5.0.

The schematic of bonding by resin-gas injection is shown in Figure 4.3. After the microfluidic platform and the lid were encapsulated in the holder, several drops of HEMA mixed with Irg 651 and a surface modification agent were injected into the platform to fill the micron- and millimeter-sized channels and reservoirs, as well as the gap between the platform and the lid (Figure 4.3a). Nitrogen gas was then pumped in to replace most of the resin inside the channels and reservoirs (Figure 4.3b). The pressure of the gas ranged from 140 to 840 kPa, depending on the channel dimensions. The remaining resin was cured by ultraviolet light (Mineralight® lamp UVGL-58, Upland CA) (Figure 4.3c). Other resins such as epoxy and unsaturated polyester can also be used for bonding. In addition to photo cure, resins can also be cured by thermal or redox initiation. Since HEMA is relatively hydrophilic, can bond PMMA well, and has been widely used in various medical applications, it was chosen as the material for boding biochips in this study.

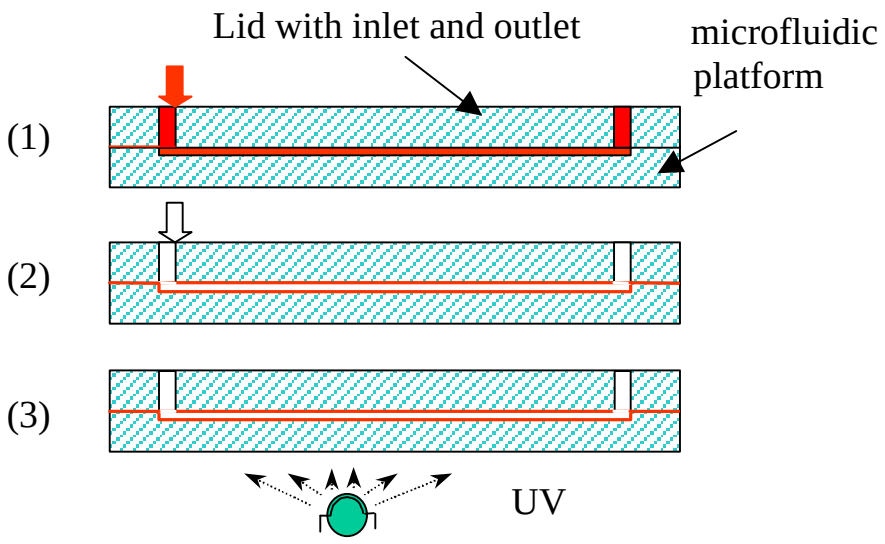

Figure 4.3. Schematic of resin-gas injection bonding process: (a) resin injection, (b) gas injection, and (c) resin curing.

4.2.4 Characterization

The bonded microfluidic device was filled with food dyes to detect any leakage. The cross section was examined by a scanning electron microscope (Philips XL 30, Philips Electron Optics) and the thickness of the PHEMA coating was then measured. The dimension and surface roughness of the fabricated microchannels were characterized by an optical profilometer (WYKO NT3300 Profiling System, Veeco Metrology Group, Tucson, AZ). The contact angle measurement between a solid surface and water can be used to determine the hydrophilicity of the surface. The advancing and receding contact angles between the surface of the microfluidic device and probe fluids (distilled water and ethylene glycol) were measured by a Dynamic Contact Angle Analyzer (DCA-322, CAHN Instruments Inc., CA). For each sample, the measurement was made at least 3 times. The substrate surface was cleaned and dried before each measurement and precautions were taken to prevent any contamination on the surface. The fluids were changed after each measurement to avoid any contamination. Two components of surface free energy of the substrate, polar (γ_s^p) and dispersion (γ_s^d) components, were calculated by using the geometric two-liquid method (DCA application software 1.0B). The interfacial free energy of the solid surface with water (γ_{sw}) was calculated by using Good-Girifalco Equation [Girifalco and Good, 1957] as follows:

$$\gamma_{sw} = \gamma_s + \gamma_w - 2(\gamma_s^d \gamma_w^d)^{\frac{1}{2}} - 2(\gamma_s^p \gamma_w^p)^{\frac{1}{2}}$$

where γ_s and γ_w are surface free energy of the platform and water, respectively; γ_w^p and γ_w^d are polar and dispersion components of surface free energy of water with values of 52 mJ/m^2 and 20.8 mJ/m^2, respectively.

4.3 Results and discussion

4.3.1 Thermal and adhesive tape bonding

Vacuum assisted heat bonding and double-sided adhesive tape bonding were also carried out in this study for comparison. Figure 4.4a shows the cross-section of a bonded micro-channel by a vacuum assisted thermal bonding. For large features (several hundreds microns to millimeters), such conventional plastic welding techniques can be used. Applying vacuum before welding may reduce voids at the welded interface, consequently, a lower pressure and temperature can be used in welding, minimizing the molten polymer from flowing into the bonded channels. Ideally, small over-flow traps should be designed along the edge of the channels to completely prevent the channels from being blocked by the molten polymer during welding. For smaller channel sizes (less than 100 microns), the design and fabrication of over-flow traps become difficult. Double-sided adhesive tape can be a useful way for micro-bonding as shown in Figure 4.4b. The main disadvantage is that the presence of adhesive tape tends to change the channel size and create an inhomogeneous interface between the substrate and the lid.

(a) (b)

Figure 4.4. SEM photos of bonded microchannels (a) by vacuum-assisted thermal bonding; (b) by adhesive tape bonding.

4.3.2 Photopolymerization

During UV curing of the resin, the UV light has to penetrate through the lid in order to reach the resin in the microchannel. The lid acts as a filter. Therefore, optical properties of the lid, such as the UV adsorption, play an important role during photo curing of the resin. The UV transparency of PC, PMMA, PDMS, and glass was examined and is plotted in Figure 4.5. It can be seen that PC is almost opaque for the UV light below the wavelength of 390 nm. Therefore, it is not suitable for the lid material. The PMMA shows some transparency at 365 nm. PDMS provides the best UV transparency in the short wavelength range. The actual UV intensity under the lid materials was measured and is summarized in Table 4.1. The data in the table confirmed that PC exhibits very poor UV transparency.

The UV photopolymerization behavior of HEMA was studied by using differential photo-calorimetry (DPC 2920, TA Instrument) at the UV intensities of 3.59 and 21 mW/cm^2. The heat flow during the progress of HEMA photopolymerization is shown in Figure 4.6. It can be seen that the reaction of the HEMA has almost finished after 60 seconds exposure to UV light (21 mW/cm^2) and about 120 seconds at 3.59 mW/cm^2, the intensity of the UV light under a PMMA lid). The total heat of polymerization can be calculated from the area under the heat flow curve. It was found that the heat of polymerization of HEMA was around 46 KJ/mol, while the heat of polymerization of HEMA reported in the literature was 50 KJ/mol [Röhm America]. Assuming that the rate of the reaction is proportional to the reaction heat exotherm, the overall conversion of the photopolymerization was found to be 92%.

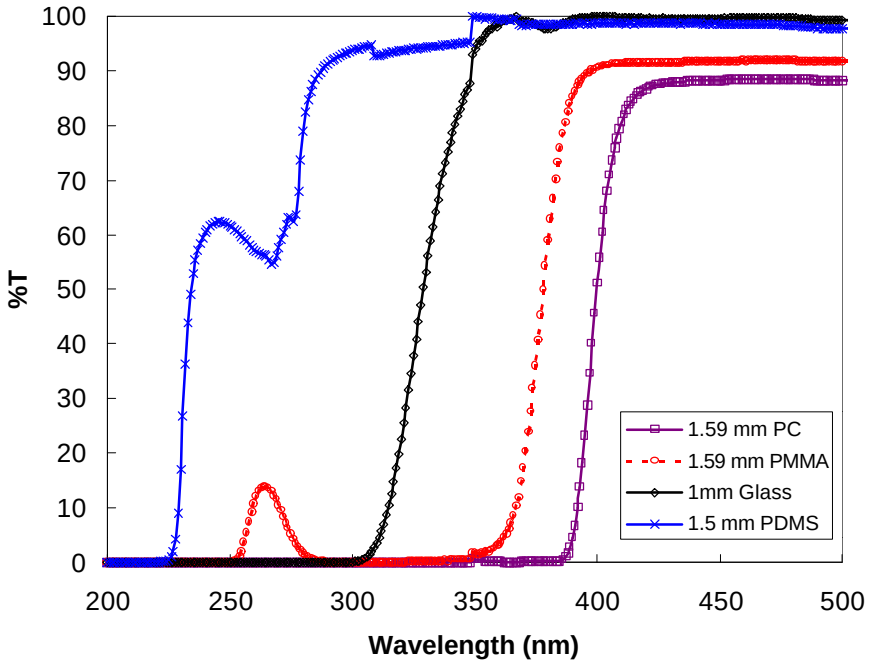

Figure 4.5. The UV transmittance spectra of PC, PMMA, PDMS, and glass.

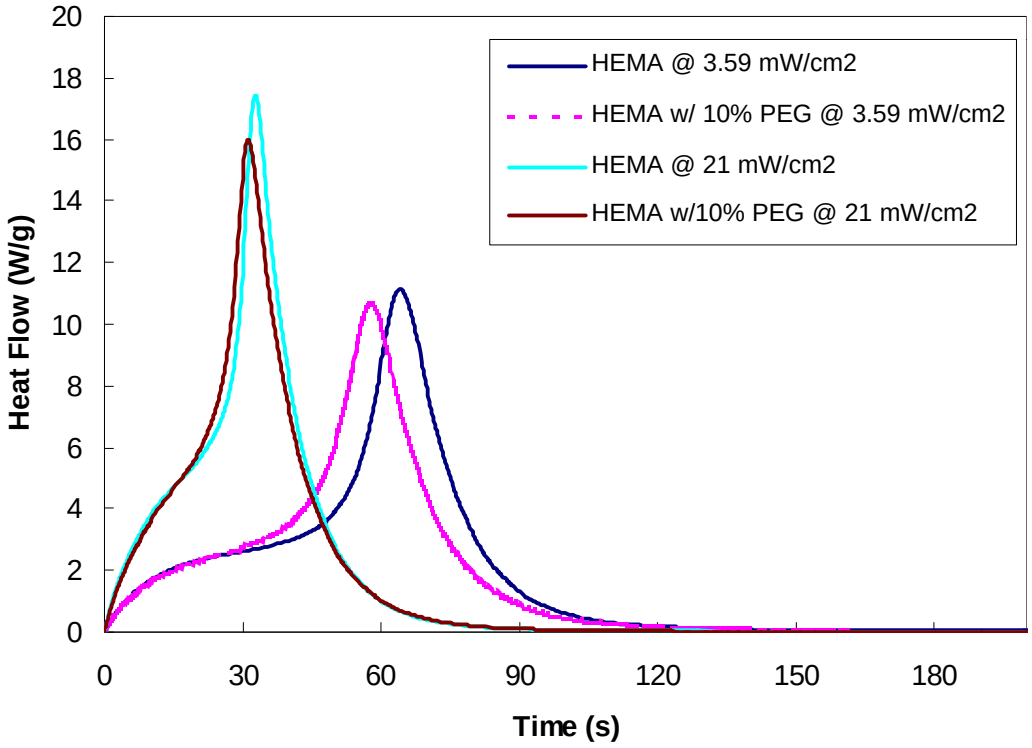

Figure 4.6. The heat flow during the photopolymerization of HEMA and HEMA w/ 10% PEG 4000 (UV intensities = 3.59 and 21 mW/cm^2).

Materials	UV intensity (mW/cm^2)	
	365 nm	All range
None	21	21
1 mm Glass	18.87	18.68
1.5 mm PDMS	19.34	19.63
1.59 mm PMMA	3.54	14.49
1.59mm PC	0.031	10.89

Table 4.1. The UV intensities under different lid materials.

Based on the photopolymerization behavior of HEMA and the UV transparency of the PMMA cover, the exposure time for the resin on the microchannel wall was set to be 10 minutes by using a UV source with the UV intensity of 21 mW/cm^2.

4.3.3 Resin-gas injection bonding

A few drops of food dye were injected into the bonded microstructure through the inlet to detect any leakage and blockage of the microchannel. It went through the inlet reservoir and the microchannel, reaching the output reservoir. A bonded channel (90 μm wide and 330 μm deep) tested by this method is shown in Figure 4.7a Complete filling of the outlet reservoir indicates that there is no block inside the microchannel. The absence of food dye outside the reservoirs and microchannel indicates no leakage. A similar result was achieved in bonding the micromixer as shown in Figure 4.7b.

A cross-section (A-A) of a bonded reservoir (3 mm wide and 300 μm deep) is shown in Figure 4.8. A close view of the reservoir corner before and after bonding is shown in Figures 4.8b and c. It can be seen that a thin layer of PHEMA resin remains in the inner surface of the reservoir and the corner is rounded after bonding. Figure 4.8a is a SEM photo of the cross-section of a bonded channel (90μm × 330μm), showing that good bonding was achieved. The surface smoothness of the bonded microchannel was examined after the bonded lid and platform was delaminated in liquid nitrogen. Very smooth channel sidewall was achieved as shown in Figure 4.9b.

In many applications, sharp corners in the microfluidic devices are undesirable since fluids may be trapped there [Madou et al., 2001]. Rounded or raindrop-shaped corner are more favorable. By using resin-gas injection bonding, the sharp corner of the

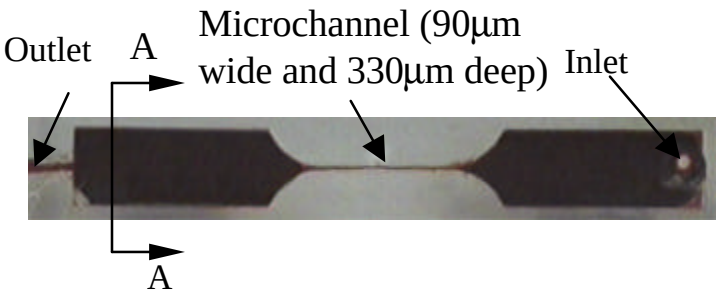

(a)

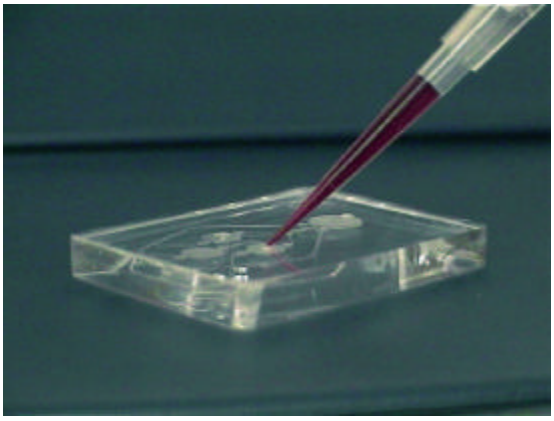

(b)

Figure 4.7. (a) Top view of a bonded microstrchannel filled with food dye and (b) a bonded cascade micromixer.

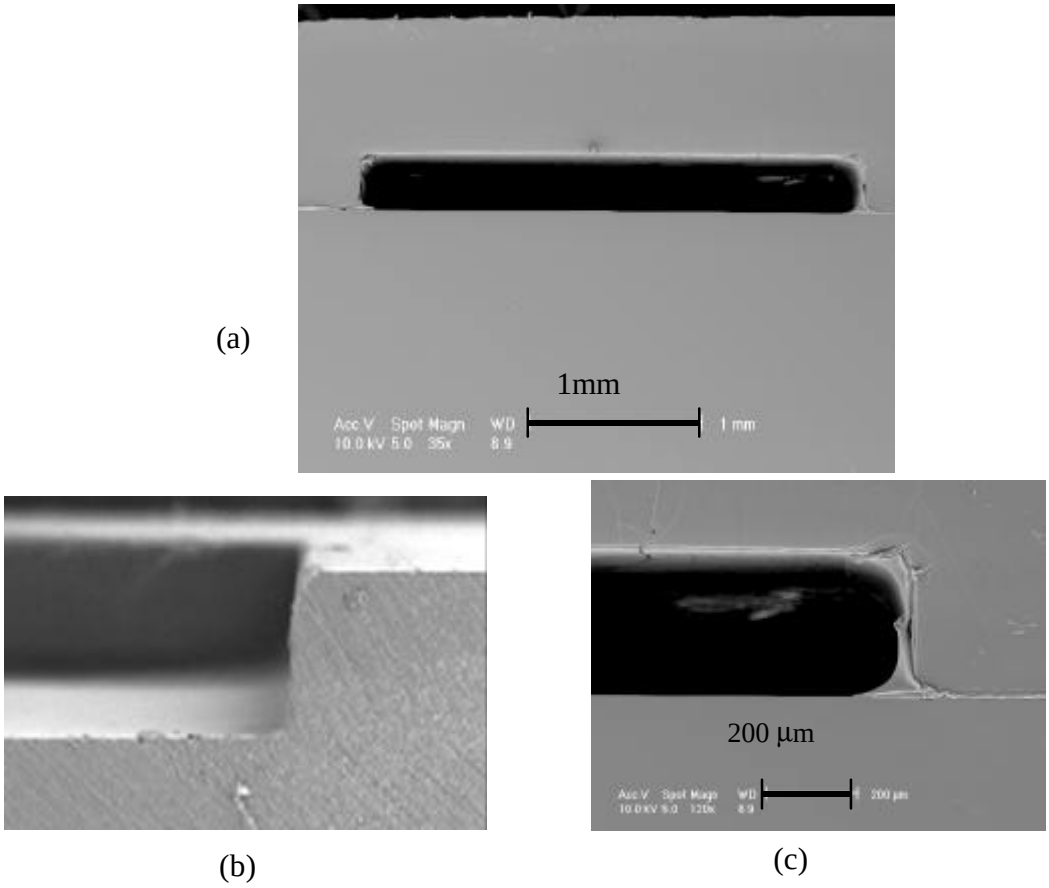

Figure 4.8. SEM photos of cross-section view of (a) a bonded reservoir, (b) enlarged view of reservoir, and (c) enlarged view of bonded reservoir.

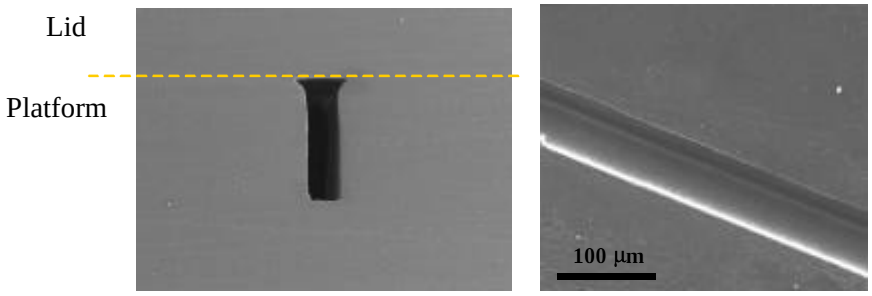

Figure 4.9. SEM photos of (a) the cross-section of a bonded microchannel (90 μm × 330 μm) and (b) the top view of a bonded microchannel after de-lamination.

reservoir can be rounded which is demonstrated in Figure 4.10. The top view of the corner of a bonded reservoir is shown in Figure 8b. It can be seen that the sharp corner was rounded like a streamline, which may facilitate the fluid flow. The cross-section view (B-B) of the same location (see Figure 4.10c) shows that more resin (HEMA) remained near the corner than in other areas (e.g., see Figure 4.10a).

4.3.4 Surface modification

The contact angle measurement between a solid surface and water can be used to determine the hydrophilicity of a material. Table 4.2 compares the measured surface properties of PMMA with several PMMA surfaces treated by resin-gas injection. It can be seen that large contact angles were observed on the untreated PMMA surface and PMMA coated with PHEMA, indicating that these surfaces are hydrophobic. The interfacial free energies of PMMA surfaces with water decreased from 12.33 to 2.76 mJ/m^2 after different surface treatments. The PMMA surface coated with PHEMA and the PEG 4000 mixture (90:10 by weight) has the lowest interfacial free energy with water and it meets the biocompatibility requirement (1~3 mJ/m^2) [Chen and Ruckenstein, 1991].

4.3.4.1 Reagent loading

In order to demonstrate the effect of surface hydrophilicity on reagent loading, a drop of food dye was placed on the tope of the inlet reservoir of the bonded microfluidic platform and the flow of the food dye was monitored by a CCD camera from the top (Figure 4.11a). Figure 4.11b shows snapshots taken at different times of a PMMA

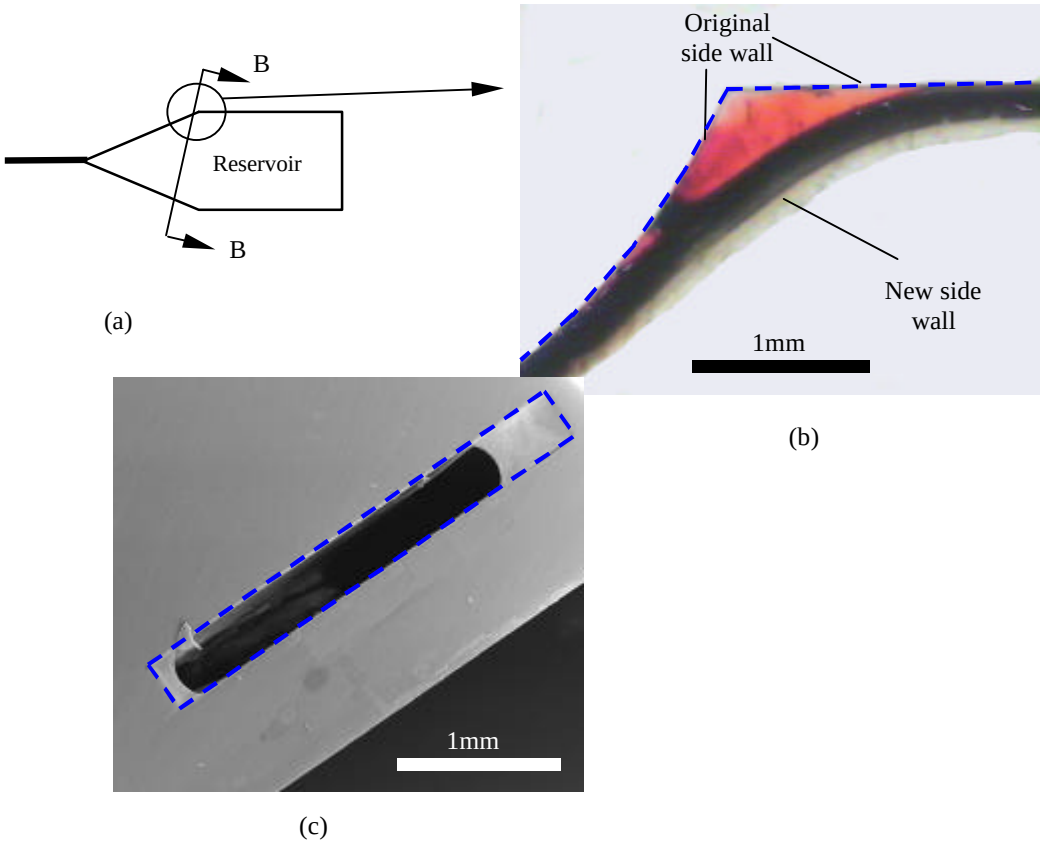

Figure 4.10. Photos at a bonded reservoir corner: (a) Schematic of the reservoir, (b) top view of the reservoir corner, and (c) SEM photo of the cross-section (B-B) at the reservoir corner. Lines were added to mark the boundary on (b) and (c).

Materials	θ_A/water	γ^p (mJ/m^2)	γ^d (mJ/m^2)	γ_s (mJ/m^2)	γ_{sw} (mJ/m^2)
Untreated PMMA	70.03±1.03	24.11±1.68	12.85±1.35	36.96±0.47	12.33
Coated with PHEMA	68.19±0.71	17.16±1.17	18.25±1.10	35.41±0.35	8.31
Coated with PHEMA and 0.5% SDS	58.15±1.82	9.76±2.52	34.57±3.63	44.32±2.04	4.10
Coated with PHEMA and 20% EG	57.12±1.68	12.68±1.23	32.09±1.25	44.77±0.48	3.44
Coated with PHEMA and 10% PEG 4000	53.01±1.72	19.31±1.28	29.91±1.32	49.22±0.91	2.76
Glass [Kaelble, 1971]	56	19.2	37.6	56.8	1.03

Table 4.2. The measured water contact angles and calculated surface free energy of treated and untreated PMMA. θ_A -the advancing contact angle between solid surface and distilled water; γ^p- polar component of surface free energy; γ^d –dispersion component of surface free energy; γ_s – surface free energy; γ_{sw} - interfacial free energy of substrate with water.

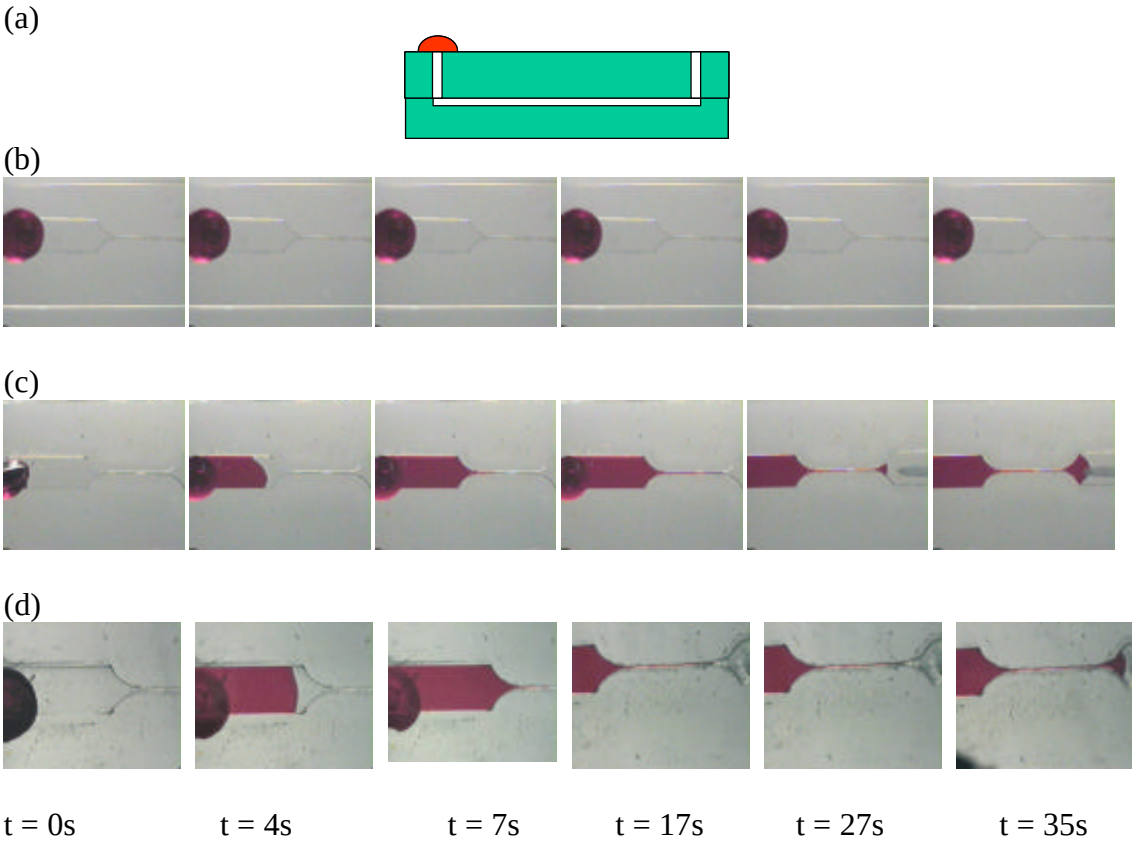

Figure 4.11. (a) Schematic of experiment to test the effect of surface modification on reagent loading; snapshots of (b) a platform bonded by PHEMA, (c) a platform bonded by PHEMA and 10% PEG 4000, and (d) a platform with local surface modification.

platform that was bonded by PHEMA only. The food dye stayed at the inlet and no flow was observed. Figure 4.11c shows snapshots for a similar platform that was bonded by PHEMA with 10% PEG 4000. It can be seen that as time elapsed, the food dye flowed into the microchannel spontaneously from the inlet to the outlet reservoir. It can be seen from Table 4.2 that the PMMA substrate coated with PHEMA and 10% PEG has a lower interfacial free energy with water than the substrate coated with PHEMA only. The former is considered more hydrophilic than the latter. Therefore, the water-based food dye can flow into the platform.

4.3.4.2 Local surface modification

Micropatterning to produce regions with different physicochemical properties has become increasingly popular for the development of improved biomaterials and microdevices. For example, protein adsorption and cell attachment can be controlled if a material is developed with regions of hydrophobic and hydrophilic. Many researchers have applied lithography techniques to manipulate the proteins, cells [Kane et al., 1999; Park et al., 1998], and other biological macromolecules [Li et al., 1999] on selectively modified silicon surfaces. Materials other than photoresists have also been applied for micropatterning by UV polymerization techniques [Ward et al, 2001; Beebe et al, 2000].

Functional microfluidic components have been produced by patterning regions inside the microchannels. Using patterned hydrophobic regions inside a silicon microchannel, nanoliter-sized liquid can be accurately metered [Handique et al., 2000], which is described in the metering section in Chapter 2. The hydrophobic regions inside the microchannel were patterned by bulk and surface machining on silicon substrate

before the platform was bonded. Microvalves inside microchannels were fabricated by liquid phase photopolymerization [Beebe et al., 2000] of hydrogel around prefabricated posts. The microvalves consist of a stimuli-responsive hydrogel structure that undergoes a volume change in response to changes in local pH. Swelling and de-swelling of the hydrogels can regulate the fluid flow in microchannels as shown in Figure 4.12. Patterns other than the circles for microvalves have also been demonstrated with the minimum feature size of 25 μm.

Combining photolithography, photopolymerization, and resin-gas injection techniques, localized surface properties in the microchannels can be achieved to perform certain functions. Figure 4.13 shows the schematic of using resin-gas injection method for local surface modification. The experimental setup and procedure were the same as previously described in resin-gas injection bonding section, except that prior to curing of the remaining resin mixture (bonding agent, such as HEMA, and surface modification agent, such as PEG), a mask (e.g., a photomask used in the lithography process) was placed between the lid plate and the UV source. The mask blocked out the UV light locally, so that the resin mixture in the locations under the mask would not cure. After the curing of the un-masked parts was complete, the uncured resin mixture was removed by bleaching the surface with water or other solvent similar to the development step in the photolithography process. Consequently, selective patterning inside the microchannel can be achieved at the same time of bonding. Selective patterning a resin mixture with hydrophilic polymers (e.g., PEG) can leave the un-patterned polymer microchannel surface hydrophobic, leading to a capillary valve for the aqueous solution (e.g., most buffer solutions used in bio-analysis).

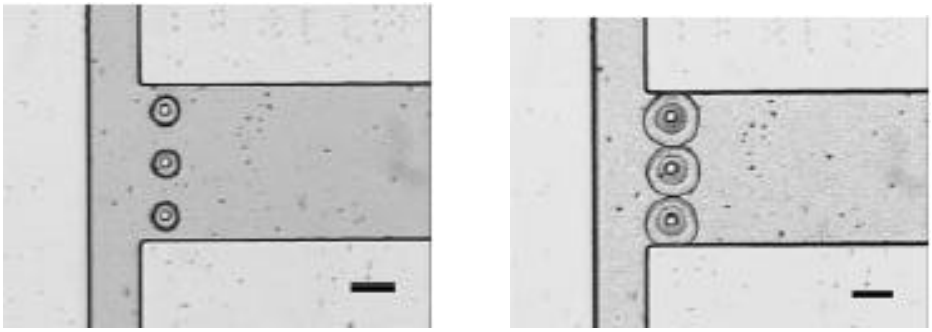

(a) (b)

Figure 4.12. Photos of fabricated microvalves: (a) The de-swelled hydrogels allow fluid to flow down the side branch and (b) swelled hydrogels block the side channel branch (Beebe et al. [2000] with permission from the author).

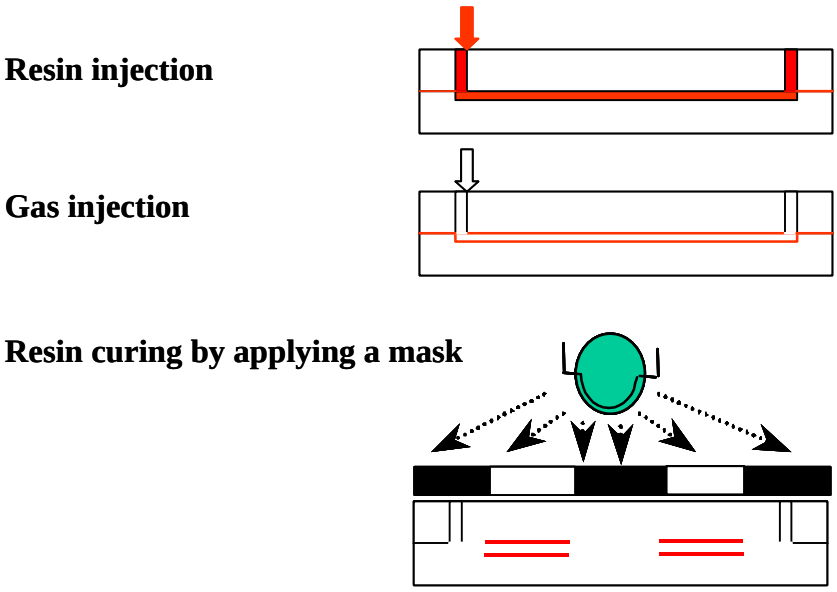

Figure 4.13. Schematic of local surface modification.

The possibility of using HEMA as the resin to create a selective pattern on PMMA substrate was tested. Figure 4.14 shows the mask and the pattern created on the PMMA substrate. It can be seen that the pattern on the mask was clearly duplicated onto the PMMA substrate. The dimension of the smallest channel on the mask is about 100 μm.

An example of local surface modification is shown in Figure 4.11d. By this method, the inlet reservoir and most of the microchannel were coated with PHEMA and 10% PEG 4000, while both the end of microchannel near the outlet reservoir and the outlet reservoir were coated only with PHEMA. Figure 4.11d shows snapshots of reagent loading on this platform. It can be seen that the food dye flowed into the microchannel spontaneously, but stopped at the end of the microchannel near the outlet reservoir where the surface changed (the fourth and fifth snapshots) from hydrophilic to hydrophobic. By applying a small pressure at the inlet, the food dye could flow to the outlet reservoir (the sixth snapshot).

4.4 A case application - DNA separation by monolithic stationary gel

4.4.1 Experimental

4.4.1.1 Materials

Acrylamide (electrophoresis grade, momomer), 2-2-dimethoxy-2-phenylacetophenone (Irg 651, photoinitiator), hydrosyethyl cellulose (HEC, average M_V

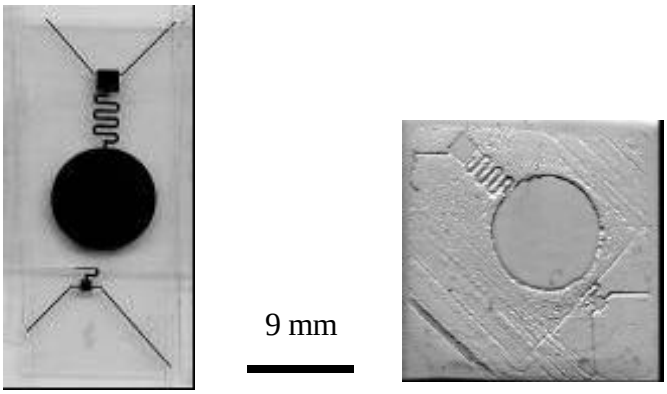

(a) (b)

Figure 4.14. (a) Mask and (b) the created pattern using HEMA on PMMA substrate.

= 720,000, sieving material), polyethylene glycol with molecular weight of 4×10^6 (PEG 4M, sieving material), thiazole orange (TO, DNA probe) were purchased from Aldrich. The crosslink agent for acrylamide, N, N'-methylene-bisacrylamide (bis, electrophoresis grade), was purchased from Fisher Scientific. A DNA standard (ΦX174 Hae III Digest, 381 μg/ml) and the 5X Tris-Borate-EDTA (TBE) buffer solution were purchased from Sigma-Aldrich (St. Louis, MO).

4.4.1.2 Microchips

Two microchip designs were used for DNA separation. A simple design (chip A) is shown in Figure 4.15a, where the separation channel is 127 μm wide, 100 μm deep, and 5.3 cm long. Four reservoirs were connected at the end of each microchannel for buffer solution, DNA sample, and wastes, respectively. They also provide the access of the electrodes. A double-T structure (see Figure 4.15b) was adopted for DNA sample injection. The detection can be carried out at any point between the sample injection point and the waste reservoir 4. Therefore, the actual separation length ranges from 0 to 5.3 cm. The second design is similar to Caliper's DNA Labchip® for multiple DNA separation as shown in Figure 4.16. In this design, a T structure was adopted for sample injection, and the channel dimensions, 127 × 100 μm, are the same as in Figure 4.15a. This design is able to separate 6 DNA samples loaded in reservoirs 2.

The two DNA sequencing microchips was fabricated by the CNC machining on a 3.2mm thick PMMA plates and bonded with a 1.59mm PMMA plate by using the resin-gas injection technique described in Section 4.2.3. A vacuum pump (DOA-P104-AA,

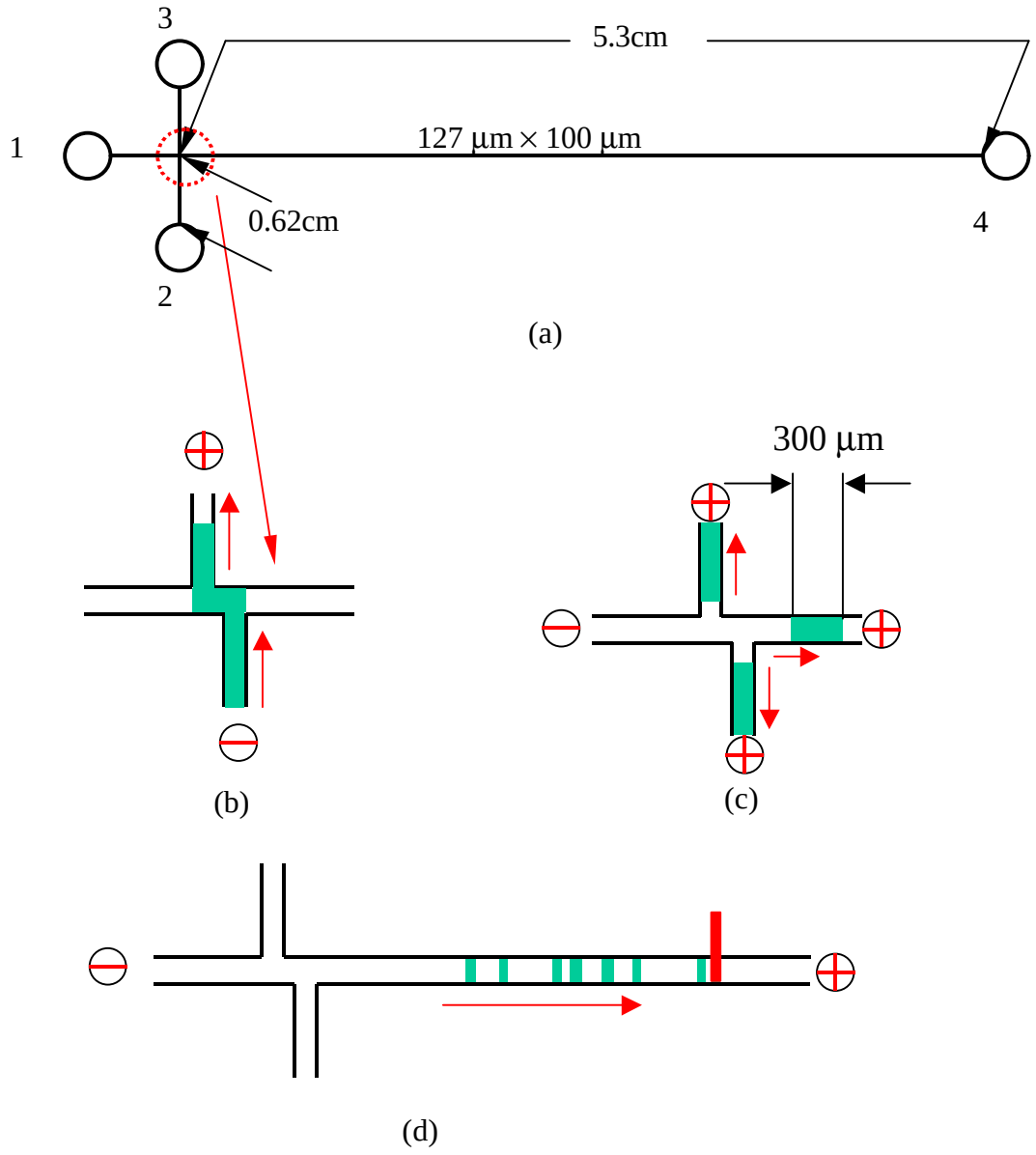

Figure 4.15. (a) Microchip design (chip A) for DNA separation (Reservoirs: 1 –buffer solution, 2 – sample, 3 – sample injection waste, and 4 – waste) and electrophoresis procedures: (b) sample injection (double-T structure for sample injection), (c) pulling back to form a sample plug, and (d) separation.

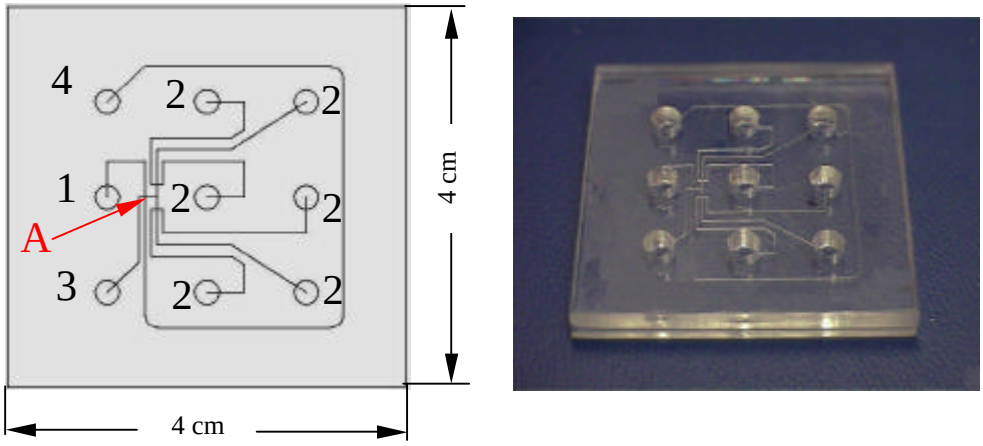

Figure 4.16. Schematic and photo of microchip design (chip B) for DNA separation. Point A refers to the sample injection point (Reservoirs: 1 –buffer solution, 2 – sample, 3 – sample injection waste, and 4 – waste).

GAST Manufacturing) was used to replace the gas cylinder and the resin inside the microchannel was removed by applying vacuum (12 ~ 25 cmHg).

4.4.1.3 Crosslinked Polyacrylamide gel

Polyacrylamide hydrogels are widely used in slab-gel electrophoresis and capillary electrophoresis for bioseparations because they are chemically and physically inert, stable to pH and to a broad range of ionic strength and compositions, and non-reactive with samples, stains, and biological materials [Hawcroft, 1997].

Crosslinked polyacrylamide gels are commonly formed from the free radical copolymerization between the monomer acrylamide and the crosslinking agent N, N'-methylenebisacrylamide (Bis). The chemical structures of acrylamide, bis, linear polyacrylamide, and crosslinked polyacrylamide are shown in Figure 4.17. The structure of polyacrylamide is similar to that of polyethylene, but having a hydrogen on every other carbon replaced by an amide group, $–CONH_2$. The molecule is composed of repeating $–CH_2–CH(CONH_2)–$ units. The free, unlinked amide groups can form hydrogen bonds with water and give the crosslinked polyacrylamide a great affinity for water.

4.4.1.4 Gel loading

The monomer gel solution was prepared by mixing acrylamide, crosslink agent bis, and photoinitiator Irg 651 in 1X TBE buffer solution. The gel loading process followed the same the resin-gas injection after the platform was bonded to the lid. After the UV exposure, the microchip was placed in an oven at 70 ^oC for 1~2 hours to achieve complete gel reaction. Prior to the electrophoresis, 1X TBE buffer solution with 5 μM

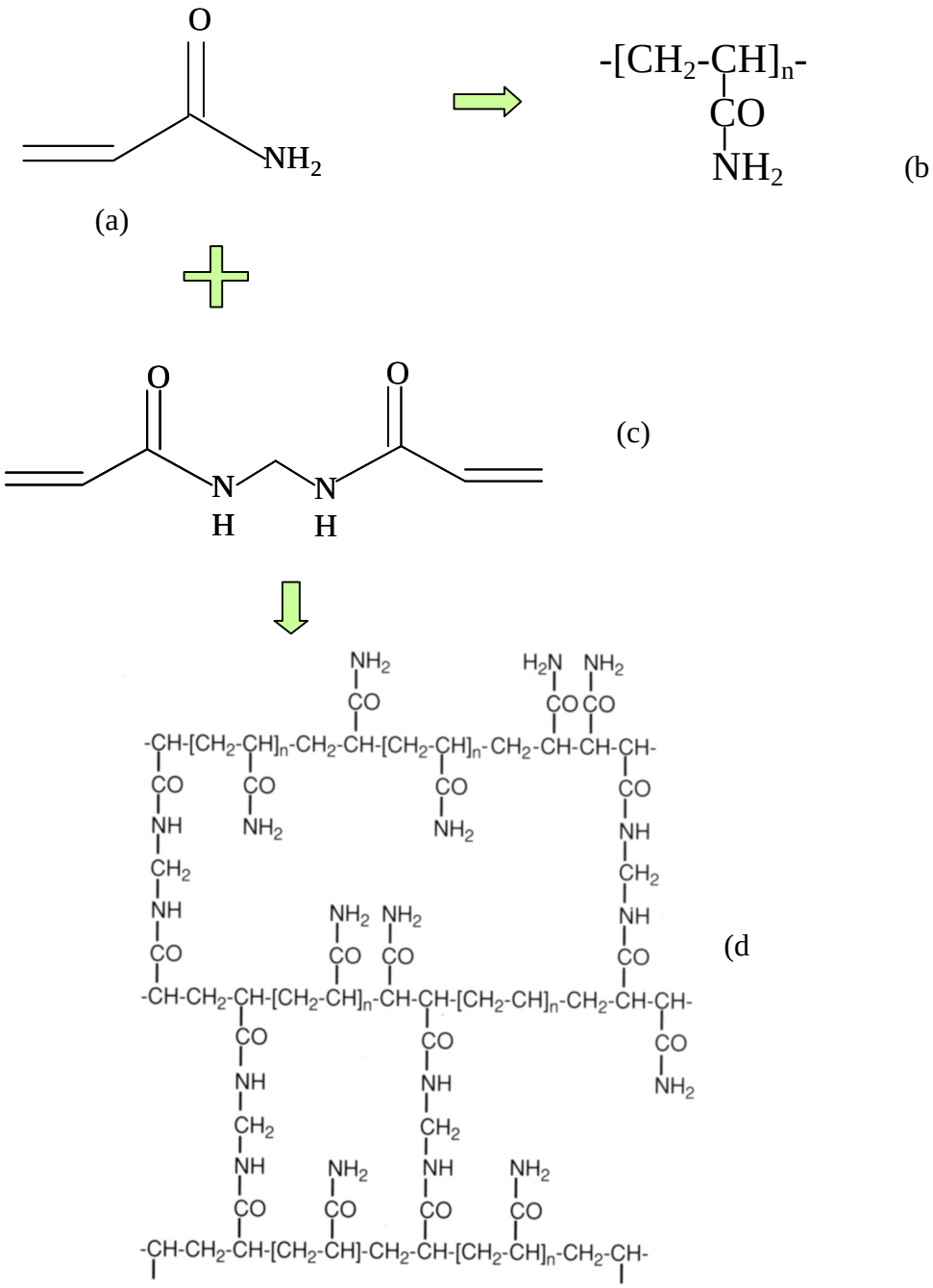

Figure 4.17. Chemical structures of (a) acrylamide, (b) non-crosslinked polyacrylamide, (c) crosslink agent N,N'-methylene bisacrylamide (Bis), and (d) crosslinked polyacrylamide.

TO was loaded into the microchannels to swell the dry polyacrylamide gel layer left on the walls of the microchannels.

4.4.1.5 Experimental procedures

The DNA standard was diluted in a 0.2X TBE buffer solution to 10 μg/ml from the stock solution (381 μg/ml). The TO dye was prepared in 100 μM in a 1X TBE buffer solution. It was further diluted to 5 μM in the sieving (HEC or PEO) solutions.

The experimental setup for DNA separation is shown in Figure 4.18. Voltages was applied to the reservoirs via a high voltage power supply system, which consists of a low voltage, programmable power supply (72-6695, Tenma® Test Equipment, Springboro OH), two miniature DC to HV (high voltage) DC converters (G10 and G20, Emco High Voltage Corp., Sutter Creek CA), and a DPDT (double pole double throw) relay (0700A, MCM Electronics). The 72-6695 power supply is capable of voltage and current outputs, timer, and over voltage/current protection. It provides the input voltages for miniature DC to HV DC converters. The G10 is used for output voltage up to 1,000 V and G20 for output voltage up to 2,000V. The relay is used to switch the polarity of the electrodes.

Detection was carried out on-chip using an inverted fluorescence microscope (Nikon ECLIPSE TE2000-U). A 100W mercury light source with a 490 nm filter and a dichroic mirror was used as an excitation source. The fluorescence signal was obtained through a dichroic mirror and a 510 nm filter. Images at the detection point were recorded sequentially by a 12-bit high-resolution monochrome digital camera system (CoolSnap HQ, Roper Scientific). The fluorescence intensities were extracted directly from the

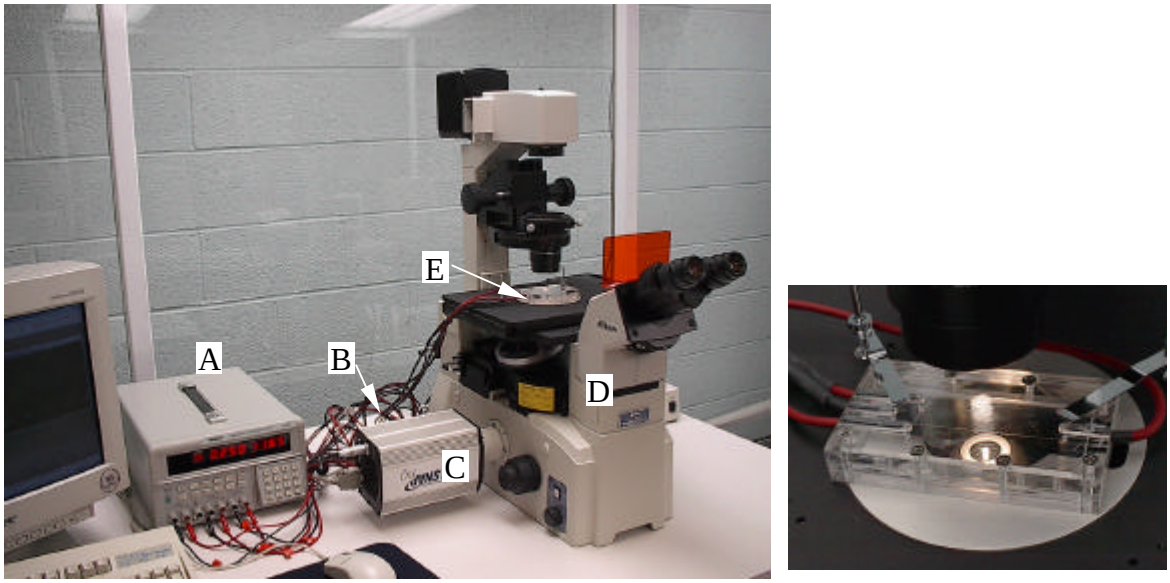

(a) (b)

Figure 4.18. (a) Experimental setup for DNA separations by microchip-based electrophoresis (A – power supply, B – relay and miniature DC to HV DC converters, C – Cool CCD camera, D – TE-2000U inverted fluorescence microscope, E – electrode holder) and (b) close view of the electrode holder.

sequential video images by using an image analysis software (Fryer Metamorph Image Analysis System). The intensity was an average over a 100 μm × 30 μm detection area.

4.4.1.6 Electrophoresis procedures

As described in the literature, the electrophoresis separation of the DNA fragments follows three steps: injection of DNA samples, pulling back to form the sample plug, and the separation as illustrated in Figure 4.15b, 15c, and 15d. The first step is the injection of DNA samples. With an electric field applied between reservoirs 2 and 3 and no voltage applied between reservoir 1 and 4, the DNA migrated from reservoir 3 towards reservoir 2 and filled the injection cross. The next step (pulling back) is to move the sample in the injection cross forward to the separation channel and pull the rest back to reservoirs 2 and 3 to form a DNA sample plug for separation. The third step is the separation with an electric filed applied between reservoirs 1 and 4. The DNAs migrated towards reservoir 4 under the electric field and were separated through the sieving materials inside the separation channel. The voltages applied and times for each step are summarized in Table 4.3.

4.4.2 Results and discussion

4.4.2.1 Substrate materials

The inherent autofluorescence background of the polymeric materials can be problematic for fluorescence detection in the electrophoresis separation of DNA. The

Process	Voltage Applied (V)				Time (s)
	1	2	3	4	
Chip A					
Injection	Float	400	0	Float	25
Pulling back	0	500	500	1100	5
Separation	0	Float	Float	1100	150
Chip B					
Injection	Float	600	0	float	50
Pulling back	0	600	600	1600	5
Separation	0	Float	Float	1600	600

Table 4.3. Voltage applied and sequences for electrophoresis separation on DNA sequencing chip A and chip B.

fluorescence background of glass and several polymeric substrates (i.e., PC, PS, PMMA, and PDMS) were examined at the excitation of 490 nm (the same excitation wavelength used in the DNA separation). The emitted fluorescence intensities from 510 nm to 550 nm were recorded. Figure 4.19 shows the fluorescence background of these substrate materials. It can be seen that PMMA and PDMS have a comparably low background, similar that of the glass. On the other hand, PC and PS have a very strong fluorescence background at 510 nm (at which the DNA is detected), higher than that of most of the DNA fragment (200 ~ 300 arbitrary unit together with background). Because of its good combination of optical clarity, mechanical strength and low cost, PMMA was selected as the dense material in the microfluidic experiments.

After its fabrication, the polymer microdevice has to be closed to perform microfluidic functions. The fluorescence background of the bonding materials may also cause problems for the detection. The fluorescence background of two bonded microdevices, one laminated with the adhesive tape and the other covered with another PMMA plate by the resin-gas injection technique with HEMA as the bonding agent, were examined. The separation channels were filled with 1% 4M PEO with 5μM TO. Figure 4.20 shows photos of the fluorescence background of these two microdevices. It can be seen that the one laminated with the adhesive tape shows very strong fluorescence background inside the microchannel (~320 arbitrary unit), while that outside the microchannel is low (~ 160 arbitrary unit). The possible reason is that materials on the adhesive tape has interaction with the dye and emits fluorescence in the detection range. We found that PMMA-based microdevices bonded with PHEMA (see Figure 4.20b) has

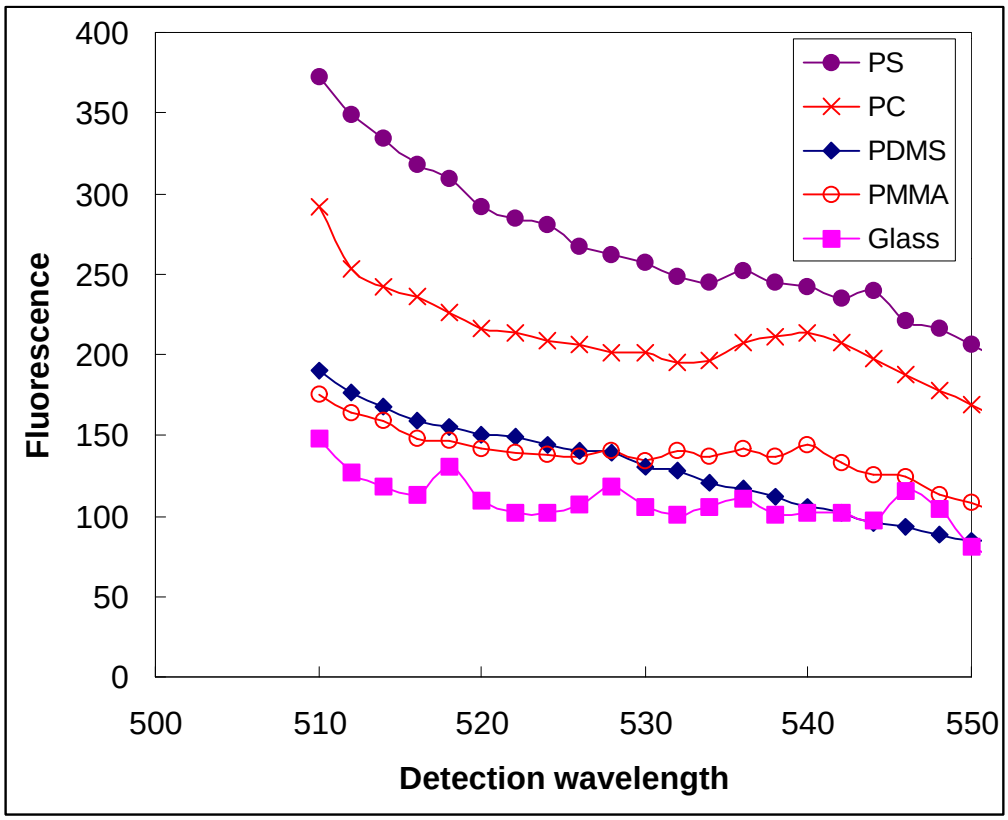

Figure 4.19. The fluorescence background (excitation at 490 nm) of several platform materials.

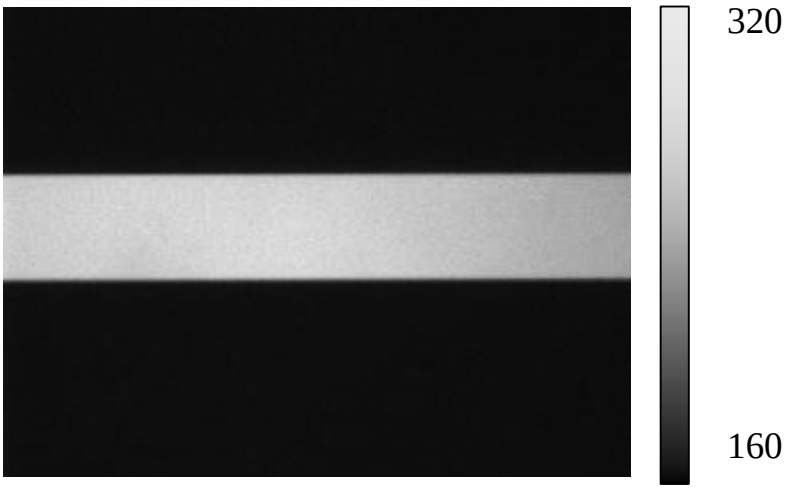

(a)

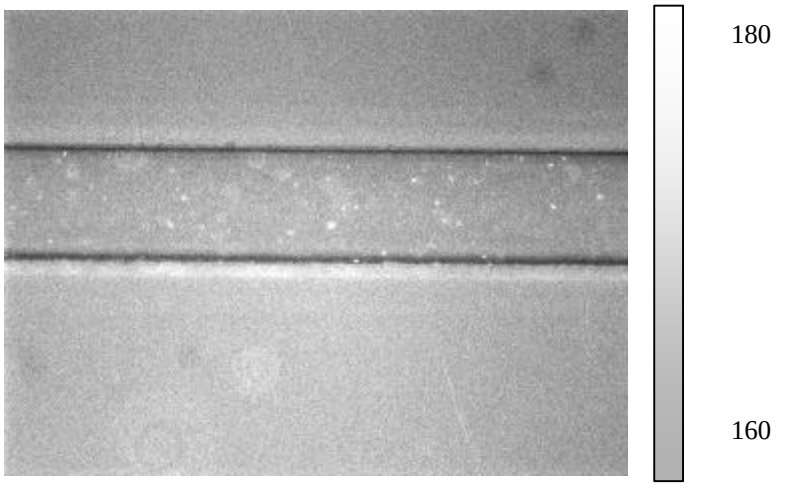

(b)

Figure 4.20. The fluorescence background (excitation at 490 nm and detection at 510 nm) of bonded microdevices: (a) by adhesive tape lamination and (b) by the resin-gas technique with HEMA as the bonding agent.

comparable low fluorescence background everywhere (~170 arbitrary unit), indicating no interaction between the PHEMA and the fluorescence dye (TO).

4.4.2.2 Photopolymerization behavior

Polyacrylamide gels are commonly produced through redox polymerization by using a mixture of ammonium persulphate and N, N, N', N'-tetramethylethylenediamine (TEMED) as the initiator of the system. This polymerization process usually requires up to an hour to complete. Photopolymerization, on the other hand, can provide much faster polymerization rate, thereby can reduce the reaction time to 5~10 minutes. The photopolymerization behavior of acrylamide was studied by using differential photo-calorimetry (DPC 2920, TA Instrument) at the UV intensity of 21 mW/cm^2.

The heat flow during the progress of UV photopolymerization of the acrylamide was shown in Figure 4.21. It can be seen that the reaction of the acrylamide has almost finished at 60 seconds, which is much shorter than the time for conventional redox polymerization. The total heat of polymerization can be calculated from the area under the heat flow curve. It was found that the heat of polymerization of acrylamide at different crosslinking agent percentage (1 ~ 5%) was 76 ±2 KJ/mol, which is very close to the heat of polymerization of acrylamide from the literature (82.8 KJ/mol) [U.S. Environmental Protection Agency, 1981]. Assuming that the rate of the reaction is proportional to the reaction heat evolved, the overall conversion of the UV-cured polyacrylamide was about 91%, which is similar to that of the conventional redox polymerization.

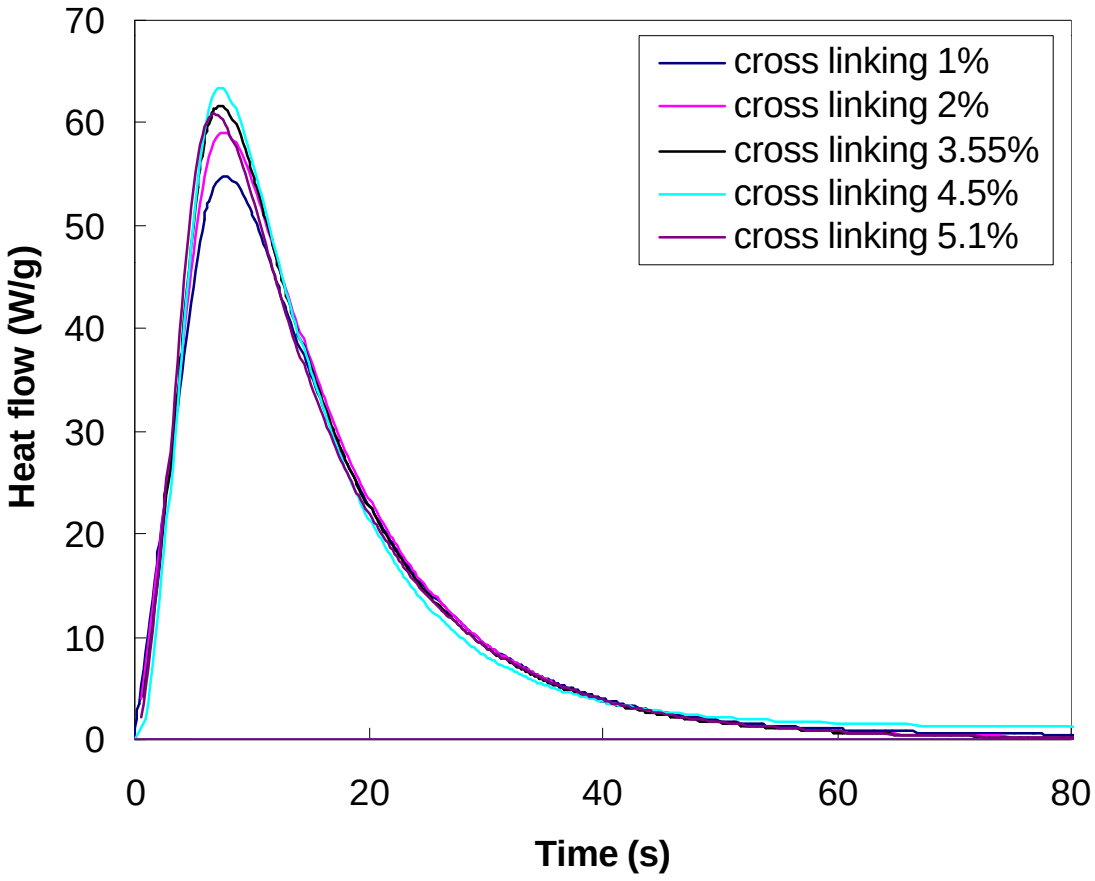

Figure 4.21. The heat flow during the photopolymerization of acrylamide (UV intensity = 21 mW/cm^2) at different crosslinking ratio.

4.4.2.3 Swelling behavior of acrylamide hydrogel

The swelling ratio is an important property of hydrogels. In general, the swelling ratio, which is defined as the ratio of the weight of the swollen sample to the weigh of the dry matrix, is used to characterize the swelling behavior of hydrogels. Factors that affect the swelling ratio mainly include the crosslinking ratio, chemical structures, and environmental conditions such as the pH value and temperature, etc. [Peppas et al., 2000].

The swelling ratio of the photopolymerized acrylamide gel in the 1X TBE buffer solution was measured as shown in Figure 4.22. It can be seen that the crosslinking ratio, the ratio of the crosslinking agent to the polymer repeating unites, has a dominating effect on the swelling behavior. The higher the crosslinking ratio, the more crosslinking agent is incorporated in the hydrogel structure. Highly crosslinked hydrogels have a tighter structure, and tend to swell less compared to the same hydrogels with a lower crosslinking ratio. The chemical structure of the polymer may also affect the swelling ratio. The equilibrium swelling ratio of poly (N-isopropylacrylamide) crosslinked by bis in water varied from 7.61 to 16.8 times of the original weight when the molar ratio of N-isopropylacrylamide (NIPA)/bis increased from 10:1 to 100:1 [Zlatanic and Petrovic, 2001].

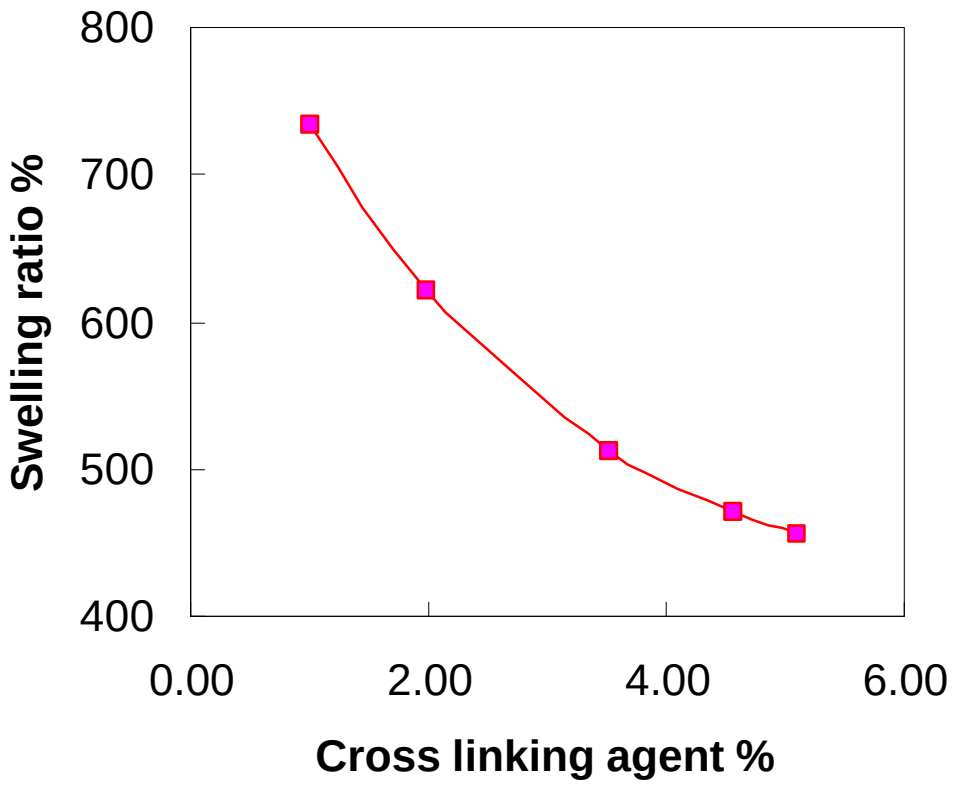

Figure 4.22. Swell ratio of the polyacrylamide gel vs. crosslinking ratio.

4.4.2.4 Loading of sieving material

Figure 4.23 shows the progresses of loading three different sieving materials by capillary force only in DNA sequencing chip A. The 0.75% 720K HEC solution and 1.0% 4M PEO solution were loaded into an empty channel with dimensions of 127μm × 100 μm. The TBE buffer solution was loaded into a channel (the same dimension) coated with a layer of dried crosslinking polyacrylamide gel. The portion of the separation channel shown in Figure 4.23 is about 1.5 cm away from the sample injection point. It can be seen that the time for the PEO, HEC, and buffer solution traveling 1cm distance are 98, 42, and 2.43 seconds, respectively. It should be noted that the loading speed of each sieving material in the separation channel was not uniform through the process. The speed in the first 5 mm distance was much faster than that in the second 5 mm distance. By the capillary force only, filling a linear polymer solution into a separation channel of 5 cm length could take more than 10 minutes. Vacuum or syringe pump could assist the loading process. However, air bubbles may be introduced into the microchannel, which is problematic in the electrophoresis process. By coating a dry polyacrylamide gel on the surface of the separation channel, sample loading (by capillary force) becomes very simple and the loading time is very short, because the TBE buffer solution has a much lower viscosity than the conventional sieving solutions.

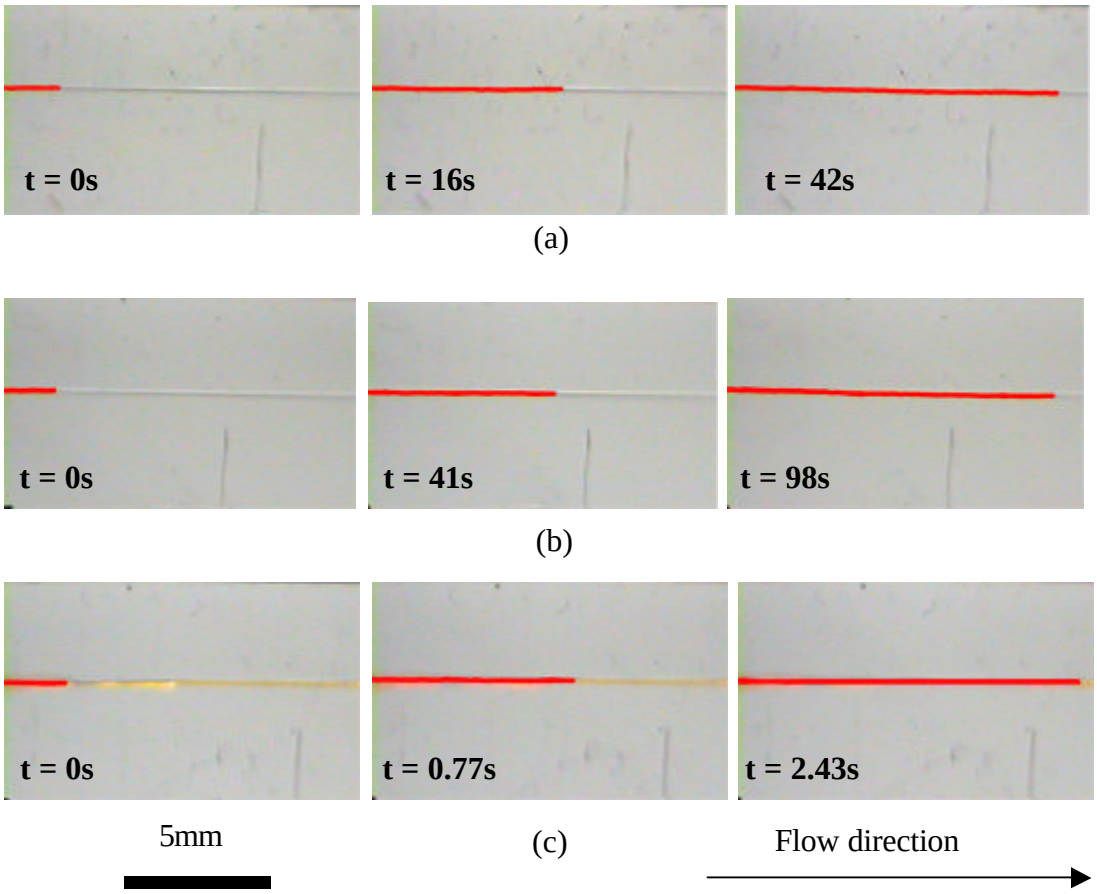

Figure 4.23. Loading of sieving materials in the separation channel: (a) 0.75% HEC (MW = 720K) in an empty channel, (b) 1.0% PEO (MW = 4M) in an empty channel, and (c) TBE buffer solution in a channel pre-filled with acrylamide gel.

4.4.2.5 DNA separation

The performance of two bonded DNA sequencing microdevices was evaluated by separating the fragments in the DNA standard (ΦX174 Hae III Digest, 11 fragments with size ranging from 78 to 1353 base pair). Figure 4.24 shows the fluorescence intensities of separated fragments in the DNA standard in chip A and chip B, using 1.0% 4M PEO or 0.75% 720K HEC as the sieving materials, respectively. All fragments are resolved.

Figure 4.25 shows the fluorescence intensities of the separated DNA fragments in chip A, with the crosslinked polyacrylamide gel (1% crosslink agent) coated on the wall of the separation channel. All fragments are resolved with the exception of the 271 and 281 base pair doublet. The imperfection of the separation may result from the insufficient polyacrylamide gel left on the channel walls and insufficient swelling of the gel to totally fill the separation channel.

4.5 Summary

A new technique, resin-gas injection, has been developed for bonding and surface modification of polymer-based microfluidic devices. This method successfully bonded microfluidic platforms from a simple single-channel structure, to more complex patterns. By adding surface modification agents, the interfacial free energy of the substrate with water decreases. By applying the masking technique, local modification of the channel surface was achieved through cascade resin-gas injection. This approach was also applied to coat a layer of crosslinked polyacrylamide gel on the walls of the separation channel,

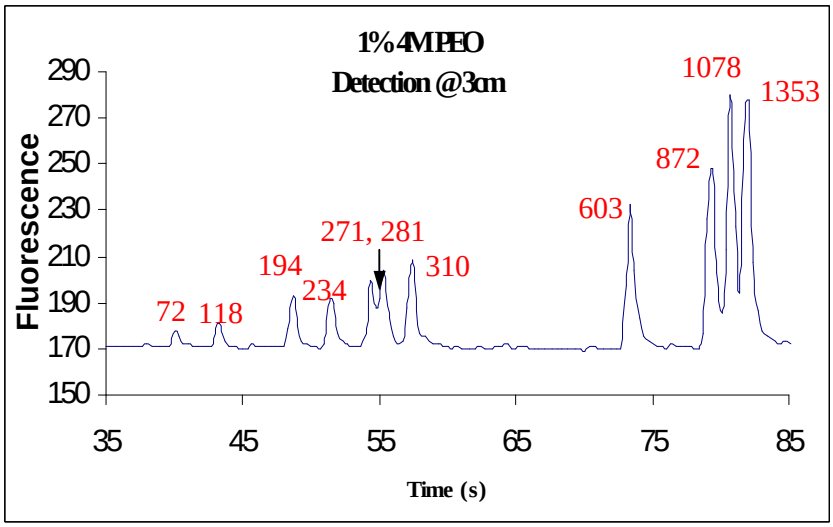

(a)

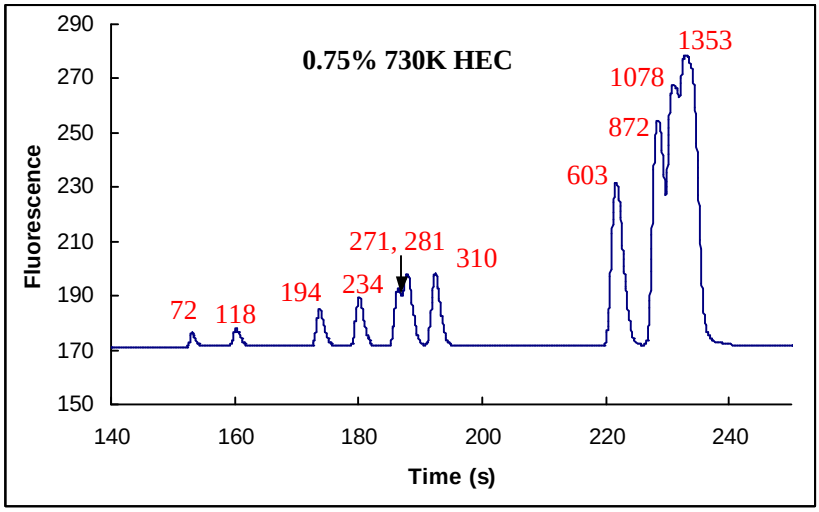

(b)

Figure 4.24. DNA standard separated in (a) chip A with 1% 4M PEO as sieving material and (b) chip B with 0.75% 720K HEC as sieving material. DNA fragment sizes in number of base pairs are denoted above each peak.

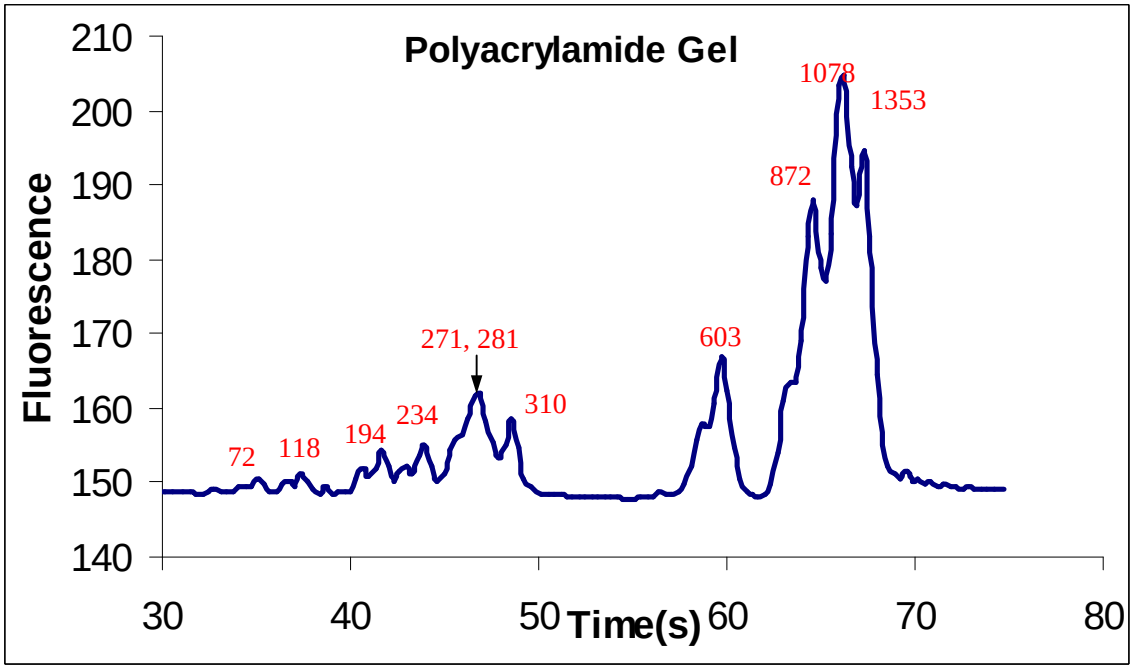

Figure 4.25. Separation of DNA standard in chip A with crosslinked polyacrylamide gel as sieving material. DNA fragment sizes in number of base pairs are denoted above each peak.

as the sieving material for electrophoresis. The gel coating method achieved the similar DNA separation efficiency as the linear polymer solution, but eliminated the tedious sieving solution preparation procedure and facilitates the sample loading process.

CHAPTER 5

CD-LIKE ELISA BIOCHIPS

The use and development of immunoassay technology in clinical, food safety, and environmental applications has drawn a great deal of interest because of its high selectivity and sensitivity. However, the conventional heterogeneous immunoassay (e.g., enzyme-linked immunosorbent assays - ELISA) needs a series of mixing (reaction) and washing steps, requires a relatively long assay time, and involves troublesome liquid-handling procedures and many expensive antibody reagents. On the other hand, microfabrication technology enables the integration of a number of fluid handling components in a single device with a network of microchannels. Due to their small scale, microdevices have advantages such as a large specific volume, little reagent consumption, and a short diffusion length.

This chapter presents an integrated microdevice on a compact disk (CD) to perform ELISA for rat IgG from hybridoma cell culture, which combined several

microfluidic functions (e.g., capillary valving, centrifugal pumping, flow sequencing, cascade micromixing, and snap-off metering) and polymer-based microfabrication techniques including a novel bonding and surface modification method we have developed and were described in the previous two chapters. Centrifugal and capillary forces were used to control the flow sequence of different solutions involved in the ELISA process. The microdevice was fabricated on a plastic CD. The surface of the plastic can be modified so that proteins are only adsorbed onto the plastic surface where the detection is carried out. Each step of the ELISA process was carried out automatically by using a computer program to control the rotation speed of the CD. The microchip-based ELISA has the advantages of fast immunoreaction, short incubation time, low reagent consumption, and automation.

5.2 Background

ELISA, typically carried out in a 96-well microtiter plate, is the most commonly used method among various immunoassays. It has been widely used for detection and quantification of biological agents (mainly proteins and polypeptides) in the biotechnology industry, and is becoming increasingly important in clinical, food safety, and environmental applications. However, conventional ELISA involves a tedious and laborious protocol that often results in large errors and inconsistent results. Figure 5.1 illustrates the general principle and procedures used in the enzyme-linked immunosorbent assay [Crowther, 2001]. The procedures are as follows:

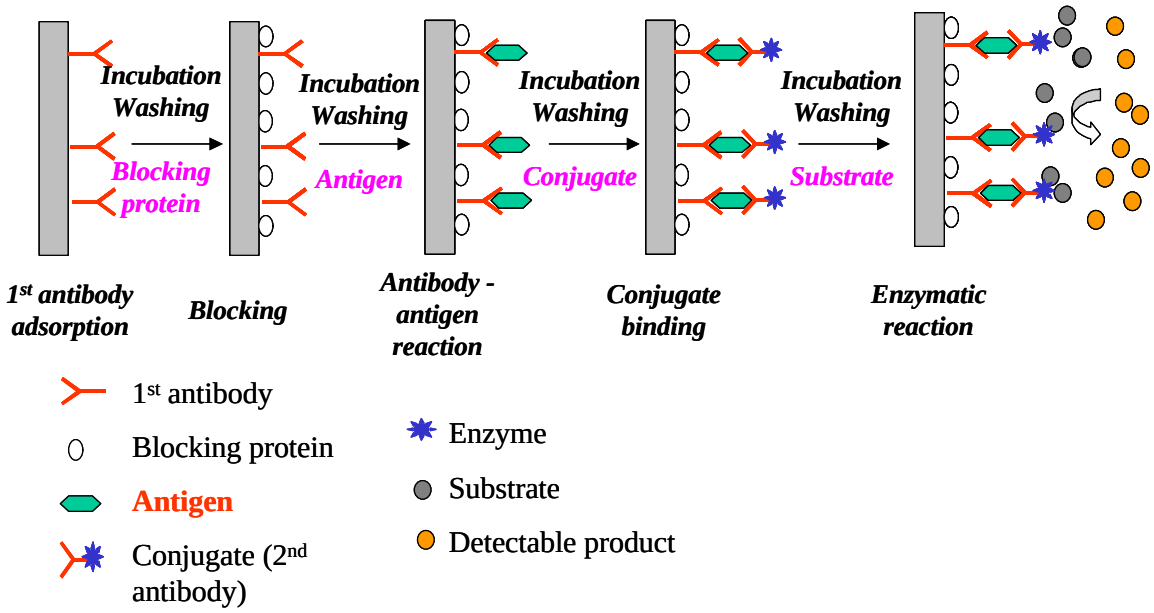

Figure 5.1. The principle and procedure of the ELISA process

(a) The first antibody (specific for the to-be-assayed antigen) is added to an ELISA plate. The first antibody is allowed to adsorb to the solid substrate surface. The excess antibody is removed from the plate after incubation.

(b). The wells are filled with blocking solution. The blocking solution provides proteins, which adsorb to all protein-binding sites and prevent subsequent nonspecific binding of antibody to the plate.

(c). The sample is added. If the sample contains the targeted antigen, it will bond to the adsorbed 1st antibody to form an antigen-antibody complex. After incubation, the plate is washed.

(d). The conjugate solution is added. The conjugate (the second antibody) is an appropriate enzyme-labeled ligand (usually an antibody), which will bond to the antigen. The conjugate solution is discard and the plate is washed after incubation.

(e). The developing solution containing the substrate is added, which reacts with the enzyme in the conjugate. Each enzyme is able to convert hundreds of substrates into products to enhance the sensitivity of the assay. The products of the reaction give fluorescence or change the color of the solution.

This process requires a series of mixing (reaction) and washing steps. It often teaks many hours to two days to perform one assay due to the long incubation times during each step. These long incubation times are mostly attributed to inefficient mass transport from the solution to the surface, whereas the immunoreaction itself is a rapid process [Rossier et al., 2001]. The CD-ELISA is designed to overcome these problems.

Microfabrication technology enables the integration of a number of fluid handling components in a single device by using a network of microchannels. Due to their small

scale, microdevices have advantages such as large specific volume, little reagent consumption, and short diffusion length. Several microchip-based ELISA have been developed, based on the immunoreaction on surfaces of a single microchannel [Rossier et al., 2001; Eteshola and Leckband, 2001] or on microbeads which are trapped in the microchannel [Sato et al., 2000]. These devices take advantage of the high surface to volume ratio of the microchannel for fast immunoreaction. However, each step of the ELISA is still carried out manually. Compared to these devices, the one designed in our lab has the advantages of possible automation and parallel analysis. On our microdevice, all solutions are loaded into the devices at the beginning of the assay and all the other steps can be carried out automatically by using a computer program to control the rotation speed of the CD. By proper design, multiple microstructures can be integrated into a single CD for multiple assays. For example, microfabricated 96-sample capillary array electrophoresis on a 5-inch CD for high-throughput DNA analysis has been developed [Mathies, 1998].

5.3 Microchip design

A prototype design of a CD-ELISA with 24 sets of ELISA microdevices on a 12 cm disk is shown in Figure 5.2. The schematic of a single assay is explained in Figure 5.3, while an actual assay on a plastic CD is shown in Figure 5.4. Each reservoir's function, volume, and burst frequency (at which the solution will release from its reservoir) are shown in Table 5.1.

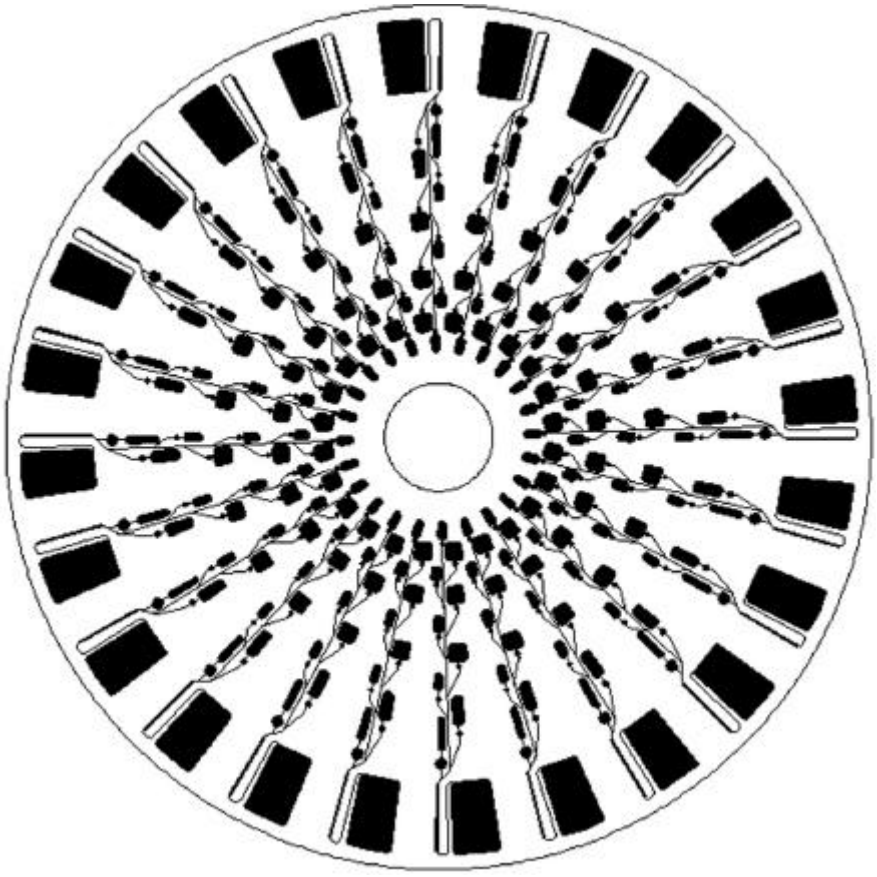

Figure 5.2. A CD-ELISA design with 24 sets of assays.

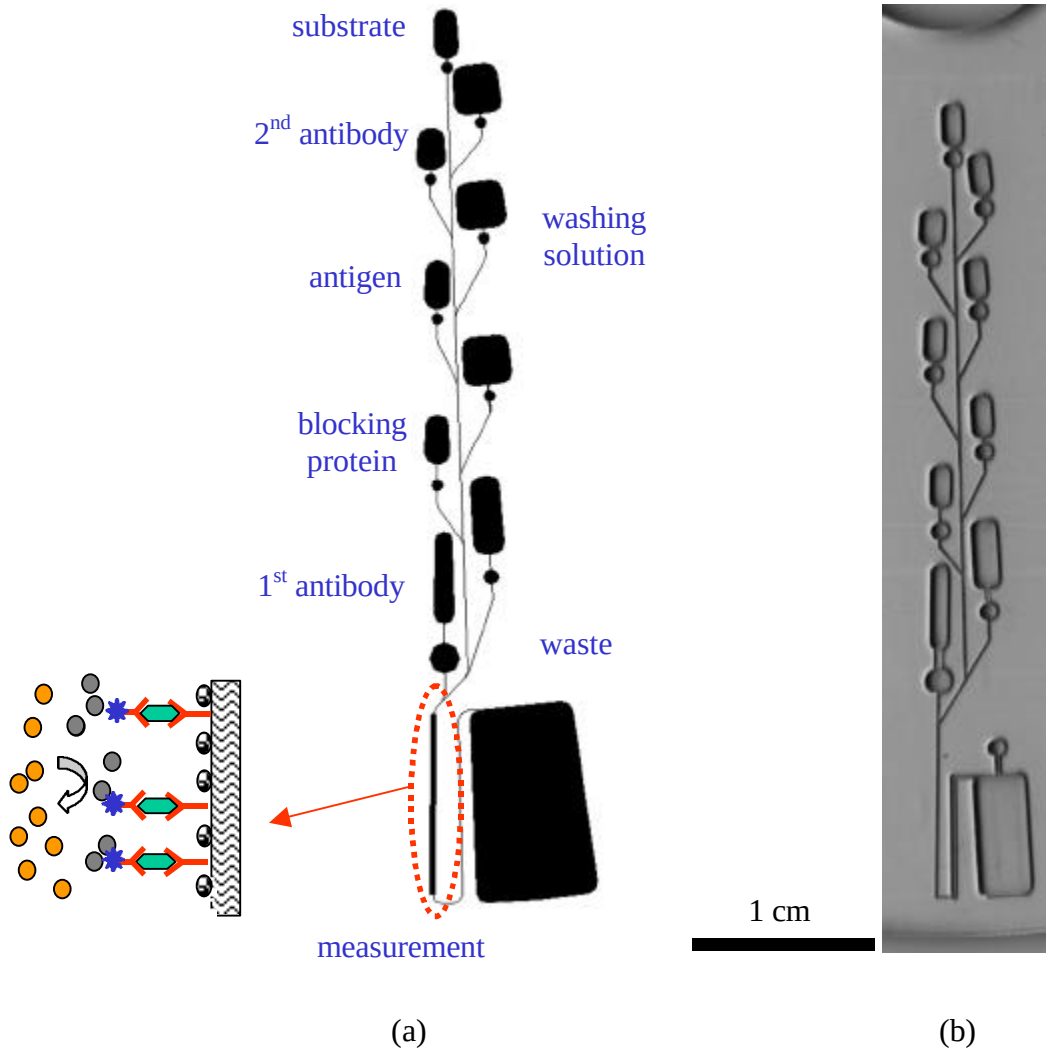

Figure 5.3. (a) Schematic and (b) photo of a single assay on CD-ELISA design.

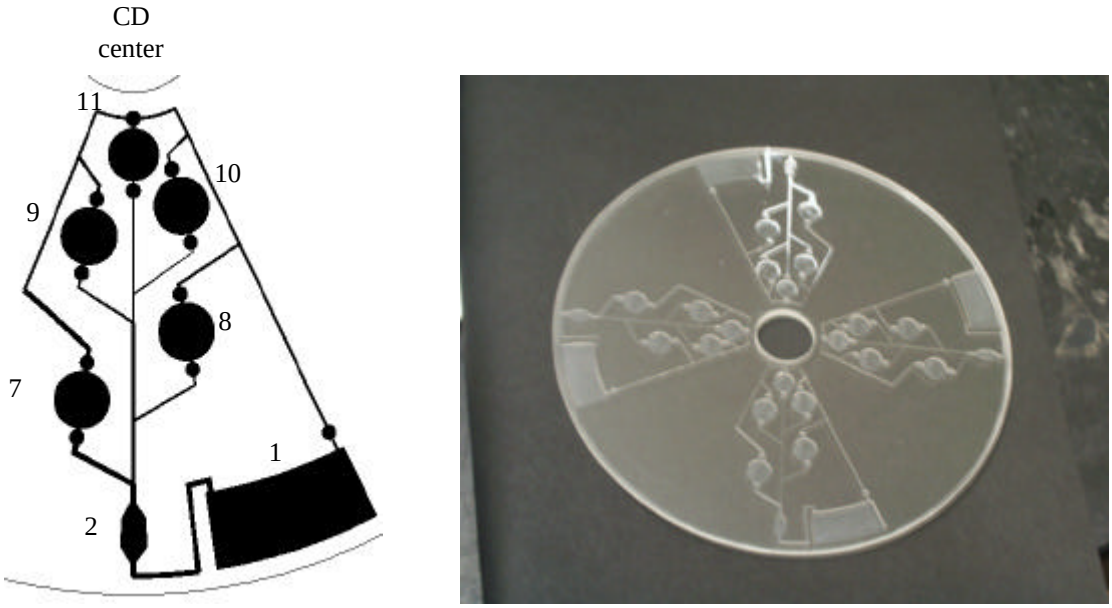

(a) (b)

Figure 5.4. (a) Schematic of 5-step flow sequencing CD (1 – waste; 2 – detection; 7 – antigen/sample; 8, 10 – washing; 9 – 2nd antibody; and 11 – substrate) and (b) a CNC-machined CD.

.

Reservoir	Solution	Volume (μl)	Burst frequency (rpm)*
1	Waste	13.5	N/A
2	Optode	0.6	N/A
3	1^{st} antibody	1.3	ω_3
4	Washing	1.3	ω_4
5	Blocking	1.3	ω_5
6	Washing	1.3	ω_6
7	Sample (antigen)	1.3	ω_7
8	Washing	1.3	ω_8
9	Conjugate (2^{nd} antibody)	1.3	ω_9
10	Washing	1.8	ω_{10}
11	Substrate	2.4	ω_{11}
* $\omega_3 < \omega_4 < \omega_5 < \omega_6 < \omega_7 < \omega_8 < \omega_9 < \omega_{10} < \omega_{11}$			

Table 5.1. A prototype of the microdevice for ELISA on CD

The substrate, conjugate, washing, primary antibody, blocking protein, and antigen solution can be preloaded into corresponding reservoirs before the test. The centrifugal and the capillary forces are used to control the flow sequence of different solutions involved in the ELISA process. The basic principle of the centrifugal pumping and capillary valving has been described in Chapter 3. In brief, the capillary force will hold the liquid from a small channel to an expanded area, while the centrifugal force may release the fluid from its reservoir when it is larger than the capillary force. The angular frequency at this moment is called the burst frequency, which can be calculated by comparing the centrifugal force and the capillary force. A computer controls the rotation speed of the disk to achieve proper flow sequencing and incubation.

The flow sequence is designed in such a way that the antigen solution is released into the measurement site first at a low rotation speed. This action allows the first antibody bind onto the microchannel surface. The solid surface at the measurement site needs to be modified so that it has a high protein affinity. After incubation, the washing solution is released to wash out the unbounded antibodies into the waste reservoir. Then the blocking protein, the washing solution, the antigen (sample or standard), the washing solution, the conjugate solution, the washing solution, and finally the enzyme substrate are delivered to the measurement site, one by one at increasing rotation speeds. All of these procedures are automated and can be completed in ~1 h with highly reproducible results because human error is eliminated or reduced to a minimal level. This novel CD-ELISA technology will have wide applications in clinical diagnostics of disease-associated antibodies and detection of pathogens, toxins, pesticides, and other hazardous contaminants present in foods and water.

5.4 EXPERIMENTAL

5.4.1 Materials

For demonstration purposes, diluted food dyes (purchased from a local grocery store) were used. The polymethyl methacrylate (PMMA) and polycarbonate (PC) sheets with different thickness for computer numerically controlled (CNC) machining and hot embossing were purchased from American Plastics. The first antibody (affinity purified antibody goat anti-rat IgG (H+L)), the antigen (rat IgG), and the second antibody (affinity purified antibody horseradish peroxidase (HRP) labeled goat anti-rat IgG (H+L)) were purchased from Kirkegaard & Perry Laboratories (KPL, Gaithersburg, MD). Dulbecco's Phosphate Buffered Saline (PBS, without calcium chloride, without magnesium chloride) was purchased from Invitrogen Life Technologies (Carlsbad, CA). All other reagents were purchased from Sigma Aldrich. All reagent were used as received.

5.4.1.1 Preparation of buffer solutions

Preparations of Tris Assay Buffer (TAB, pH 7.5), Tris Wash Buffer (TWB, pH 7.5), and 0.15M Tris-HCl buffer solution (pH8.5) are listed in Table 5.2. For the PBS buffer solution (1X, pH7.5), 9.55g of PBS powder were dissolved in 1L de-ionized water and NaOH (1M) or HCL (1M) solution was used to adjust the pH value.

(a)

Component	Mass/Liter
NaCl	29.22 g
Trizma Prset Crystal, pH 7.5	7.09 g
Tween 20	1.0 ml
BSA (Bovine Serum Albumin)	10.0 g
NaN_3 (Sodium azide)	1.0 g
Deionized water	1000 ml

(b)

Component	Mass/Liter
NaCl	29.22 g
Trizma Prset Crystal, pH 7.5	2.84 g
Tween 20	1.0 ml
BSA (Bovine Serum Albumin)	0.2 g
NaN_3 (Sodium azide)	0.5 g
De-ionized water	1000 ml

(c)

Component	Mass/Liter
NaCl	29.22 g
Trizma Prset Crystal, pH 7.5	18.15 g
12M HCl	4.83ml
De-ionized water	1000 ml

Table 5.2. Preparation of Tris assay buffer (TAB, pH 7.5), Tris wash buffer (TWB, pH7.5), and Tris-HCl buffer solution (0.15M, pH8.5).

5.4.1.2 Pre-preparation of antigen/antibody solution

All antigen and antibody (0.5mg or 1mg) were dissolved in 1 ml 50% glycerol solution (mixture of 0.5ml glycerol and 0.5 ml reagent quality water) and stored in a frozen state.

5.4.2 Fabrication

The designed microfluidic patterns were drawn using commercial AutoCAD software (AutoCAD 2000, AutoDesk, Inc). Channels and reservoirs (with depths ranging from 60 μm to 800 μm and widths ranging from 127 μm to 762 μm) were generated on a polymethyl methacrylate (PMMA) plate (12 cm in diameter) by a CNC machine (Dynapath Delta CNC, Chevalier®). The end mills (single-end two-flute sub-miniature end mill) were purchased from McMaster-CARR (Chicago, IL) and the diameter of the mills ranged from 127 μm to 762 μm.

5.4.3 CD microfluidic testing setup

The same experimental setup described in Chapter 3 and shown in Figure 3.4 was used for CD-ELISA testing. The sealing and sample loading procedures were similar to those described in Section 3.2.4.

5.4.4 Experiment procedures

For comparison, the ELISA was carried out both on 96-well microtiter plate and on the microchip.

5.4.4.1 Procedure for 96-well microtiter plate

(a) Coating

The first antibody was diluted to 2.5 μg/ml in TAB and 100 μl dilute solution was added to each well on the plate. The plate was covered and incubated at 4 ^{o}C for overnight or at room temperature for 6 hours. The plate was emptied (dumping the solution from the plate) and the inverted plate was tapped on paper towels. The wells were then filled with 300 μl washing buffer (TWB) solution, emptied, and tapped. The washing step was repeated three times.

(b) Blocking

300 μl TAB was added to each well. The plate was incubated at least 1hr at 37 ^{o}C. After incubation, it was washed with TWB solution three times.

(c) Sample or Standard loading

A series of 2-fold dilute solution of standard (rat IgG) was prepared in the TAB solution at 80, 40, 20, 10, 5, 2.5, and 1.25 μg/ml respectively. 100 μl diluted standard IgG solution was added into each well, and 100 μl TAB solution was added into each negative control wells. Each sample needs at least one duplicate sample well. The plate was then incubated at least 1hr at 37 ^{o}C or overnight at 4 ^{o}C. After incubation, it was washed with TWB solution three times.

(d) Second antibody

The second antibody was diluted to 2 μg/ml in the diluting TAB solution. 100 μl diluted second antibody solution was added into each well. The plate was incubated at 37 ^{o}C for 1.5 hrs, and then washed once with TWB solution and twice with PBS.

(f) Substrate (HPPA)

3mg/ml HPPA was prepared in 0.15M Tris-HCl buffer solution (pH 8.5). 1 μl 30% hydro peroxide was added to 7.5 ml HPPA solution and mixed thoroughly just prior the use. 100 μl substrate was added to each well.

(g) Detection

Detection was carried out on CytoFlour® Multi-well Plate Reader (Series 4000, Perspective Biosystems) with excitation at 360/40 nm and emission at 460/40 nm. The fluorescence signal from the enzymatic reaction of the enzyme substrate (HPPA) is proportional to the analyte to the IgG concentration in the test sample [Eteshola and Leckband, 2001].

5.4.4.2 Procedure for CD-ELISA

For prototyping, a five-step flow sequencing CD (see Figure 5.4) was used. The first-antibody and the BSA blocking were carried out off-chip. First, the first antibody (2.5 μg/ml) was applied to the detection reservoir (reservoir 2). The antibody was allowed to adsorb onto the surface of this reservoir. After incubation, the excess antibody was removed by washing solution (TWB solution). The TAB solution was then added to block all protein-binding sites on the surface of the microchip.

After the incubation and washing off excess BSA, the antigen/sample, washing, 2nd antibody, and substrate solutions were loaded into their corresponding reservoirs. The

CD was mounted onto the motor plate. The rotation speed of the CD was set to 360 rpm (± 15 rpm) to release the sample solution (in reservoir 7, containing to-be-assayed antigen) into reservoir 2 for the binding process of antigen-antibody. According to the literature, several minutes of incubation is sufficient to reach equilibrium of the immunoreaction in a microchannel with a similar dimension of reservoir 2 [Rossier et al., 2000].

After incubation, reservoir 2 was washed with washing solution (in reservoir 8) at a rotation speed of 560 rpm (± 30 rpm). Based on previous experience [Madou et al., 2001], 3-fold of the washing solution is sufficient to displace the existing water-based solution in reservoir 2. The washing solution was set at about 3-fold of the volume of reservoir 2 in the CD.

The conjugate solution (2^{nd} antibody solution in reservoir 9) was released into reservoir 2 at a rotation speed of 790 rpm (± 35 rpm)to let the enzyme-labeled secondary antibody bond to the primary antibody. After incubation, reservoir 2 was washed with washing solution (in reservoir 10) at a rotation speed of 1190 rpm (± 55 rpm).

The substrate solution (in reservoir 11) was released at a rotation speed of 1280 rpm (± 65 rpm) into reservoir 2 . Immediately after the release of the substrate, the detection was carried out using an inverted fluorescence microscope (Nikon ECLIPSE TE2000-U). A 100W mercury light source with a 335/20 nm filter and a dichroic mirror was used as an excitation source. The fluorescence signal was obtained through a dichroic mirror and a 405/40 nm filter. Images were recorded by a 12-bit high-resolution

monochrome digital camera system (CoolSnap HQ). The intensity of the fluorescence was analyzed using the Fryer Metamorph Image Analysis System.

5.5 Results and Discussion

An ELISA analysis of rat IgG from hybridoma cell culture was used to compare the performance between the conventional 96-well microtiter plate and a microfabricated microfluidic device.

5.5.1 Medium effect

The effect of medium on the antibody adsorption onto the solid surface was also examined. In this experiment, the antibody adsorption was carried out by adsorbing the 2^{nd} antibody (diluted in the TAB and the DI water, respectively) onto the substrate surface in the 96-well microtiter plate. The substrate (HPPA, 3mg/ml) was added after the incubation and washing. The fluorescence intensity of the enzymatic reaction product was used as an indicator of the amount of antibody adsorption. As shown in Figure 5.5, for antibody diluted in DI water, the fluorescence intensity of the product increases with the increase of the antibody concentration at low antibody concentration range (<2 μg/ml), but reaches a maximum at a higher antibody concentration (>2.5 μg/ml), indicating that the antibody adsorption onto the polymer surface reaches equilibrium (or the surface is saturated). Further increase of the antibody concentration would waste the expensive reagent. For the antibody diluted in TAB (see Figure 5.5b), the higher concentration of the antibody, the stronger the florescence intensity of the product detected. It should also be noted that even at a very high antibody concentration (40

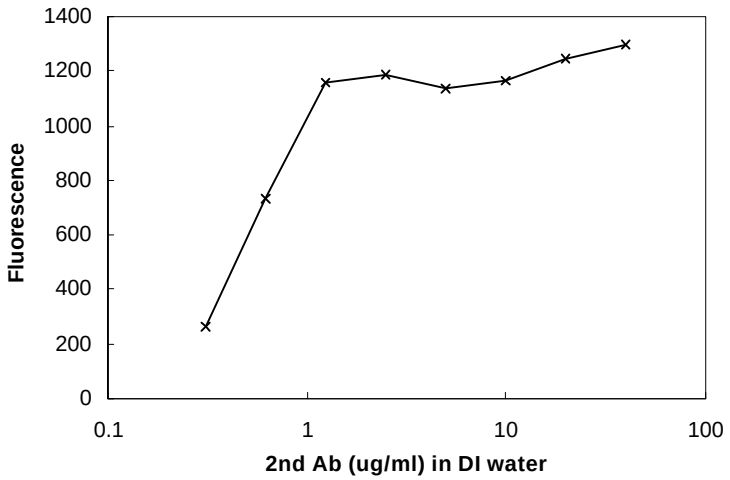

(a)

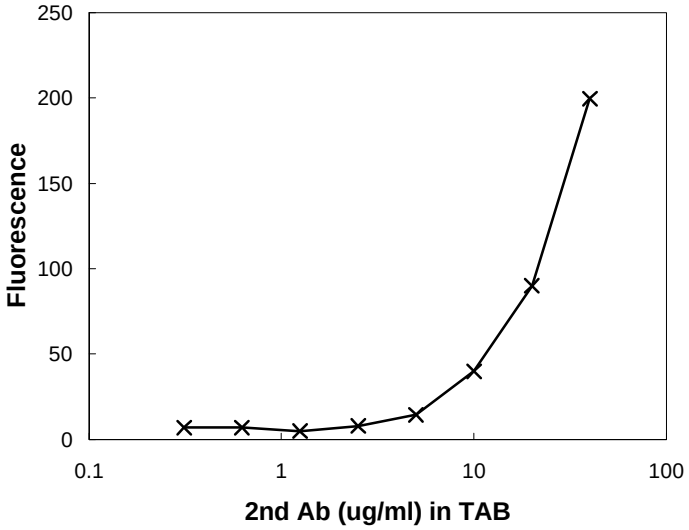

(b)

Figure 5.5. Effect of medium on the antibody adsorption on 96-well microtiter plate (HPPA = 3mg/ml and enzymatic reaction time = 30 min), (a) antibody diluted in DI water and (b) antibody diluted in TAB buffer.

ug/ml), the fluorescence intensity is much weaker than the results from antibody diluted in DI water (Figure 5.5a). It implies that much less antibody in the TAB solution was adsorbed onto the solid surface than that in the DI water. This is because there is10mg/ml BSA in the TAB solution, which competes strongly with the antibody for the protein binding sites on the solid surface. This illustrates the excellent ability of the BSA to block the protein-binding site on the solid surface, therefore, limit the non-specific binding.

5.5.2 Enzymatic reaction

The time course of the enzymatic reaction of HPPA was examined. The 2nd antibody (HRP linked) was adsorbed onto the substrate surface on the 96-well microtiter plate. After the incubation and washing out the excess antibody, the substrate was added. The fluorescence intensity of the enzymatic reaction product was used as an indicator of the extent of the enzymatic reaction and was monitored as a function of time. A comparison of the enzymatic reaction rate between the microchip and the microtiter plate is shown in Figure 5.6. The enzymatic reaction in a microtiter plate took almost 120 minutes to complete or reach the equilibrium (see Figure 5.6a), while it only took about 200 seconds in the microchannel (see Figure 5.6b).

In a 96-well microtiter plate, the specific surface area of 100 μl solution in each well (6.5 mm in diameter and 3 mm in height) is about 944 m^2/m^3. A microchannel with dimensions of 140 μm ×100 μm × 2 mm has a specific surface area of 34300 m^2/m^3, which is about 36 times larger than that of the microtiter plate. This provides more reaction area for the substrate (in unit volume) to react with the enzyme on the solid

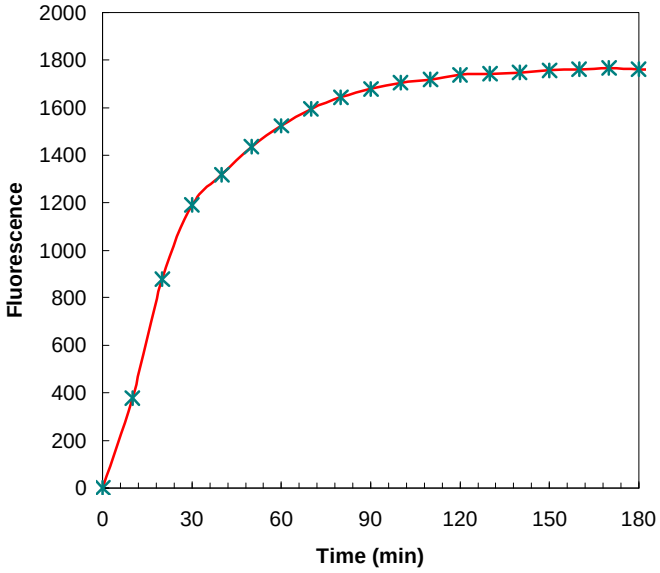

(a)

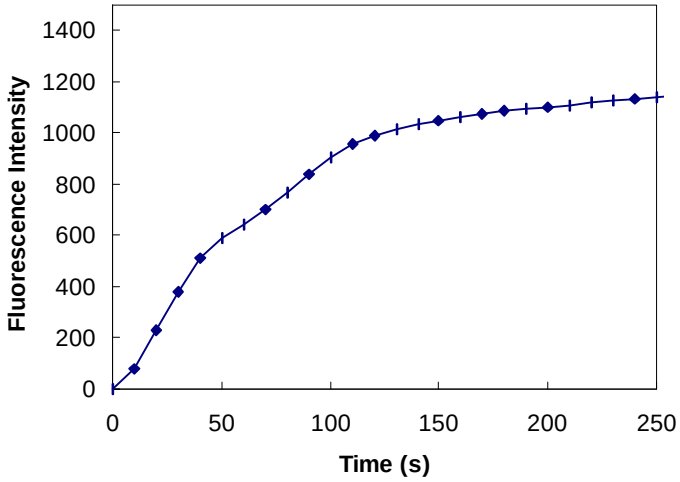

(b)

Figure 5.6. The enzymatic reaction of HPPA in (a) a 96-well microtiter plate and (b) a microchannel (140 μm ×100 μm).

surface. The diffusion length in the microtiter plate is 3 mm (the height for 100 μl liquid in each well), whereas that of the microchannel is only 50 μm. According to Eq. (2-4), the characteristic time required for a molecule to diffuse is proportional to the square of the diffusion length. Therefore, the diffusion time of the substrate to the enzyme on the microchannel surface can be 3600 times faster than that in the 96-well microtiter plate. The larger surface to volume ratio and the shorter diffusion length contribute to the fast enzymatic reaction.

From these reasons, we determined that the time for the enzymatic reaction was 5 minutes on the microchip.

5.5.3 Analysis of rat IgG from hybridoma cell culture

Figure 5.7 shows the calibration curves of the standard rat IgG from the 96-well microtiter plate and the microchip on fluorescence signal. It can be seen that the microchip has higher signal and is in the same detection range as that of the microtiter plate. The detection limit is 5 mg/L (31nM) of the rat IgG (MW ~ 160,000). Since the concentration of the rat IgG from the hybridoma culture is typically in the range of 1 to 100 mg/L, this microfluidic platform is expected to be suitable for practical measurement.

5.5.4 Comparison of processing conditions

The reagent consumption and assay times of each step were compared in Table 5.3. It can be seen that the consumption of reagents (the most expensive ones are antigen and antibodies) on the microchip was 30 μl, which is one tenth that of the 96-well

	Reagent volume (µl)		Incubation time(min)		Microchip (target)	
	96-Well	Microchip *	96-Well	Microchip*	Volume (µl)	Incubation time (min)
Antigen binding	100	10	480	30	1	5
Blocking protein	300	10	60	15	1	5
IgG/sample	100	10	60~120	15	1	5
Conjugate	100	10	60~120	15	1	5
Substrate (HPPA)	100	100	20-40	1	1	1
Total	700	**140**	680~82	**76**	**5**	**21**

Table 5.3. ELISA comparison between a 96-well microtiter plate and a microchip (*Microchannel: 150 µm wide, 140 µm deep, and 1.25 cm long).

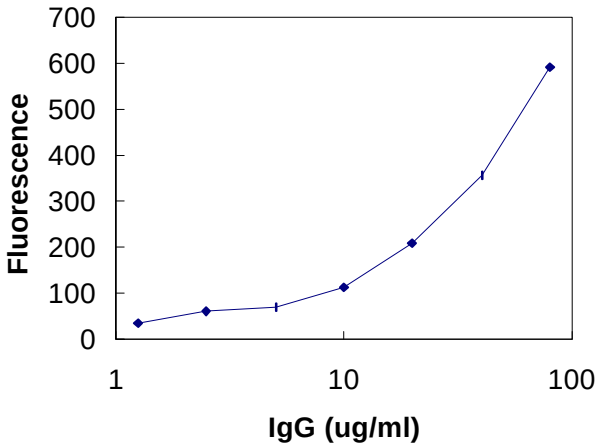

(a)

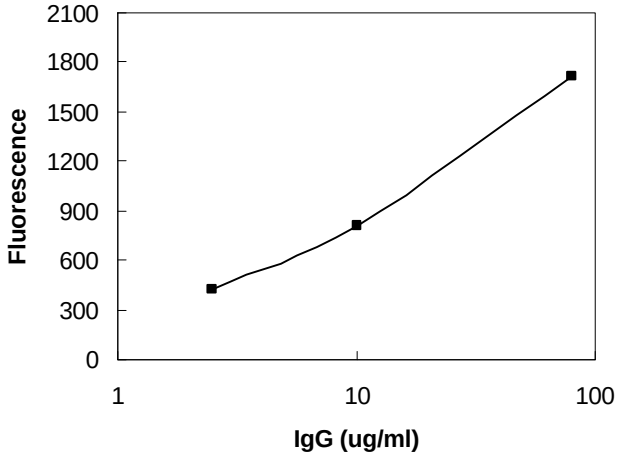

(b)

Figure 5.7. Calibration curves of rat IgG from (a) a 96-well microtiter plate and (b) a microchip.

microtiter plate (300 μl). The assay time on the microchip was a little more than an hour, which is also about one tenth of that required for the microtiter plate. With further improvement, the reagent consumption can be reduced to less than 1 μl for each step and each assay can be finished within half an hour.

5.6 SUMMARY

A polymer microfluidic platform integrated with different fluidic features has been designed and fabricated for enzyme-linked immunosorbent assays. It has been demonstrated successfully that flow sequencing can be achieved on a CD-like microfluidic platform by integrating the necessary microfluidic functions such as centrifuge pumping and capillary valving. Burst valves with well-defined and well-separated critical frequencies can be constructed on the disk by varying channel dimensions and distance of the burst valve from the center of rotation. The preliminary analysis of rat IgG from hybridoma culture shows that the microchip-based ELISA has the same detection range as the conventional method on the 96-well microtiter plate and has advantages such as less reagent consumption and shorter assay time over the conventional one.

CHAPTER 6

CONCLUSIONS AND RECOMMENDATIONS

6.1 Conclusions

The overall goal of this study is to design and fabricate polymer-based microfluidic devices for BioMEMS (biological micro-electro-mechanical systems) applications. The emphasis is on the design of microfluidic functions and the development of a new packaging technique. Low-cost microfabrication techniques are used to produce polymer-based microfluidic devices for research studies.

First, a microfluidic platform has been designed on a compact disk (CD) for medical diagnostics, which includes functions such as pumping, valving, sample/reagent loading, mixing, metering, and separation. The fluid propulsion is based on centrifugal

force, which is achieved through rotationally induced hydrostatic pressure. A passive capillary valve, which is based on a pressure barrier that develops when the cross-section of the capillary expands abruptly, was used to control the fluid flow. Micromixing is achieved by impinging mixing and bend-induced vortices by flowing fluids through an S-shaped channel. Integration of these microfluidic functions was applied in a two-point calibration system for medical diagnostics and a cascade micromixer for protein reconstitution.

A polymer CD microfluidic platform integrated with these different fluidic features was designed and fabricated for enzyme-linked immunosorbent assays. We have demonstrated successfully that flow sequencing can be achieved on a CD-like microfluidic platform by integrating the necessary microfluidic functions such as centrifuge pumping and capillary valving. The preliminary analysis of rat IgG from hybridoma culture shows that the microchip-based ELISA has the same detection range as the conventional method on the 96-well microtiter plate and has advantages such as less reagent consumption and shorter assay time over the conventional one.

For fabrication of microfluidic platforms, we have applied computer numerically controlled (CNC) machining for prototyping and UV-LIGA (UV lithography, electroforming, and plastic molding) techniques for mass production. Currently, packaging (surface modification, bonding, and reagent loading) of polymer microfluidic platforms is a challenging issue. A new resin-gas injection technique has been developed, which both bonds the polymer-based microfluidic platforms and modifies their surface properties (such as changing the hydrophilicity, protein adsorption and rejection properties, etc.) of microchannels. . This method can easily bond biochips with complex

flow patterns. A cascade micro-mixer and a multi-channel DNA sequencing chip were demonstrated experimentally. By adding surface modification agents, the interfacial free energy of the substrate with water can be controlled. Local modification of the channel surface can also be achieved through sequential resin-gas injection in conjunction with the masking technique.

For application, this technique was used to form a layer of dry monolithic stationary hydrogel on the walls of a microchannel, serving as a sieving material for electrophoresis separation of DNA fragments. It has been demonstrated that the photopolymerization of the acrylamide was much faster than the traditional redox polymerization and can achieve the similar conversion. The regent loading, and the electrophoresis separation efficiency of this new technique were compared experimentally with the conventional linear polymer solution method used in the microchannel based DNA sequencing process. It was found that our method has the advantages of more user-friendly operation, easier and faster sample loading, and better separation efficiency.

6.2 Recommendations

6.2.1 Microfluidic simulations

Up to now, the development of microfluidic devices is mainly based on trial-and-error process. There is a growing interest in using simulation and modeling to guide the design of microfluidic devices. Jensen et al [1998] used finite element simulations to design microfluidic devices for chemical reactions. Two- and three-dimensional fluid

flow, thermal fields, and chemical species concentrations in microfluidic devices were simulated to predict the performance of microreactor systems. The reactor simulations are in excellent agreement with experimental observations, demonstrating the ability of FEM solution to provide accurate simulations of microfluidic chemical devices. Bergkvist et al [2002] investigated a silicon microextraction chip (SMEC) structure both numerically and experimentally. The finite element analysis of the microfluidic flow in the microchip was analyzed numerically by the use of computational fluid dynamics module FLOTRAN in the ANSY software package. The overall analysis performance was verified by the experimental result.

Several companies have developed commercial simulation software for modeling MEMS, microsystems, sensors and acutators, and microfluidics devices. FlumeCAD^{TM} (Fluid-molecular CAD, now called Biochip Developer software) by Microcosm Technologies (renamed to Coventor) is the first integrated CAD system targeting the general design of integrated chemical and biochemical analysis or synthesis systems. Biochip Developer software (then FlumeCAD) uses finite element methods to solve the Navier-Stokes equations including the thermal fields in fluidic devices. In addition, it calculates the coupled electrostatic equations for applications in ionic transport in microchannels. Biochip Developer software supports 3D simulation of chemical transport in electrophoretic, electroosmotic, and pressure driven systems and includes tools for the design and analysis of DNA separation and PCR amplification systems on chip. It also includes 3D modeling of fluidic microcomponents; performing flow, chemical transport, and containment analysis; enabling the analysis of complex fluidic networks; and calibrating microchemical flows with valid simulations. This software has been applied in

the analysis of micromixing [Wang et al., 2001] and optimization of sample injection components in electrokinetic microfluidic systems [Bousse et al., 1999].

CFD Research Corporation provides software (CFD-ACE$^+$) for biochip and microfluidic development for microreactions, bioanalytical (genomics, proteomics, cellomics), medical and pharmaceutical applications. CFD-ACE$^+$ enables the strongly coupled simulation of fluid flow, heat and mass transfer, particle magnetics, structural dynamics, and others. It is capable of modeling microfluidic functions such as sample preparation, extraction, injection, cleaning, dispensing, filling, mixing, preconcentration, separation, fluid and particle handling, electrochemical sensing, biochemical sensing, and PCR. This software system has been applied in optimization of DNA hybridization kinetics [Lenigk et al, 2002], thermal management (i.e., heater input power, fluid flow rate, sensor placement, and air-gap size and placement) inside microchannels for PCR [Sadler et al, 2002; Chou et al, 2002], DNA analysis (i.e., extraction, concentration of DNA from fluidic samples and on PCR amplification, hybridization, and electrophoretic separation) in microfluidic networks on a chip [Przekwas et al., 2000], and convective-diffusive mass transport as well as biochemical reaction kinetics in a coupled manner [Makhijani et al., 1999].

Computer simulation can help design engineer to gain insight into the physics of a microdevice, as well as the interaction between physical domains that can greatly affect device performance. It can also lead to the answers to following questions: what is the optimal channel dimension? What is the optimal voltage for injection? What is the optimal flow rate? Is Joule heating critical? How to minimize dispersion? Compared to traditional empirical and laboratory analysis, this method provides a fundamental and

detailed understanding of the microdevice and leads to higher performance designs in less time and at lower cost.

The computer simulation can improve the performance of CD microfluidic platforms. For example, the two-point calibration system has a five-step flow sequence and the gap between the burst frequency for each step is about 150 ~ 200 rpm in order to prevent the bundle release. With the computer simulation, it should be able to model the centrifugal pumping and capillary valving precisely and predict the burst frequency in more accurate way. Therefore, more steps should be able to be placed onto the same disk to provide multiple-point calibration, or the same two-point calibration system can be placed onto a smaller disk for miniaturization. High throughputs on the CD microfluidic platform can be realized too.

6.2.2 Coating thickness

The thickness of the coating on the wall of the microchannel is an important parameter to be controlled in the resin-gas injection method because it determines the final dimension of bonded microchannel. In the case of coating hydrogel for electrophoresis separations, knowing the coating thickness will help in the selection of hydrogels, such as sufficient swell ratio of the hydrogel to ensure the totally filled separation channel after swelling. To this end, further analysis of the process to better understand how to control the coating thickness is necessary.

The flow of a gas bubble through fluids in capillary tubes has been studied extensively with interesting practical applications, such as gas-assisted injection molding [Huzyak,

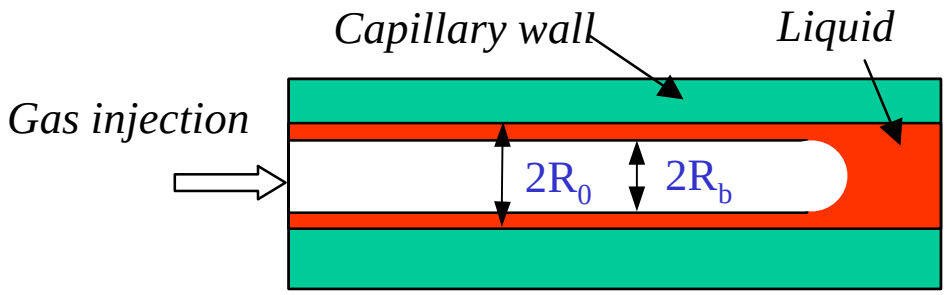

Figure 6.1. Schematic of gas bubble penetration through liquid in a capillary tube.

1995; Huzyak and Koelling, 1997; Gauri and Koelling, 1999]. The schematic of the gas bubble penetration through a liquid in a capillary tube is shown in Figure 6.1. A dimensionless quantity called fractional coverage (*m)* can be used to characterize the hydrodynamic coating thickness. The fractional coverage *m* is defined as:

$$m = \frac{R_0^2 - R_b^2}{R_b^2} \tag{6.1}$$

where R_0 is the capillary radius and R_b is the radius of the penetrating bubble as shown in Figure 6.1 . The fractional coverage is the ratio of the cross-sectional area coated by the fluid to the tube cross-sectional area. Another important dimensionless group in this process is the capillary number (*C*a), defined as:

$$Ca = \frac{U_g \eta}{\gamma_{gl}} \tag{6.2}$$

where U_g is the gas velocity, η is the viscosity which is a function of the shear rate ($\dot{\gamma}$) in the case of non-Newtonian fluids, and γ_{gl} is the liquid and gas interfacial tension.

Gas penetration in capillary tubes filled with Newtonian [Fairbrother and Stubbs, 1935; Taylor 1961; Kolb and Cerro, 1991] and non-Newtonian [Poslinski et al., 1995; Huzyak, 1995; Huzyak and Koelling, 1997; Gauri and Koelling, 1999] fluids have been studied by many researchers. The first experiment of gas penetration in Newtonian fluids, conducted by Fairbrother and Stubbs [1935], yielded an empirical correlation for the fractional coverage as a function of capillary number for capillary numbers between 10^{-3} and 10^{-2}.

$$m = 1.0 \cdot Ca^{1/2} \tag{6.3}$$

Taylor [1961] extended its validity to capillary number of 0.1. By plotting the fractional coverage as a function of capillary number, all data were merged into a single curve. He showed that the fractional coverage asymptotically approaches 0.56 at higher capillary number. Further experimental and theoretical work confirmed these results but with an asymptotic value of 0.6 at high capillary numbers. The studies of non-Newtonian fluids showed that at low capillary numbers, the fractional coverage is identical to that of Newtonian fluids at the same capillary number. At high capillary number, the fractional coverage for the shear thinning fluids also reached an asymptotical value, but less than that of Newtonian fluids [Poslinski et al., 1995]. The fractional coverage of the fluids with viscoelasticity was found to be dependent on the Deborah numbers (De) [Huzyak and Koelling, 1997]. At small Debroah numbers (De < 1), the fractional coverage is the same as that of Newtonian fluids. However, it deviates form the Newtonian fluids when De > 1. The fractional coverage can be 30% greater than that of the Newtonian fluids. Figure 6.2 shows the plots of the fractional coverage as a function of capillary number for Newtonian, Boger (ideal elastic), and shear thinning fluids.

The gas displacement of Newtonian fluids in square tubes has also been studied [Kolb and Cerro, 1991]. It was found that the fractional coverage increases with the capillary number and approaches an asymptotic value of 0.64. Above capillary number of 0.1, the gas forms a circular hollow core (axisymmetric); below capillary number of 0.1, the hollow core takes on the square shape of the tube (nonaxisymmetric).

In the literature, experiments of gas penetration were conducted in relatively large capillary tubes with tube diameters large than 1mm. In the case of microfluidic platforms, the width and the depth of microchannels are typically in the order of 10 ~100 μm.

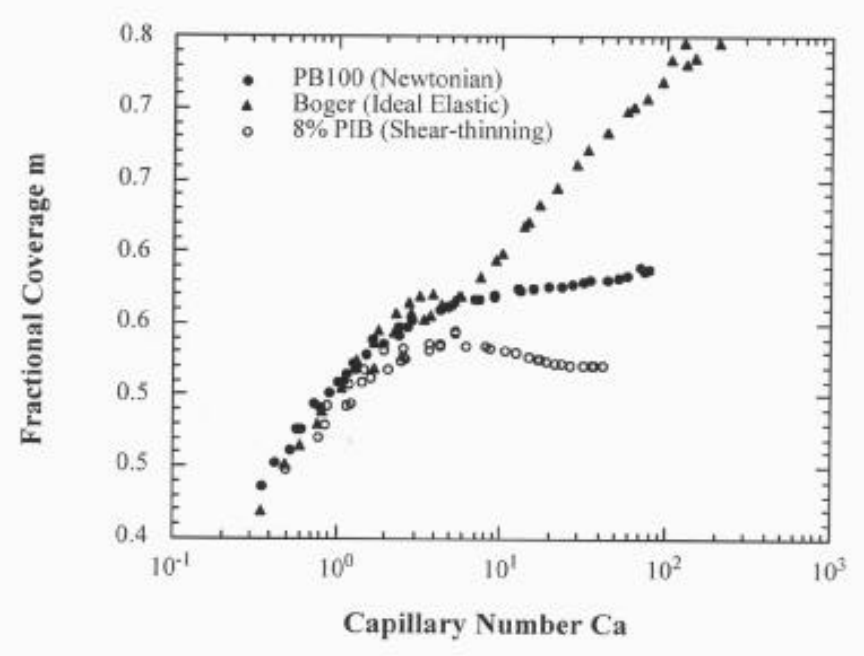

Figure 6.2. Fractional coverage as a function of capillary number for Newtonian, Boger, and shear thinning fluids [from Huzyak, 1995].

Because of the dimension of the channel, the shear rate inside the channel is very high (on the order of 10^5~10^6 s^{-1}). The microchannel is fabricated through either photolithography or CNC machining. The cross-section of the microchannel is commonly in rectangular shape. In some cases, dissimilar materials are bonded to cover the microchannel. The questions to be addressed include:

(a) Will the relationship between the fractional coverage and capillary number still be valid in the microchannel? How is the result from microchannels compared with that from literature?

(b) Under such high shear rate, will the rheological properties change of the fluid affect the coating thickness?

(c) Will the liquid-solid surface properties, such as wettibility, contact angle, and interfacial tension affect the coating thickness?

The answers to these questions will provide a fundamental understanding of the resin-gas injection process. The coating thickness can be examined by the scanning electron microscope (SEM) after curing the coating layer. The effect of the processing conditions, channel dimensions, and liquid properties on the coating thickness should be studied. The Finite Element Method (FEM) and molecular modeling method can be used to simulate the process inside the square microchannel. The relationship between the fractional coverage and capillary number in microchannels should be compared with that in the relatively large capillary tubes studied in the literature.

6.2.3 CD-ELISA

The current design of the CD-ELISA has 24 sets of ELISA on a 5” CD. The sample and reagent solutions have to be loaded into the reservoir one by one prior to the experiment. In order to be comparable to the most advanced microtiter plate (e.g., 384-well microtiter plate), a smaller CD platform with denser microfluidic patterns and more automatic sample loading is highly desirable. Figure 6.3 shows the schematic of this ideal CD platform with 28 sets of ELISA tests on a 3.6” CD. A single ELISA design is explained in Figure 6.4a. In this design, the first antibody is per-coated on the detection chamber and the remaining fluidic surface is then blocked with BSA. Thus, less numbers of reservoirs (5 reservoirs compared to 9 reservoirs in previous design) are necessary. Therefore, a 3.6” CD is able to hold 28 sets of the ELISA.

By using the capillary force, a commonly used washing solution can be loaded into all washing reservoir automatically through the loading channel near the edge of the CD (see Figure 6.4a, point B is where the washing solution will be injected). If the 2^{nd} antibody and the substrate (in the solid means) can be pre-loaded into corresponding reservoirs, then a buffer solution can be automatically loaded intro each reservoir by the capillary force through the loading channel near the center of the CD (see Figure 6.4a, point A is where the buffer solutions will be injected). A microarray design can also be incorporated onto the CD-ELISA. Figure 6.4b shows 10 dot-arrays in a detection reservoir. Each array can be pre-loaded with different antibodies to detect different antigens in the sample (e.g., food-borne toxins). Thus, The microarray technique can expand the number of assays on the CD up to 280, which is close to that of the 384-well microtiter plate.

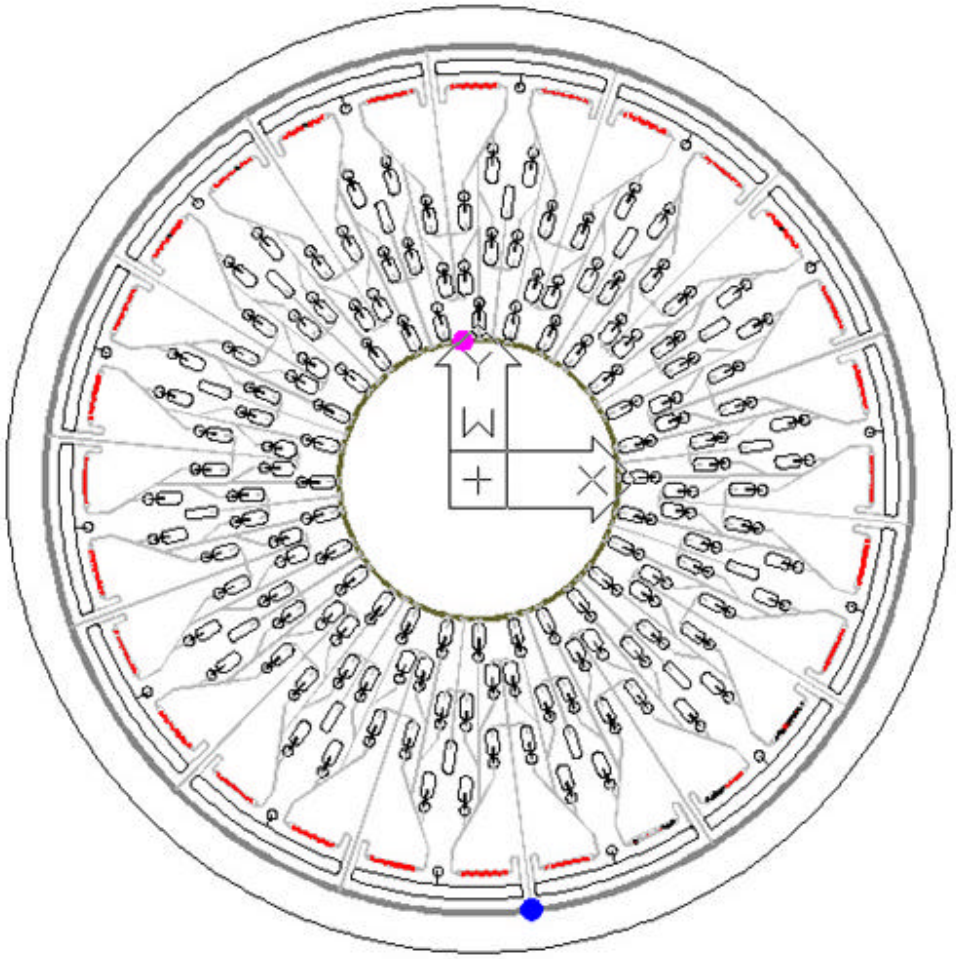

Figure 6.3. A CD-ELISA design with 28 sets of assays, automatic sample loading, and microarrays.

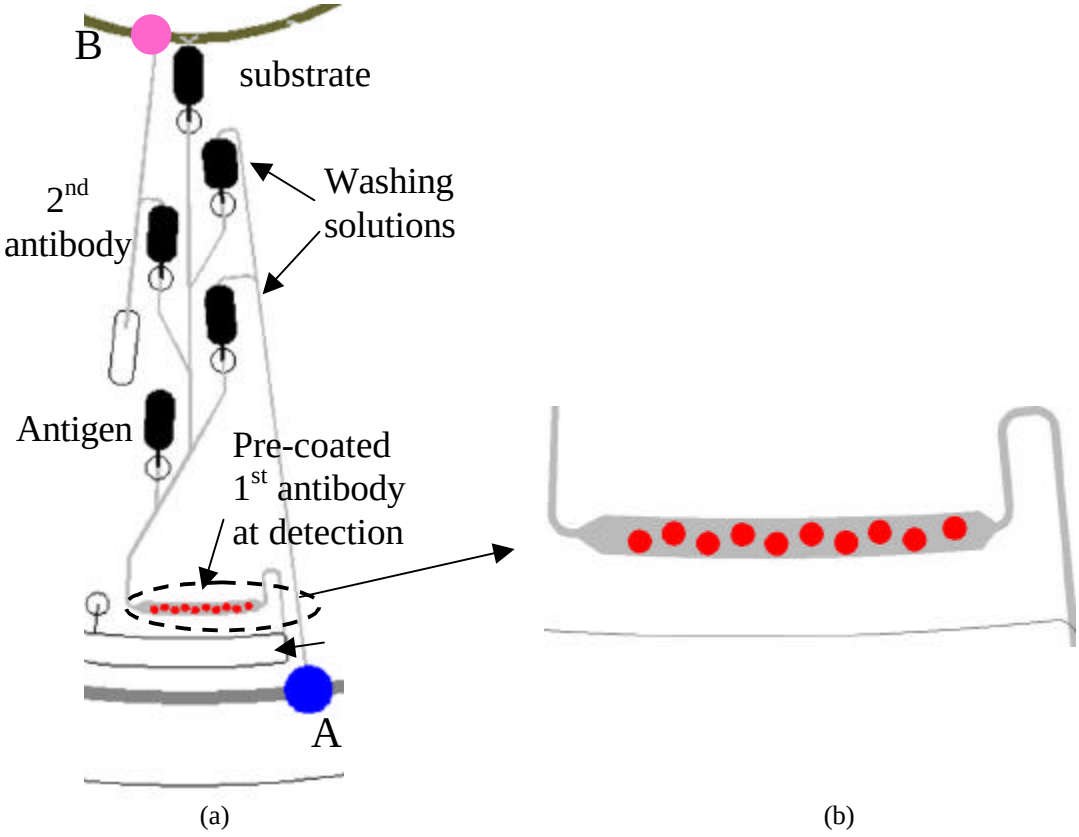

Figure 6.4. (a) Schematic of a single ELISA design with automatic sample loading (A - washing solution loading point, B – buffer solution loading point) and (b) microarrays.

To increase the detection sensitivity, surface modification techniques to improve the protein's adsorption and immobilization efficiency are very valuable. For example, proteins can be immobilized on a polymer surface by first activating the hydroxyl groups of the polymer with tosyl chloride and then forming a covalent bond with the protein. The application of this novel CD-ELISA can be extended for fast detection of food-borne pathogens and toxins.

BIBLIOGRAPHY

Ahmed F., Alexandridis P., and Neelamegham S., "Synthesis and application of fluorescein-labeled pluronic block copolymers to the study of polymer-surface interactions," *Langmuir*, 17, pp. 537-546 (2001).

Alcantar N. A., Aydil E. S., and Israelachvili J. N., "Polyethylene glycol—coated biocompatible surfaces," *J. Biomed. Mater. Res.*, 51(3), pp. 343-351 (2001).

Anderson R. C., Bogdan G. C., Puski A., and Su X., "Genetic analysis systems: improvements and methods," *Proc. Solid State Sensors and Actuators Workshop*, pp. 7-10 (1998).

Arenkow P., Kukhtin A., Gemmell A., Voloshchuk S., Chupeeva V., and Mirzabekov A., "Protein microchips: use for immunoassay and enzymatic reactions," *Analytical Biochemistry*, 278, pp. 123-131 (2001).

Bao J. J., "Capillary electrophoretic immunoassays," *Journal of Chromatography B*, 699, pp. 463-480 (1997)

Becker H. and Dietz W., "Microfluidic devices for μ-TAS applications fabricated by polymer hot embossing," *Proc. SPIE*, 3515, pp.177-182 (1998).

Becker E. W., Ehrfeld W., Hagmann, P., Maner A., and Munchmeyer D., Fabrication of microstructures with high aspect ratios and great structural heights by synchrotron radiation lithography, galvanoforming and plastic moulding (LIGA process). *Microelectron. Eng*., 4, pp. 35-56, (1986).

Becker H. and Gartner C., "Polymer microfabrication methods for microfluidic analytical applications," *Electrophoresis*, 21, pp. 12-26 (2000).

Becker H. and Heim U., "Silicon as tool material for polymer hot embossing" *IEEE Int. Conf. Micro Electro Mech. Syst., Tech. Dig*., 12, pp. 228-231 (1999).

Beebe D. J., Moore J. S., Bauer J. M., Yu Q., Liu R. H., Devadoss C., and Jo B-H., "Functional hydrogel structures for autonomous flow control inside microfluidic channels," *Nature*, 406, pp 588-590 (2000).

Bergkvist J., Ekstrom S., Wallman L., Lofgren M., Marko-Varga G., Nilsson J., Laurell T., "Improved chip design for integrated solid-phase microextraction in on-line proteomic sample preparation," Proteomics, 2(4), pp. 422-429 (2002).

Bertsch A., Heimgartner S., Cousseau P., and Renaud P., "Static micromixers based on large-scale industrial mixer geometry," Lab on a Chip, 1, pp. 56-60 (2001).

Bousse L., Cohen C., Nikiforov T., Chow A., Kopf-Sill A. R., Dubrow R. and Parce J. W., " Electrokinetically controlled microfluidic analysis systems," *Annu. Rev. Biophys. Biomole. Struct.*, 29, pp. 155-81 (2000).

Bousse L., Dijkstra E., and Guenat O., "High-density arrays of valves and interconnects for fluid switching," *Proceedings of Solid Sensor and Actuators Workshop*, pp. 272-275 (1996).

Bousse L., Minalla A., Deshpande M., Greiner. K.B., and Gilbert J.R., "Optimization of sample injection components in electrokinetic microfluidic systems," *Technical Digest of IEEE International Conference on Micro Electro Mechanical Systems*, 12th, pp. 309-314 (1999).

Brady R. F., "In search of non-stick coatings," *Chem. Ind*., 6, pp. 219-222 (1997).

Brahmasandra S. N., Handique K., Krishnan M., Namasivayam V., Burke D., Mastrangelo C. H., and Burns M. A., "Microfabricated devices for integrated DNA analysis," Biochip Technology, Cheng J. and Larry Kricka L. J. eds., Harwood Academic Publishers, PA, pp. 229-250 (2001).

Brahmasandra S. N., Ugaz V. M., Burke D. T., Mastrangelo C. H., and Burns M. A., "Electrophoresis in microfabricated devices using photopolymerized polyacrylamide gels and electrode-defined sample injection," *Electrophoresis*, 22, pp. 300-311 (2001).

Branebjerg J., Gravesen P., Krog J. P., and Nielsen C. R., "Fast Mixing by Lamination," *Proceedings IEEE Micro Electro Mechanical Systems (MEMS)*, pp. 441-446 (1996).

Brott L. L. Naik R. R., Pikas D. J., Kirkpatrick S. M., Tomlin D. W., Whitelock P. W., Clarson S. J., and Stone. M. O., "Ultrafast holographic nanopatterning of biocatalytically formed silica," *Nature*, 413, pp. 291-293 (2001).

Burns M. A., Johson B. N., Brahmasandra S. N., Handique K., Webster J. R., Krishnan M., Sammarco T. S., Man P. M., Jones D., Heldsinger D., Mastrangelo C. H., Burke D. T., "An integrated nanoliter DNA analysis device," *Science*, 282, pp. 484-487 (1998).

Cao X., Lai S., and L.J. Lee, "Design of a self-regulated drug delivery device," *BioMedical Microdevices*, 3(2), pp. 109-117 (2001).

Casey B.G., Monaghan W. and Wilkinson C. D. W., "Embossing of nanoscale features and environments," *Microelectron. Eng*., 35(1-4), pp. 393-396 (1997).

Casey B.G., Cumming D. R. S., Khandaker I. I., Curtis A. G. S. and Wilkinson C. D. W., "Nanoscale embossing of polymers using a thermoplastic die," *Microelectron. Eng*., 46(1-4), pp. 125-128 (1999).

Chen J. H. and Ruckenstein E., "Surface modification by a two-phase deposition of a surfactant," *J. Colloid and Interface Sci*. 142(2), pp. 544-553, 1991.

Chiem N. and Harrison D. J., "Microchip-based capillary electrophoresis for immunoassays: analysis of monoclonal antibodies and tehophylline," *Anal. Chem*., 69(3), pp. 373-379 (1997).

Chiem N., and Harrison D. J., "Microchip systems for immunoassay: an integrated immunoreactor with electrophoretic separation for serum theophylline determination," Clinical Chemistry, 44(3), pp. 591-598 (1998).

Choi J-W and Ahn C.H., "An Active Micro Mixer Using Electrohydrodynamic (EHD) Convection," *Solid-State Sensor & Actuator Workshop*, Hilton Head, pp. 52-55 (June 2000).

Chou C.F., Changrani R., Roberts P., Sadler D., Burdon J., Zenhausern F., Lin S., Mulholland A., Swami N., Terbrueggen R., "A miniaturized cyclic PCR device-modeling and experiments," *Microelectronic Engineering*, 61-62, pp. 921-925(2002).

Chou S.Y., Krauss P.R. and Renstrom P. J., "Imprint Lithography with 25-Nanometer Resolution," *Science*, 272, pp. 85-87 (1996).

Cohen c. B., Chin-Dixon E., Jeong S., and Nikiforov T. T., "A microchip-based enzyme assay for protein kinase A," *Analytical Biochemistry*, 273, pp. 89-97 (1999).

Colgate E. and Matsumoto H., "An investigation of electrowetting-based microactuation," *J. Vac. Sci. Technol.*, A8(4), pp. 3625-3633 (1990).

Crowther J. R., The ELISA guidebook, Humana Press, Totowa, NJ (2001).

Desai T.A., Hansford D. J., Kulinsky L., Nashat A. H., Rasi G., Tu J., Wang Y., Zhang M., and Ferrari M., "Nanopore technology for biomedical applications," Biomedical *Microdevices*, 2(1), pp. 11-40 (1999).

Deshpande M., Greiner K. B., West J., Gilber J. R., Bousse L., and Minalla A., “Predictive design of reverse injection mechanism for electrokinetic DNA sample injection,” *Solid State Sensor & Actuator Workshop*, pp. 128-131 (2000).

Despont M., Lorenz H., Fahrni N., Brugger J., Renaud P., and Vettiger P., “High-aspect-ratio, ultrathick, negative-tone near-UV photoresist for MEMS applications," *IEEE MEMS, Nagoya, Japan*, 10, pp. 518-522 (1997).

Douglass P.M., Wenner B.R., Lai S., Bachas L., and Daunert S., “Centrifugal microfluidics in pharmaceutical analysis: phenothiazine detection employing fluorescently-labeled calmodulin as the biorecognition element,” submitted to *Analytical Chemistry* (2002).

Dreuth H. and Heiden C., “A method for local application of thin organic adhesive films on micropatterned structures”, *Materials Science and Engineering*, C5, pp. 227-231 (1998).

Duffy D. C., Gills H. L., Lin Joe, Sheppard N. F., and Kellogg G. “Microfabricated Centrifugal Microfluidic Systems: Characterization and Multiple Enzymatic Assays” *Anal. Chem.*, 71(20), pp. 4669-4678 (1999).

Duffy D. C., McDonald J. C., Schueller O. J. A., and Whitesides G. M., “Rapid prototyping of microfluidic systems in poly(dimethylsiloxane),” *Anal. Chem.*, 70(23), 4974-4984 (1998).

Dunke K., Bauer H-D, Ehrfeld W., Hobfeld J., Weber L., Horcher G. and Muller G., "Injection-moulded fiber ribbon connectors for parallel optical links fabricated by the LIGA technique," *J. Micromech. Microeng.*, 8, pp. 301-306 (1998).

Edwards T.L., Mohanty S.K., Edward R.K. and Thomas C.L., "Rapid tooling using SU-8 for injection molding microfluidic components," *Proc. SPIE*, 4177 (Microfluidic Devices and Systems III), pp. 82-89 (2000).

Effenhauser C. S., Bruin G. J. M., Paulus A., and Ehrat M., “Integrated Capillary Electrophoresis on Flexible Silicone Microdevices: Analysis of DNA Restriction Fragments and Detection of Single DNA Molecules on Microchips,” *Anal. Chem.*, 69, pp. 3451-3457 (1997).

Ehler St., Elgeti K., Menzel T., and Wiebmeier G., “Mixing in offstream of a microchannel system,” *Chem. Eng. and Proc.*, 39, pp. 291-298 (2000).

Elwenspoek M., Lammerink T. S., Miyake J. R., and Fluitman J. H. J., “Towards integrated microliquid handling systems,” *J. Micromech. Microeng.*, 4, pp. 227-245 (1994).

Ehrfeld W. and Lehr H., "Deep x-ray lithography for the production of three-dimensional microstructures from metals, polymers and ceramics," *Radiat. Phys. Chem*., 45(3), pp. 349-365 (1995).

Eteshola and Leckband, "Development and characterization of an ELISA assay in PDMS microfluidic channels," *Sensors and Actuators B*, 72, pp. 129-133 (2001).

Evans J., Liepmann D. and Pisano A. P., "Planar laminar mixer," *Proceedings IEEE Micro Electro Mechanical Systems (MEMS)*, pp. 96-101 (1997).

Fahrenberg J., Bier W., Mass D., Menz W., Rupercht R. and Schomburg W. K.," A microvalve system fabricated by thermoplastic molding," *J. Micromech. Microeng.*, 5, pp.169-171 (1995).

Fairbrother F. and Stubbs A. E., "Studies in electroendosmosis Part VI: The 'bubble tube' methods of measurement," *J. Chem. Soc*., 1, pp. 527-529 (1935).

Findlay J. B., Atwood S., Bergmeyer M. L., Chemelli J., Christy K., Cummins T., Donish W., Ekeze T., Falvo J., and Patterson D., "Automated closed-vessel system for in vitro diagnostics based on polymerase chain reaction," *Clin. Chem.*, 39, pp. 1927-1933 (1993).

Freemantal M., "Downsizing Chemistry", *Chem. Eng. News*, pp. 27-36, February 22 (1999).

Fujii T., "Microchip-based biochemical analysis devices for 'bioarchitect' research," *Riken Review*, 41, pp. 98-99 (2001).

Gandhi K., Dubrow R. S., and Bousse L. J., "Methods of fabricating polymeric structures incorporating microscale fluidic elements," US patent 6,123,798 (2000).

Gauri V., Koelling K. W., "The motion of long bubbles through viscoelastic fluids in capillary tubes," *Rheol. Acta*, 38, pp. 458-470 (1999).

Gelfi C., Debesi P., Alloni A., Righetti P. G., Lyubimova T., and Briskman V. A., "Kinetics of acrylamide photopholymerization as investigated by capillary zone electrophoresis," *Journal of Chromatography*, 598(2), pp. 277-285 (1992).

Girifalco L. A. and Good R. J., "A theory for the estimation of surface and interfacial energies I: Derivation and application to interfacial tension," J. Phys. Chem., 61, pp.904-909 (1957).

Glasgow I. K., Beebe D. J., and White V. E., "Design rules for polyimide solvent bonding", *Sensors and Materials*, 11(5), pp. 269-278 (1999).

Goll C., Bacher W., Bustgens B., Maas D., Ruprecht R. and Schomburg W. K., " An electrostatically actuated polymer microvalve equipped with a movable membrane electrode," *J. Micromech. Microeng.,* 7, pp. 224-226 (1997).

Gottschalch F., Hoffmann T., Sotomayor T. C. M., Schulz H. and Scheer H-C, " Polymer issues in nanoimprinting technique," *Solid-State Electron*., 43, pp. 1079-1083 (1999).

Gravesen P., Branebjerg J., and Jensen O.S., "Microfluidic – a Review", *J. Micromech. Microeng.*, 3, pp. 168-182 (1993).

Green R. J., Davies M. C., Roberts C. J., and Tendler S. J. B., "A surface plasmon resonance study of albumin adsorption to PEO–PPO–PEO triblock copolymers," *J. Biomed. Mater. Res.*, 42, pp. 165-171 (1998).

Griffith L. G., "Polymeric Biomaterials," *Acta Mater*., 48, pp.263-277 (2000).

Hadd A. G., Raymond D. E., Halliwell J. W., Jacobson S. C., and Ramsey J. M., "Micorchip device for perfrorming enzyme assays," *Anal. Chem.*, 69, pp. 3407-3412 (1997).

Handique K., Burke D.T., Mastrangelo C.H. and Burns M.A., "Nanoliter liquid metering in microchannels using hydrophobic patterns," *Anal. Chem*., 72, pp. 4100-4109 (2000).

Harder P., Grunze M., Dahint R., Whitesides G. M., Laibinis P. E., "Molecular conformation in oligo(ethylene glycol)-terminated selfassembled monolayers on gold and silver surfaces determines their ability to resist protein adsorption," *J. Phys. Chem. B*, 102, pp. 426–36 (1998).

Harris J. M, "Poly(ethylene glycol) chemistry: Biotechnical and biomedical applications," Plenum Press, New York, 1992.

Hawcroft D. M., Electrophoresis: The Basics, OIRL press (1997).

He, B., Burke B. J., Zhang X., Zhang R., and Regnier F. E., "A Picoliter-Volume Mixer for Microf luidic Analytical Systems," Analytical Chemistry, 73(9), pp. 1942-1947 (2001).

Hinsmann P., Frank J., Svasek P., Harasek M., and Lendl B., "Design, simulation and application of a new micromixing devices for time resolved infrared spectroscopy of chemical reactions in solution," *Lab on a Chip*, 1, pp. 16-21 (2001).

Hoffman A. S., "Hydrogels for biomedical applications," *Advanced Drug Delivery Reviews*, 43, pp. 3-12 (2002).

Horvath J. and Dolnik V., “Polymer wall coatings for capillary electrophoresis,” *Electrophoresis*, 22, pp. 644-655 (2001).

Huang Y., Mather E.L., Bell J.L., and Madou M., “MEMS-based sample preparation for molecular diagnostics,” Anal. Bioanal Chem., 372, pp. 49-65 (2002).

Huzyak P. C., "The effects of rheology on the penetration of a gas bubble through viscoelaastic fluids," Thesis, The Ohio State University (1995),

Huzyak P. C. and Koelling K. W., “The penetration of a long gas bubble through a viscoelastic fluids in a capillary tube,” *J. Non-Newtonian Fluid. Mech*., 71, pp. 73-88 (1997).

Israelachvili J., “The different faces of poly(ethylene glycol),” *Proc. Natl. Acad. Sci. USA*, 94, pp. 8378-8379 (1997).

Ito Y., “Surface micropatterning to regulate cell functions,” *Biomaterials*, 20, pp. 2333-2342 (1999).

Jacobson S. C., Ermakov S. V., and Ramsey J. M., “Minimizing the number of voltage sources and fluid reservoirs for electrokinetic valving in microfluidic Devices,” *Anal. Chem.*, 71(15), pp. 3273-3276 (1999).

Jacobson S. C., Hergenroder R., Koutny L. B., and Ramsey J.M., “High-Speed Separations on a Microchip,” *Anal. Chem.*, 66(7), pp.1114-1118 (1994).

Jaszewski R.W., Schift H., Gobrecht J. and Smith P., "Hot embossing in polymers as a direct way to pattern resist," *Microelectron. Eng*., 41/42, pp. 575-578 (1998).

Jaszewski R.W., Schift H., Groning P. and Margaritondo G., "Properties of thin anti-adhesive films used for the replication of microstructures in polymers," *Microelectron. Eng*., 35(1-4), pp. 381-384 (1997).

Jaszewski R.W., Schift H., Schnyder B., Schneuwly A. and Groning P., "The deposition of anti-adhesive ultra-thin Teflon-like films and their interaction with polymers during hot embossing," *Appl. Surf. Sci*., 143(1-4), pp. 301-308 (1999).

Jeong J. H., Lim D. W., Han D. K., and Park T. G., “Synthesis, characterization and protein adsorption behaviors of PLGA/PEG di-block co-polymer blend films,” *Colloids and Surfaces B: Biointerfaces*, 18, pp. 371-379 (2000).

Jensen K. F., Hsing I-M. Srinivasan R., Schmidt M. A., “Reaction engineering for microreactor systems,” Microreaction Technology-Proceedings of the International Conference on Microreaction Technology, 1st, pp. 2-9 (1997).

Johnson R. D., Badr I. H. A., Barrett G., Lai S., Lu Y., Madou M. J., and Bachas L. G., "Development of a fully integrated analysis system for ions based on ion-selective optodes and centrifugal microfluidics," *Analytical Chemistry*, 73, pp. 3940-3946 (2001).

Jun T. K. and Kim C-J, "Valveless pumping using traversing vapor bubbles in microchannels," *J. Appl. Phys.*, 83(11, Pt. 1), pp. 5658- 5664 (1998).

Kaelble D. H., Physical Chemistry of Adhesion, Wiley, New York, (1971).

Kaetsu I., Uchida K., Shindo H., Gomi S., and Sutani K., "," *Radiation Phys. Chem.*, 55, pp. 193- (1999).

Kane R. S., Takayama S., Ostuni E., Ingber D. E., Whitesides G., "Patterning proteins and cells using soft lighography," *Biomaterials*, 20, pp. 2363-2376 (1999).

Kelly K. W., *Proceedings of Novel Microfabrication Options for BioMEMS Conference*, Chapter 6, The Knowledge Foundation, San Francisco, CA, July (1999).

Kim E., Xia Y. and Whitesides G. M., "Polymer microstructures formed by moulding in capillaries," *Nature*, 376, pp. 581-584 (1995).

Kingshott P. and Griesser H. J., "Surfaces that resist bioadhesion," *Current Opinion in Solid State and Materials Science*, 4, pp. 403–412 (1999).

Kiss E., Samu J., Toth A., and Bertoti I., "Novel ways of covalent attachment of poly(ethylene oxide) onto polyethylene: surface modification and characterization by XPS and contact angle measurements," *Langmuir* 12, pp. 1651-1657 (1996).

Koch M., Chatelain D., Evans A. G. R., and Brunnschweiler A., "Two simple micromixers based on silicon," *J. Micromech. Microeng*, 8, pp. 123-126 (1998).

Kolb W. B. and Cerro R. L., "Coating the inside of a capillary of square cross section," *Chemical Engineering Science*, 46(9), pp. 2181-2195 (1991),

Kopp M.U., Crabtree H.J. and Manz A., "Developments in technology and applications of microsystems," *Current Opinion in Chem. Biol*., 1, pp. 410-419 (1997).

Kopp M. U., de Mello A. J., and Manz A., "Chemical amplification: continuous-flow PCR on a chip," *Science*, 280, pp. 1046-1048 (1998).

Koutny L. B., Schmalzing D., Taylor T. A., and Fuchs M., "Microchip electrophoretic immunoassay for serum cortisol," *Anal. Chem*., 68(1), pp. 18-22 (1996).

Lagally E. T., Emrich C. A., and Mathies R. A., "Fully integrated PCR-capillary electrophoresis microsystem for DNA analysis," *Lab on a Chip*, 1(1), pp. 102-107 (2001).

Lee J. W. and Colbrun W. A., "Immunoassay techniques," *Drugs and the Pharmaceutical sciences*, v117 (Handbook of Pharmaceutical analysis), edited by Ohannesian L. and Streeter A. J., pp. 225-312 (2002).

Lee L. J., Madou M. J., Koelling K. W., Daunert S., Lai S., Koh C. G., Juang Y-J, Lu Y., and Yu L., "Design and fabrication of CD-like microfluidic platforms for diagnostics: microfabrication," *Biomedical Microdevice*, 3(4), pp. 339-351 (2001).

Lee Y-K, Deval J., Tabeling P., and Ho C-M., "Chaotic mixing in electrokinetically and pressure driven microflows," *IEEE-MEMS*, pp. *483-486* (2001).

Li Y., Pfohl T., Kim J. H., Yasa M., Wen Z., Kim M. W., and Safinya C. R., "Selective surface modification in channels for micromanipulation of biological macromolecules," *Biomedical Microdevices*, 3(3), pp. 239-244 (2001).

Lin L-W, Chiu C-J, Bacher W. and Heckele M., "Microfabrication using silicon mold inserts and hot embossing," *Seventh International Symposium on Micro Machine and Human Science*, pp. 67-71 (1996).

Liu R.H., Yu Q., Bauer J.M., Moore J.S., and Beebe D.J., "Hydrogel Microvalves Fabricated Using in-situ Polymerization", *Solid-state Sensor & Actuator workshop*, pp. 222-225 (2000).

Lum P. and Greenstein M., "Microfluidic structure assembly with mating microfeatures," US Patent 5,932,315 (1999).

Lyman D. J., Muir W. M.,, and Lee I. J., "The effect of chemical structure and surface properties of polymers on the coagulation of blood. I. Surface free energy effects," *Trans. Amer. Soc. Artif. Int. Organs*, 11, pp. 301-306 (1965).

Madou M. J., Fundamental of Microfabrication, CRC Press, Boca Raton (1997).

Madou M. J. and Kellogg G. J., "The LabCD^{TM}: A centrifuge-based microfluidic platform for diagnostics". *Proc. SPIE.*, V3259, pp. 80-93 (1998).

Madou M.J., Lee L.J., Koelling K.W., Lai S., Koh C. G., Juang Y-J., Yu L. and Lu Y., "Design and fabrication of polymer microfluidic platforms for biomedical application," *Annu. Tech. Conf. - Soc. Plast. Eng*. 59th (Vol. 3), pp. 2534-2538, (2001).

Madou M.J., Lu Y., Lai S., Lee L. J., and Daunert S., "A Centrifugal Microfluidic platform- A comparison", *Micro Total Analysis Systems*, pp. 565-570 (2000).

Madou M.J., Lu Y., Lai S, Juang Y-J, Lee L.J., and Daunert S., “A Novel design on a CD disc for two-point calibration measurement”, *Solid-state Sensor & Actuator workshop*, pp. 191-194 (2000).

Makhijani V.B., Raghavan J., Przekwas A., Przekwas, A., “Simulation of biochemical reaction kinetics in microfluidic systems,” Microreaction Technology-Proceedings of the International Conference on Microreaction Technology, 3rd, pp. 441-450 (1999).

Malmsten M., Emoto K., and Van Alstine J. M., “Effect of chain density on inhibition of Protein adsorption by poly(ethylene glycol) based coatings,” *Journal of Colloid and Interface Science*, 202, pp. 507–517 (1998).

Manz A., Harrison D. J., Verpoorte E. M. J., Fettinger J. C., Paulus, A., Ludi H., Wilmer H. M., “Planar chips technology for miniaturization and integration of separation techniques into monitoring systems: capillary electrophoresis on a chip” *J. Chromatogr*., 593, pp. 253-258 (1992).

Mathies R. A., “High-throughput genetic analysis using microfabricated 96-sample capillary array electrophoresis microplates,” *Proc. Natl. Acad. Sci. USA*, 95, pp. 2256-2261 (1998).

McCormick R. M., Nelson R. J., Alonso-Amigo M. G., Benvegnu D. J., and Hooper H. H., “Microchannel electrophoretic separations of DNA in injection-molded plastic substrates,” *Anal. Chem*., 69, pp. 2626-2630 (1997).

McDonald J. C., Duffy D. C., Anderson J. R., Chiu D. T., Wu H., Schueller O. J. A. and Whitesides G. M., “Fabrication of microfluidic systems in poly (dimethylsiloxane),” *Electrophoresis*, 21, pp. 27-40 (2000).

Medintz I. L., Paegel B. M., and Mathies R. A., “Microfabricated capillary array electrophoresis DNA analysis systems,” *Journal of Chromatography*, 924, pp. 265-270 (2001).

Metz S., Holzer R., and Renaud P., “Polyimide-based microfluidic devices,” *Lab on a Chip*, 1, pp. 29-34 (2001).

Momma C., Nolte S., Chichkov N., Alvensleben B. V., and Tunermann F. A., "Precise laser ablation with ultrashort pulses," *Appl. Surf. Sci.*, 109/110, pp. 15-19 (1997).

Moroney R. M., White R. M., and Howe R. T., “Fluid motion produced by ultrasonic lamb waves,” *Ultrasonics Symposium Proceedings*, 1, pp. 355-358, Honolulu, HI (1990).

Ogura M., Agata Y., Watanabe K., McCormick R. M., Hamaguchi Y., Aso Y., and Mitsuhashi M., "RNA chip: quality assessment of RNA by microchannel linear gel electrophoresis in injection-molded plastic chips," *Clinical Chemistry*, 44(11), pp. 2249-2255 (1998).

Otsuka H., Nagasaki Y., and Kataoka K., "Self-assembly of poly ethylene glycol -based block copolymers for biomedical applications," *Current Opinion in Colloid & Interface Science*, 6, pp. 3-10 (2001).

Park A., Wu B., and Griffith L. G., "Integration of surface modification and 3D fabrication techniques to prepare patterned poly(L-lactide) substrates allowing regionally selective cell adhesion," *J. Biomater. Sci. Polymer Edn.*, 9(2), pp. 89-110 (1998).

Paul P. H., Garguilo M. G., and Rakestraw D. J., "Imaging of pressure- and electrokinetically driven flows through open capillaries," *Anal. Chem.*, 70, pp. 2459-2467 (1998).

Peppas N. A., Bures P., Leobandung W., and Ichikawa, "Hydrogels in pharmaceutical formulations," *European Jouranl of Pharmaceutics and Biopharmaceutics*, 50, pp. 27-46 (2000).

Petersen K. E., "The future of DNA diagnostic testing," *Proceedings of SPIE*, **V4560**, pp. 1-7 (2001).

Pethig R., Burt J. P. H., Parton A., Rizvi N., Talary M. S., and Tame J. A., "Development of biofactory-on-a-chip using eximer laser micromachining," J. Micromech. Microeng., 8, pp. 57-63 (1998).

Piotter V., Benzler T., Hanemann T., Wollmer H., Ruprecht R. and Haubelt J., "Innovative molding technologies for the fabrication of components for microsystems," *Proc. SPIE-The International Society for Optical Engineering*, V3680, pp. 456-463 (1999).

Poslinski A. J., Oehler P. R., and Stokes V. K., "Isothermal gas-assisted displacement of viscoplastic liquids in tubes," Polymer Engineering and Science., 35(11), pp. 877-892 (1995).

Prime K. L., Whitesides G. M., "Adsorption of proteins onto surfaces containing eng-attached oligo(ethylene oxide) - a model system using self-assembled monolayers," *Journal of the American Chemical Society*, 115(23), pp. 10714-10721 (1993).

Przekwas A., Makhijani V., Athavale M., Klein A., Bartsch P., "Computational simulation of bio-microfluidic processes in integrated DNA biochips," Proceedings of the μTAS Symposium, 4th, pp. 561-564 (2000).

Qin D., Xia Y., Rogers J. A., Jackman R. J., Zhao X-M, and Whitesides G. M., "Microfabrication, microstructures and microsystems," *Topics in Current Chemistry*, 194, pp. 1-20 (1998).

Ramos B. L., Choquette S. J. and Nicholas F. F., "Embossable Grating Couplers for Planar Waveguide Optical Sensors," *Anal. Chem*., 68, pp. 1245-1249 (1996).

Röhm America, LLC product literature: http://www.rohmamerica.com/Methacrylates/Monomers/aliphatics.html.

Robert M. A., Rossier J. S., Bercier P., and Girault H., "UV laser machined polymer substrates for the development of microdiagnostic systems," *Anal. Chem.*, 69, pp. 2035-2042 (1997).

Rossier J. S., Schwarz A., Reymond F., Ferrigno R., Bianchi F., and Girault H. H., "Microchannel networks for electrophoretic separations," *Electrophoresis*, 20, pp. 727-731 (1999).

Rossier J. S., Girault H. H., "Enzyme linked immunosorbent assay on a microchip with electrochemical detection," Lab on a Chip, 1(2), pp. 153-157 (2001).

Ruckenstein E., and Lee S. H., "Estimation of the equilibrium surface free energy components of restructuring solid surfaces.," *J. Colloid Interface Sci*. 120(1), pp. 153-161 (1987).

Sadler D.J., Changrani R., Roberts P., Chou C-F., and Zenhausern F., "Thermal management of BioMEMS," *Proceedings of Intersociety Conference on Thermal and Thermomechanical Phenomena in Electronic Systems*, 8th, pp. 1025-1032 (2002).

Sammarco T. S. and Burns M. A., "Thermocapillary pumping of discrete drops in microfabricated analysis devices," *AIChE J*., 45(2), pp. 350-366 (1999).

Sander G. H. W., and Manz A., "Chip-based microsystems for genomic and proteomic analysis," *Trends in Analytical Chemistry*, 19(6), pp. 364-378 (2000).

Sato K., Tokeshi M., Odake T., Kimura H., Ooi T., Nakao M., and Kitamori T., "Integration of an immunosorbent assay system: analysis of secretory human immunoglobulin A on polystyrene beads in a microchip," Anal. Chem., 72(6), pp. 1144-1147 (2000).

Sato K., Tokeshi M., Kimura H., and Kitamori T., "Determination of carcinoembryonic antigen in human sera by integrated bead-bed immunoassay in a microchip for cancer diagnosis" Anal. Chem., 73(6), pp. 1213-1218 (2001).

Sayah A., Solignac D., Cueni T., and Gijs M. A. M., “Development of novel low temperature bonding technologies for microchip chemical analysis applications,” Sensors and Actuators A, 84, pp. 103-108 (2000).

Schmalzing D., Buonocore S., and Piggee C., “Capillary electrophoresis-based immunoassays,” *Electrophoresis*, 21, pp. 3919-3930 (2000).

Schmidt M. A., “Wafer-to-wafer bonding for microstructure formation,” Proc. IEEE, 86, pp. 1575-1585 (1998).

Schneegab I., Brautigam R., and Kohler J. M., "Miniaturized flow-through PCR with different template types in a silicon chip thermocycler," *Lab on a Chip*, 1(1), pp. 42-49 (2001).

Schwarz, A., Rossier J. S., Bianchi F., Reymond F., Ferrigno R., and Girault H. H., “Micro-TAS on polymer substrates micromachines by laser photoablation,” Proceedings Micro-TAS, pp. 241-244 (1998).

Schift H., Jaszewski R.W., David C. and Gobrecht J., "Nanostructuring of polymers and fabrication of interdigitated electrodes by Hot Embossing Lithography," *Microelectron. Eng*., 46(1-4), pp. 121-124 (1999).

Schwesinger N., Frank T., and Wurmus H., “A Modular Microfluidic System with an Integrated Micromixer,” *J. Micromech. Microeng*, 6(1), pp. 99-102 (1996).

Sheth S. R. and Leckband D., “Measurements of attractive forces between proteins and end-grafted poly(ethylene glycol) chains,” *Proc. Natl. Acad. Sci. USA*, 94, pp. 8399-9404 (1997).

Sheth S. R., Efremova N., and Leckband D., “Interactions of poly(ethylene oxide) brushes with chemically selective surfaces,” *J. Phys. Chem. B*, 104, pp. 7652-7662 (2000).

Simpson P. C., Roach D., Woolley A. T., Thorsen T., Johnston R., Sensabaugh G. F., and Mathies R. A., “High-throughput genetic analysis using microfabricated 96-sample capillary array electrophoresis microplates,” *Proc. Natl. Acad. Sci. USA*, 95, pp. 2256-2261 (1998).

Snyder M. R., ‘Micromolding technology extends sub-gram part fabrication capability’ *Modern Plastics*, pp. 85-87, January (1999).

Stroock A. D., Weck M., Chiu D. T., Huck W. T. S., Kenis P. J. A., Ismagilov R. R., and Whitesides G. M., “Patterning electro-osmotic flow with patterned surface charge,” Physical review letters, 84(15), pp. 3314-3317 (2000).

Taylor G. I., "Deposition of a viscous fluid on the wall of a tube," *J. Fluid Mech*., 10, pp. 161-165 (1961).

Taylor J., Picelli G., and Harrison D. J., “An evaluation of the detection limits possible for competitive capillary electrophoretic immunoassays,” Electrophoresis, 22, pp. 3699-3708 (2001).

Tsibouklis J., Stone M., Thorpe A. A., Graham P., Peters V., Heerlien R., Smith J. R., Green K.L., and Nevell T.G., "Preventing bacterial adhesion onto surfaces: the low-surface-energy approach," *Biomaterials*, 20(13), pp. 1229-1235 (1999).

Tsibouklis J., Stone M., Thorpe A.A., Graham P., Nevell T. G., and Ewen R. J., "Inhibiting bacterial adhesion onto surfaces: the non-stick coating approach," *Int. J. Adhes. Adhes*., 20(2), pp. 91-96 (2000).

U.S. Environmental Protection Agency. Toxic Substances Control Act (TSCA) Chemical Assessment Series, Washington, D.C., April 15, 1981.

van Oss C. J., “Hydrophobicity of biosurfaces – origin, quantitative determination and interaction energies,” *Colloids and Surfaces B: Biointerfaces*, 5, pp. 91-110 (1995).

Wang H., Masood S., Iovenitti P., and Harvey E. C., “Application of fused deposition modeling rapid prototyping system to the development of microchannels,” *Proceedings of SPIE- BioMEMS and Smart Nanostructures*, V4590, pp. 213-220 (2001).

Wang P., Tan K.L., Kang E.T., Neoh K.G., “Plasma-induced immobilization of poly(ethylene glycol) onto poly(vinylidene fluoride) microporous membrane,” *Journal of Membrane Science*, 195, PP. 103–114 (2002).

Wang Y., "Polymer impregnation and surface modification using supercritical fluids," Thesis, The Ohio State University (2001).

Waters L. C., Jacobson S. C., Kroutchinina N., Khandaurina J., Foote R. S., and Ramsey J. M., “Multiple sample PCR ampilification and electrophoretic analysis on a microchip,” *Anal. Chem*., 70(24), pp. 5172-5176 (1998).

Ward J. H., Bashir R., and Peppas N. A., “Micropatterning of biomedical polymer surfaces by novel UV polymerization techniques,” *Journal of Biomedical Materials Research*, 56(3), pp. 351-360 (2001).

Warrington R. O., "An overview of micromechanical machining processes for BioMEMS," *Proceedings of Novel Microfabrication Options for BioMEMS Conference*, Chapter 7, pp. 67-84, July (1999).

Waters L. C., Jacobson S. C., Kroutchinina N., Khandaurina J., Foote R. S., and Ramsey J. M., "Multiple sample PCR amplification and electrophoretic analysis on a microchip," *Anal. Chem*., 70(24), pp. 5172-5176 (1998).

Wenner B. R., Douglass P. M., Shrestha S., Sharma B. V., Lai S., Madou M. J., and Daunert S., "Genetically designed biosensing systems for high-throughput screening of pharmaceuticals, clinical diagnostics, and environmental monitoring," *Proceedings of SPIE* V. 4252 *–Advances in Fluorescence Sensing Technology V*, pp. 59-70 (2001).

Wild D., "The immunoassay handbook-products," Stockton Press, New York (1994).

Wimberger-Friedl R., "Injection molding of sub-μm grating optical elements," *Proc. SPE ANTEC*, 57(1), pp. 476-480 (1999).

Woias P., Hauser K., and Yacoub-George E., "An active silicon micromixer for TAS applications" *Micro Total Analysis Systems*, pp. 277-282 (2000).

Woolley A. T., Sensabaugh G. F., and Mathies R. A., "High-speed DNA genotyping using microfabricated capillary array electrophoresis chips," *Analytical Chemistry*, 69, pp. 2181-2186 (1997).

Wroblewski D. E., et al., "MEMS micro-valve arrays for fluidic control," *MEMS, ASME Proceedings*, pp. 145-151 (1998).

Xia Y., Kim E., Zhao X-M, Rogers J. A., Prentiss M. and Whitesides G. M., "Complex optical surfaces formed by replica molding against elastomeric masters," *Science*, 273, pp. 347-349 (1996).

Xia Y., McClelland J. J., Gupta R., Qin D., Zhao X-M, Sohn L. L., Celotta R. J. and Whitesides G. M., "Replica molding using polymeric materials. A practical step toward nanomanufacturing," *Advanced Materials*, 9, pp. 147-149 (1997).

Xia Y. and Whitesides G.M., "Soft lithography," *Angew. Chem. Int. E.*, 37, pp. 550-575 (1998).

Yi M.and Bau H., "The kenematics of bend-induced stirring in micro-conduits," *ASME MEMS*, pp. 489-496 (2000).

Zhang F., Kang E.T., Neoh K.G., Wang P., Tan K.L., "Surface modification of stainless steel by grafting of poly(ethylene glycol) for reduction in protein adsorption," *Biomaterials*, 22, pp. 1541-1548 (2001).

Zhang M., Desai T., and Ferrari M., "Proteins and cells on PEG immobilized silicon surfaces," *Biomaterials*, 19, pp. 953-960 (1998).

Zeng J., Banerjee D., Deshpande M., Gilbert J., Duffy D.C., and Kollogg G.J., "Design Analyses of Capillary Burst Valves in Centrifugal Microfluidics", *Micro Total Analysis Systems*, pp. 579-582 (2000).

Zheng H. J. and Dasgupta P. K., "Concentration and optical measurement of aqueous analytes in an organic solvent segmented capillary under high electric field," *Anal. Chem.*, 66(22), pp. 3997-4004, (1994).

Zlatanic A., and Petrovic Z. S., "Effect of crosslinking on swelling, transitions and mechanical properties of poly(N-isopropylacrylamide) responsive hydrogels," ANTEC Proc. SPE, 59th, pp. 3319-3323 (2001).

APPENDIX A PHOTORESIS CD MICROFLUIDIC PLATFORM

Photolithography has also been applied to fabricate the photoresist CD in the case that all feature sizes have same depths. The structures on the CD were first designed by computer-aided design software such as AutoCAD 2000 or Freehand 8.0. This design was then converted into a photomask, which was a pattern of emulsion printed onto a transparency using a high-resolution (3386dpi) imagesetting system (Yeager Graphics, Columbus OH). The resulted transparent film was then place onto a 4"×4" glass plate and was used as the photomask during the photolithography process. The negative photoresist SU-8 100 (MicroChem Inc.) was used and PMMA was selected as the substrate. The photolithography produced channels have the same depth around 300μm and widths ranging from 80μm to 508μm. The structure developed by photolithography was covered with adhesive tape and attached to a specific position on a blank CD for the burst frequency testing. CNC machining can provide features containing channels and reservoirs with different depths while photolithography cannot. However, features produced by photolithography have much better surface quality and accuracy in dimension. In addition, the geometries of the channel (e.g., no sharp turns) and shapes of the reservoir (such as, raindrop liked shape) are more feasible in the photolithography process. Figure A.1 shows the burst frequency test result of photolithography developed

structure. The observed burst frequencies were consistently high than the calculated values because the design is based on the contact angle between the testing fluid and the PMMA (SU-8 data is not available). The SU-8 is more hydrophobic than PMMA. Higher contact angle between the testing fluid and the SU-8 is expected. According to Eq. (3.4), the higher the contact angle, the higher burst frequency.

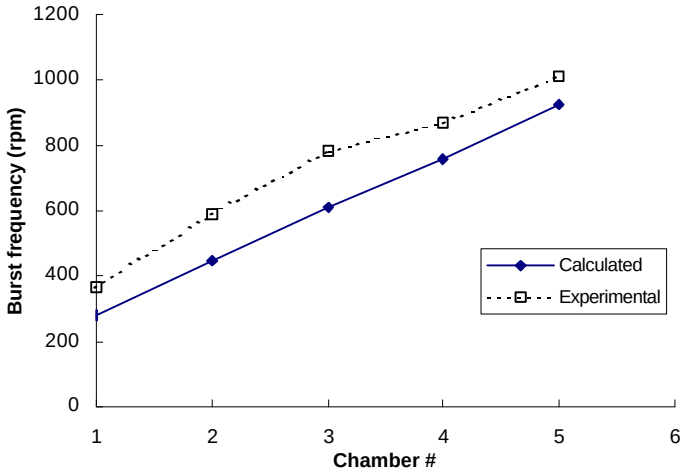

Figure A.1. Burst frequencies of photolithography-made CD (TP2).

APPENDIX B NICKEL ELECTROPLATING

Electroplating is the electrochemical deposition of metals, alloys or semiconductors. Nickel is the typical metal materials for electroplating due to its well-known electroplating process, high replication accuracy, and low internal stresses. The basic principle for the nickel electroplating is shown in Figure B.1. The reactions occurred at the anode and cathode are expressed in Eqs. (B.1) to (B.3):

Anode:

$$Ni\ (s) \rightarrow Ni^{2+}\ (aq) + 2e^{-} \qquad (B.1)$$

Cathode:

$$Ni^{2+}\ (aq) + 2e^{-} \rightarrow Ni\ (s) \qquad (B.2)$$

$$2H^{+}\ (aq) + 2e^{-} \rightarrow H_2\ (g) \qquad (B.3)$$

The electroplating time (*t)* is governed by Eq. (B.4) [Madou, 1997]:

$$t = \frac{zFdAt_s}{IM} \qquad (B.4)$$

where z = Valence (for Ni^{2+}, $z = 2$),

F = Faraday's constant (96,487 Coulomb/mol),

d = Density of Ni (8.9 g/cm^3),

M = Molecular weight of Ni (58.69 g/mol),

t_s = Thickness (cm),

A = Area to be electroplated (cm^2),

I = Current applied (A = Coulomb/sec),

Materials and equipment:

Current control: galvanostat (DCH1, PC4/750, Gamry Instruments),

Temperature control and agitation: a digital hot plate with a Teflon thermocouple

Nickel anode (Gallon- Nickel Anode Set, Technic Inc.)

Nickel solution: Nickel Sulfamate RTU solution (Mechanical, from Technic Inc.)

Wetting agent: sodium dodecyl sulfate (SDS)

Process Conditions:

Temperature = 50 ^oC

pH = 3.8 ~ 4.5

Current density = 10 ~ 30 A/cm^2

Agitation = 550 ~ 650 rpm.

The input parameters for the Galvanostat in the Gamry system are listed in Table B.1.

Parameters	Input
Initial I (mA/cm2)	-30
Initial Time (s)	20000*
Final I (mA/cm2)	0
Final Time (s)	0
Sample Period (s)	5
Sample Area (cm2)	0.8
Density (gm/cm3)	8.9
Equiv. Wt	29.4
Red + White (Anode)	Nickel Bar**
Green + Blue (Cathode)	Substrate

Table B.1. The input parameters for the Galvanostat in the Gamry system (* the electroplating time is based on a two-point calibration system. ** The nickel bar and the substrate should be placed as parallel as possible in the electroplating bath).

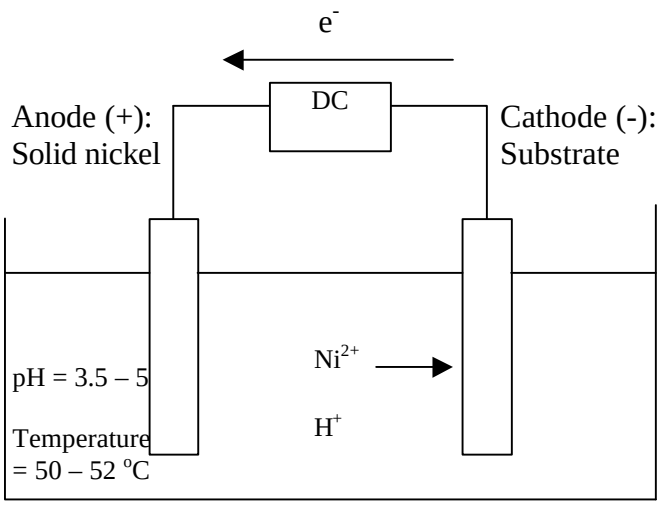

Figure B.1. Schematic of nickel electroplating setup.